Comrisk - Subproject SP 7

Risk assessment for the Wadden Sea

September 2004

Kystdirektoratet
Trafikministeriet

INTERREG III B North Sea Region Programme of the Eropean Union

COMRISK

Comrisk - Subproject SP 7

Risk assessment for the Wadden Sea

September 2004

Note:
In this report the Danish formatting of numbers is applied where decimal places are indicated by a comma and the separation by thousand is indicated by a point. This stands in contrast to the British formatting of numbers.

Kystdirektoratet
Højbovej 1
Postbox 100
DK - 7620 Lemvig
Tlf. (+45) 99 63 63 63 63
E-post: KDI@kyst.dk
www.kyst.dk

Pictures on the front cover show a breach at Juvre Dike caused during the storm surge on December 3rd, 1999 and the subsequent inundations in the northeast part of the island of Rømø, Denmark.

All photographs used in the report were taken by G. Mensel, Skærbæk, Denmark, apart from the photographs used in Appendix A which were taken by A. Kortenhaus, Braunschweig, Germany.

Preface

The design of flood defence systems has undergone extensive development in the last decades. Traditionally, flood defence systems are designed on the basis of deterministic or quasi-deterministic approaches, normally referring to a design water level. However, these approaches adopt simplistically fixed design values for the various parameters of hydrodynamic and geotechnical processes taking place at a flood defence system during a storm surge.

Hence, new design methods, including probabilistic approaches, have been subjected to constant development during the last years. The probabilistic approaches allow engineers to account for uncertainties in the input parameters and the models describing all possible versions of the various types of flood defence structures. Probabilistic approaches are, however, only applicable to the concept of risk analysis.

The present report has been prepared under the framework of the Interreg III B project "Common Strategies for Storm Flood Risk" (COMRISK) and presents the results of the SP7 subproject "Risk Assessment for the Wadden Sea". The objective of the subproject has been assessment of the flood risk for the Ribe sea defence system by means of a risk analysis. The Danish Coastal Authority (DCA) has been responsible for the completion of the SP7 subproject, which has been carried out in the period from January 2003 to September 2004.

The support of Ribe Municipality, Ribe County and Ribe Tourist Office and their supply of valuable data and information about the Ribe area are gratefully acknowledged. Special thanks are due to Dr. A. Kortenhaus of the Leichtweiss Institute at the Technical University of Braunschweig, Germany, for his performing of the probabilistic calculations as well as for his inexhaustible support.

September 2004

Danish Coastal Authority
Lemvig, Denmark

Contents

List of figures

List of tables

Abstract

Within the framework of the Interreg III B project "Common Strategies for Storm Flood Risk" (COMRISK) coastal flood risk management is being improved through transfer and evaluation of knowledge, methodologies as well as pilot studies. One of the pilot studies, the SP7 subproject, concerns the risk analysis of a flood defence system located in the Danish part of the Wadden Sea. The pilot study area is located about 50 km north of the German-Danish border and is mainly characterised by a large rural area of former marshland and by an urban area, Ribe town.

The study in hand assesses the flood risk of this flood defence system based on the state of the art in the literature. The flood risk of the Ribe defence system is hereby defined as the product of the flooding probability and the subsequent consequences of flooding. The study is performed in two major steps which comprise on the one hand a hazard analysis calculating the overall probability of flooding for the area, and on the other hand an analysis of vulnerability determining the damage potential of the hinterland in case of flooding.

Within the hazard analysis the report deals with the set-up of a detailed fault tree for the dike structure, a sluice and three outlets considering 23 failure mechanisms and their related limit state equations. The uncertainties of the input parameters and the models are evaluated and supplemented by a sensitivity analysis of the input parameters. The overall failure probability of the individual sections of the system are calculated after splitting the defence system into representative sections based on predefined criteria.

The vulnerability analysis considers the valuation of tangible risk elements in the flood-prone hinterland. Damage functions are defined for each element at risk. Moreover, inundation scenarios are set up in order to assess the extension and depth of different inundation scenarios. The combination of the value of risk elements and the related damage factors determines the damage within a specific scenario.

Finally, the overall flooding probability is multiplied with the damage within a risk assessment, which is the final formal step in the risk analysis.

1. Introduction

There is a long tradition of coastal flood defence systems along the North Sea coast. The overall objective of flood defence systems is to protect low-lying coastal areas against flooding. However, throughout history many low-lying areas around the North Sea have been flooded during storm surges due to flood defence system failure. A great effort has therefore been made to improve and strengthen flood defence systems during the last decades. The knowledge regarding the technical processes concerning loads and the resistance of flood defence systems has been considerably broadened. However, the risk of flooding is present and will be present in future.

Though no major flooding disasters have taken place in the North Sea region for decades, the challenge of climate change and the increasing vulnerability of more intensively used coastal areas call for new management approaches to the handling of the risk of coastal flooding. About 14 million people, corresponding to approx. 20 % of the total population in the North Sea region, live in coastal lowlands. Major economic activities, e.g. the seaports of Rotterdam, London and Hamburg or the tourist industry, are concentrated in these lowlands. Hence, social progress and economic growth prerequisite appropriate coastal defence measures embedded in new innovative strategies of managing the risk of coastal flooding.

Figure 1-1: Low-lying coastal areas in the North Sea region.

1.1 The "Common Strategies to reduce the Risk of Storm Floods in Coastal Lowlands" (COMRISK) project

In 1996 national and regional coastal defence authorities in the UK, Belgium, the Netherlands, Germany and Denmark initiated a high-level network of co-operation, the North Sea Coastal Managers Group (NSCMG). The NSCMG is an important platform for exchanging knowledge and achieving a balanced approach to a more comprehensive international co-operation on risk management throughout the North Sea region. Based on these considerations, the idea of a project named COMRISK was born.

The "Common Strategies for Storm Flood Risk" (COMRISK) project aims to improve coastal flood risk management through transfer and evaluation of knowledge, methodologies as well as pilot studies.

COMRISK is divided into two parts: the 'umbrella project' and nine subprojects. The umbrella project focuses on the exchange of experience and on the coordination of the overall project and the subprojects. The specific objectives of the project are as follows:

- To bring together coastal defence experts from administrations, science centres and private companies in the North Sea region and beyond.
- To exchange experiences and studies of good practise on coastal risk management.
- To evaluate and further develop innovative integrated risk management strategies, considering national regulations and responsibilities.
- To initiate and support transnational cooperation on integrated coastal risk management (network).
- To integrate coastal risk management into strategies for sustainable management of the coastal zones in the North Sea region.

The nine subprojects are closely connected to each other and consist either of evaluation studies or pilot studies. There is one general objective of each subproject that contributes to the above-mentioned main objectives. In four of the nine subprojects, the objective is to perform a risk assessment of a relevant coastal flood unit located in Belgium, UK, Germany and Denmark. This report presents the results of the risk assessment of the Danish flood unit. The objectives of the remaining five subprojects are

- to improve national policies and strategies for coastal risk management,
- to achieve common strategic planning tools for coastal risk management,
- to achieve common methods to improve the public's perception of, and participation in, coastal risk management,

- to achieve common approaches and indicators to establish the performance of risk management measures,
- and to achieve common approaches to establish the hydraulic boundary conditions for technical measures.

The COMRISK project runs from July 2002 to June 2005 and is co-financed by the Interreg III B North Sea Region Community Initiative Programme of the European Union. The project period is divided into three phases. During the first phase, necessary preparations to coordinate and implement the project involving seven partners have been carried out. The subprojects are carried out in the second phase. During the second phase a workshop has to be organized for each subproject where the project progress as well as relevant (local) topics will be discussed by the participants. The second phase ends with the reporting of the outcome of the subprojects. Finally, an international conference will be organized during the third phase. The conference is an opportunity to present the outcomes of the pilot and evaluation studies to a broader audience of risk management experts from administrations, research institutes and private companies.

On the basis of the conference proceedings and the preceding activities a brochure will be prepared, containing principles and recommendations for innovative and integrated risk management strategies in the North Sea region.

1.2 Background and objectives of the SP7 subproject

The report in hand presents the results of the SP7 subproject "Risk assessment for the Wadden Sea". The SP7 subproject is one of the four pilot studies to perform a risk assessment. The pilot study area is located in the Danish part of the Wadden Sea.

The Wadden Sea is a major part of the North Sea region. It fringes the Dutch, German and Danish coasts over a distance of nearly 500 km with a maximum width of approximately 35 km (CPSL, 2001). Towards the North Sea, the Wadden Sea is bordered by 20 large and many small barrier islands, peninsulas and sandy shoals. In between these barrier islands and the mainland coast lies the largest tidal flat area in Europe. The low-lying mainland coasts are mainly protected against flooding by dikes.

Based on the increasing socio-economic pressure in the low-lying hinterlands behind the Wadden Sea dikes, the awareness and the perception of the coastal flood risk are well established in all Wadden Sea countries. Coastal defence authorities have to react to the public's request for maintenance of the present safety level. This demand is increased by the public discussion about the long-term consequences of climate change.

Scientists and risk management experts are therefore developing instruments and methods in order to assess the risk of flooding. For this purpose, risk is defined as the combination of the probability of occurrence of a hazardous event and the magnitude of subsequent consequences. The method of combination is generally to multiply the probability of occurrence by the consequences. Although the concept of multiplying two figures looks quite simple, the implementation is quite complicated. Instruments and methods used to calculate the probability of hazardous events or the determination of consequences have to be applicable for coastal defence authorities in charge and they must be in conformity with national policies. Weak spots in the models and application difficulties normally appear during practical application. Hence, the feasibility of these methods and models for risk assessment have to be tested and evaluated at different flood units with changing boundary conditions.

The main objective of SP7 subproject is to perform a risk assessment of a sea defence system located in the Danish part of the Wadden Sea. The risk assessment will be based on knowledge found in the literature. This way, the project will not contribute to new development of instruments or methods, but instead apply existing methods and models. To achieve the main objective, the following tasks and topics will be dealt with:

– The present state of knowledge of terms, methods and models concerning risk handling will be studied in a literature review. The literature review shall identify practicable methodologies and tools which may be used for assessing the flood risk in the Danish pilot study area.
– In the discipline of flood protection the main goal is the prevention of flooding danger to the public. However, a hazard to the public occurs if the protection against flooding can not be maintained in a particular situation, e.g. in case of a dike breach during a storm surge. This implies the question in what kind of situations the protection against flooding is lost. A hazard analysis aims at identifying these situations, including the definition of relevant hazard types (e.g. wave overtopping or dike breach), the location and intensity of the hazard as well as the calculation of the hazard probability.
– Furthermore, it is necessary to know the consequences if the flood defence system fails and the hinterland is inundated. If inundation occurs, the result will be different types of damage – material/nonmaterial, direct/indirect, tangible/intangible damage. By inventorying the flood-prone area and defining damage functions in relation to the inundation depth for different types of damage, the consequences of a particular flood (scenario) can be estimated.
– In case of failure of the sea defence system during a storm surge, a specific water volume will enter the area behind the defence line and inundate the hinterland. The volume of inflow depends on a number of parameters, e.g. location and number of openings in the defence system, time-dependent growth of the gaps as well as the time of dike breach in relation to the outer storm surge water level. Furthermore, the expansion of the flood water pouring into the hinterland

must be described properly in order to allow an adequate assessment of all assets which might be damaged by the flood water. For this purpose, the topography of the flood-prone hinterland must be known.

A more specified description of the objectives and the methodology of the investigation will be given in Chapter 3.

As mentioned above, each subproject included a workshop during the second project phase. At the workshops of the four pilot studies, differences and similarities in relation to the applied methods and tools as well as the geographical conditions of the pilot areas have been discussed extensively. Experience gained when performing a risk assessment, comprising a hazard analysis and vulnerability analysis, has been exchanged. This way, the SP7 subproject has been especially linked to the other three pilot studies involving risk assessment.

1.3 The pilot study area of Ribe – history and present situation

The pilot study area for the performance of a risk assessment is located approximately 50 km north of the German-Danish border. The study area is more than 95 km² and mainly characterised by a large rural area of former marshland and by an urban area, Ribe town, which is located 5-6 km from the sea. Ribe town is the oldest town in Denmark and today it has about 9.000 inhabitants. Ribe town and the westward marshland are protected by an 18,4 km long sea dike called Ribe Dike. The dike has a constant profile over its total length and is interrupted by one sluice (Kammerslusen) and three smaller outlets.

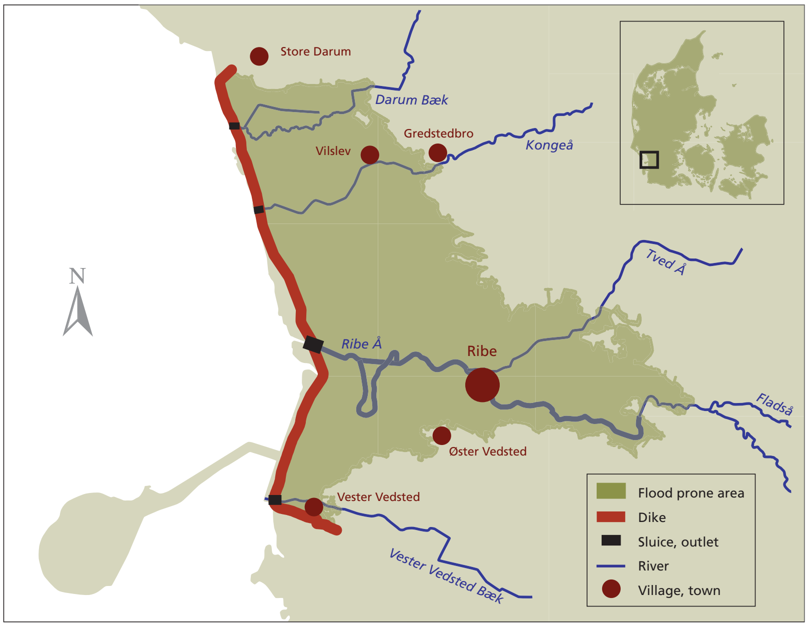

Figure 1-2: Location of Ribe town and its flood unit.

The Ribe flood site has been chosen as pilot study area due to a) suitable and sufficient input data, b) a simple cross-section of the flood defence system, and c) the composition of the flood site by rural and urban areas is characterised by a high degree of tourism which to a great extent has to do with the long and interesting history of Ribe town.

The history of Ribe town and its hinterland goes back to the period before the year 800. The town was founded along the periphery of a small market place on high sandy land, which was separated by a river and wetlands. Already before the time of Apostle Ansgar, who obtained land from the Danish king around the year 860, the market place was an important international meeting place (Ribe Tourist Office, 2004).

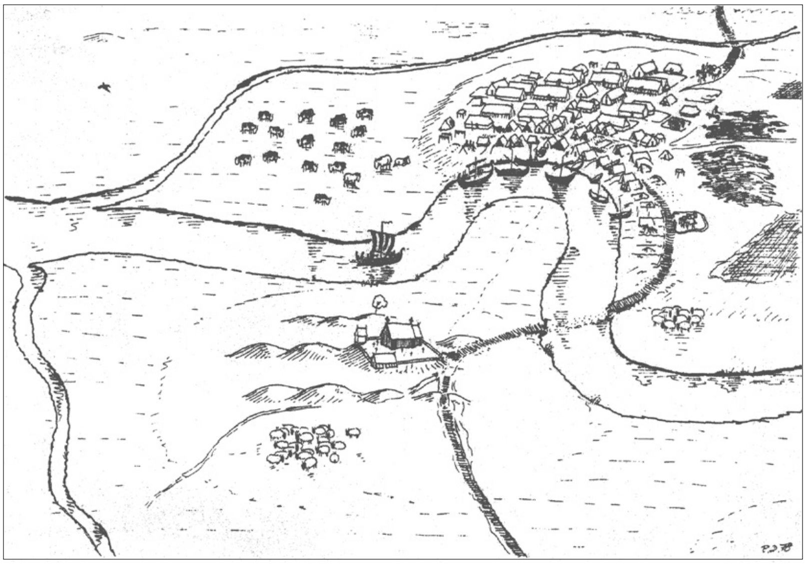

Figure 1-3: Drawings showing Ribe during the 9th century (Peter Dragsbo in BYGD, 1989).

The 12th century was the most dramatic period of development for Ribe. The Ribe Cathedral was erected. The medieval town expanded to the western side of the river which resulted in a kind of twin city with activities on both sides of the river. The town of Ribe developed during the next four centuries into the most important medieval North Sea port of the kingdom characterised to a high degree by its religious and political life as well as trade (Tougaard & Meesenburg, 1974). The principal trade of Ribe was the export of agricultural produce to Flanders, on the other hand import and sale comprised clothing and luxury articles (Ribe Tourist Office, 2004).

By the middle of the 17th century, the import and export activities slowed down and Ribe lost its economic importance. Trade had found other routes and new trading centres evolved in other places. Shipping on the river dramatically decreased and the river slowly sanded up.

Figure 1-4: The course of Ribe River in the year 1873 (Tougaard & Meesenburg, 1974).

In the middle of the 19th century increasing coal imports from England and timber exports from Norway held out hopes of a new period of profit-yielding trade. However, the conditions made loading and unloading of ships and prams difficult. The silting of the river and the increase in ship size enabled the turnover of goods only to a limited degree. In 1844, the Ribe harbour board decided to invest in the construction of a canal for the purpose of shortening the shipping way from the river mouth through the marsh towards Ribe town to three kilometres (see Figure 1-4). Due to lack of money, the second part of the canal project was not finished before 1918-19 (Tougaard & Meesenburg, 1974). As a result of this, the river course was clearly shortened and the distance that ships had to sail to get into Ribe town would have been much shorter, if the Ribe era of trade and shipping had not finally ended around 1900.

Since the first settlements along the periphery of a small market place, no sea defence system protected Ribe town against flooding during storms. The marsh area west of Ribe town was frequently flooded. During severe storms, the water even reached the town resulting in many casualties. Hence, settlements were erected further inland on higher dry land and the large marsh areas remained unsettled for many centuries. From 1911 to 1914 the Ribe dike was built – reaching from Vester Vedsted in the south to Tjæreborg in the north – including the construction of a sluice at the estuary of Ribe river and three smaller outlets.

During the following years, efforts were made to drain the marshland of agricultural activities and scattered settlements. Around 1966, after the severe storm surges in Holland in 1953 and in Germany in 1962, local policy makers began discussing the possible reinforcement of Ribe dike. The discussion was mainly driven by three factors (Ribe Amtsråd, 1966):

1. The existing profile of Ribe dike no longer corresponded with the state of knowledge at the time.
2. The storm surges of 1953 and 1962 had shown that even reliable dike constructions designed by experienced engineers could collapse under special load conditions.
3. The sea level rise.

However, the Ribe dike was not reinforced to its present safety level before 1978 - 1980. A detailed description of the dike geometry will be given in Chapter 4.

Today, Ribe town is the oldest and best preserved town in Denmark. The preservation of many old timber framed houses, which go back to the 17th century, was initiated by Ribe Tourist Association in 1899 in the hope of promoting the historical importance of Ribe as a tourist attraction. Today, the tourist association's hope has come true. About 1 million day-visitors visit Ribe every year, which has made tourism the most important economic source of revenue for Ribe town and its hinterland (personal communication with Ribe Tourist Office, 2003).

1.4 Contents of the report

Chapter 2 will provide a short literature review of risk handling and existing conceptual approaches, including risk assessment, risk analysis and risk management. Relevant definitions will be given and the concept of a probabilistic framework, including failure modes and fault trees, will be introduced.

Objectives and the methodology of the study will be specified in detail in Chapter 3. Furthermore, the chapter will present selected models and tools which have been applied in the study.

Chapter 4 will describe the calculation of failure probability of a number of failure mechanisms as well as the overall failure probability of the Ribe sea defence system. In order to calculate the overall failure probability, a detailed fault tree will be presented in the chapter explaining the correlations between the failure mechanisms. A detailed description of the methodology used in chapter 4 will be given in Chapter 3.

Chapter 5 will relate to the determination of the damage or loss associated with the occurrence of an inundation. A valuation of all elements at risk and their geographical position will be registered. The chapter will deal with damage functions which relate the damage to a risk element to an inundation depth. Dike breach scenarios will be set up in order to calculate the inundation behaviour in the flood-prone area. A more detailed description of the methodology used in Chapter 5 will be given in Chapter 3.

Finally, the flood risk for the Ribe flood unit will be assessed in Chapter 6 based on the results of the hazard analysis and the vulnerability analysis.

The report ends with a discussion on methodology and results, and recommendations for further work will be given.

2. Literature review of flood risk assessment

A short literature review of risk handling and natural hazards will be given in the following. This will comprise general definitions of terms and methodical approaches. A conceptual reflection on risk handling will be presented together with a more detailed explanation of risk analysis and risk assessment. Finally, an overview of some practicable methods and models to support the performance of a risk analysis will end Chapter 2.

2.1 Risks and natural hazards in coastal areas

The terms "risk" and "natural hazard" are keywords which are often heard in the media. A short discussion of the terms "risk" and "natural hazard" therefore seems reasonable, starting with a simple example.

Imagine two persons living in the same low-lying flood-prone area within the same distance to the sea. The property of person A is protected against flooding by a 2 m high ring dike surrounding his house. The house of person B is protected against flooding by a 4 m high ring dike.

The hazard of being exposed to a storm surge and a subsequent inundation of the low-lying coastal area in which they live is the same for both persons. However, the risk of getting his property flooded due to dike breach or wave overtopping is higher for person A than for person B because A's property is protected only by a 2 m high ring dike.

The term "risk" is often misused as a synonym for the term "hazard" (Reese, 2003). Hazard is defined as natural or man-made processes or events with the potential to result in harm. However, a hazard may not necessarily lead to harm. Hence, natural hazards in coastal areas are extreme natural events (storm surges) of a specific intensity in a specific area, which may result in danger to individuals, property and infrastructure (Reese, 2003). The systematic process of identifying events, situations or actions with the potential to result in danger to human life and property in a specific area is carried out through a hazard analysis. It determines the combination of the intensity and probability of a specific hazardous event or situation. The practical implementation of a hazard analysis will be explained in Chapter 2.3.

Returning to the example mentioned above, risk includes the feature of impact or consequence due to the hazardous event: Getting their property flooded due to dike breach or wave overtopping during a storm surge. Risk is hence a combination of a hazard in a specific area – characterised by intensity and probability – and the consequences that this hazard may have if it occurs (see e.g. Reese, 2003; DEFRA, 2002).

Furthermore, the example comprises the aspect of failure or collapse of a construction, namely the persons' ring dike surrounding their property. Thus, in this case the magnitude of the consequences depends on the failure or collapse of both persons' defence construction (dike ring) protecting them against flooding. Therefore, the assessment of risk also includes the failure and/or collapse of the defence system. Although the two terms of failure and collapse are commonly used as having almost identical meanings, there is a clear distinction (CUR, 1990). The term "failure" relates to the principal functions of the construction. This way, a dike fails if it can no longer prevent inundation of a protected area. The term "collapse" relates to the construction itself. If the dike undergoes deformations of such magnitude that the original geometry and integrity is lost, the dike collapses (CUR, 1990). In general, the collapse of the construction is attended by an increased failure probability of the construction. The construction may collapse without losing its main functions, e.g. en-bloc-slide on the seaward slope. However, the opposite may occur, too. In the event of wave overtopping the dike fails without necessarily collapsing. For reasons of simplification, the term "failure" will be used in the following for both "failure" and "collapse". However, Chapter 4 will show that both definitions of "failure" and "collapse" must be considered when assessing the risk of a coastal defence system.

The expected consequences of a failure event may be desirable or undesirable. The engineering discipline of flood protection is, however, mainly focused on the prevention of inundation to protect society against loss of life or injury and financial losses. Normally, the consequences are estimated by assessing the potential damage of a number of risk elements (i.e. buildings, household goods, livestock, agricultural areas) in a specific area. A major difficulty in estimating consequences is how to compare direct financial losses at risk elements (building damage, production losses), indirect losses (impact on economic growth, unemployment) and non-monetary losses like loss of human life or injury. In many cases, the consequences of a failure event are therefore often only described through direct damage where the monetary value of risk elements can be sufficiently assessed.

The systematic approach used to assess the potential damage to risk elements in a specific area is defined as a vulnerability analysis. In Chapter 2.5, the practical implementation of a vulnerability analysis will be explained.

Finally, to determine persons A and B's risk of getting their property flooded, natural hazards, failure events and the consequences have to be assessed. In a mathematical formula, the risk R is determined by multiplying the probability P_f of a failure event by the expected consequences E(D) that this event will have (see e.g. Kortenhaus & Oumeraci, 2002; Faber & Stewart, 2003):

$$R = P_f \times E(D) \qquad \text{(Eq. 1)}$$

2.2 Conceptual reflection on risk handling

In general, risk handling aims at a judgment of whether an engineering system satisfies the requirements of society with regard to safety and economy. Concepts of risk analysis are in fact multidisciplinary engineering fields which have entered various engineering application areas, such as nuclear power, dam engineering or bridge construction. Different methodologies and concepts of risk handling have been compiled. However, these concepts are often characterised by a high degree of complexity. Moreover, the concepts comprise interdisciplinary approaches which intend to involve different interest groups such as scientists, policymakers and the public, each having an individual understanding of risk handling. The task of compiling standardized concepts of risk handling is therefore quite difficult. Since the 1980s, Germany has made an attempt to standardise concepts and methodologies for the handling of natural hazards and the correlated risk. However, this attempt has only had little success so far (Reese, 2003).

In the field of flood protection and flood risk a number of aspects are of interest:

- The danger and probability that the public will be harmed or killed by flooding.
- The intensity and probability of damage to property and infrastructure.
- The intensity, depth and duration of flooding.
- The frequency of different locations in the potential flood area to be flooded in return, taking account of the failure probability of the defence system and geographical circumstances of the potential flood area.
- The degree of risk inherent in each defence structure, i.e. the predicted annual consequences of failure of the defence structure.
- Scenarios, i.e. considering the effect of sea level rises or changes in the frequency and intensity of storms.

Due to the aspects mentioned above and the idea of harmonising design and safety standards in various engineering disciplines, conceptual frameworks for handling the risk of flooding have been recently published (see e.g. Reese, 2003; Oumeraci, 2001; Oumeraci & Kortenhaus, 2002). The comparison of the concepts shows a generic approach to risk handling, including the following elements: risk analysis, risk evaluation and risk management (see Figure 2-1).

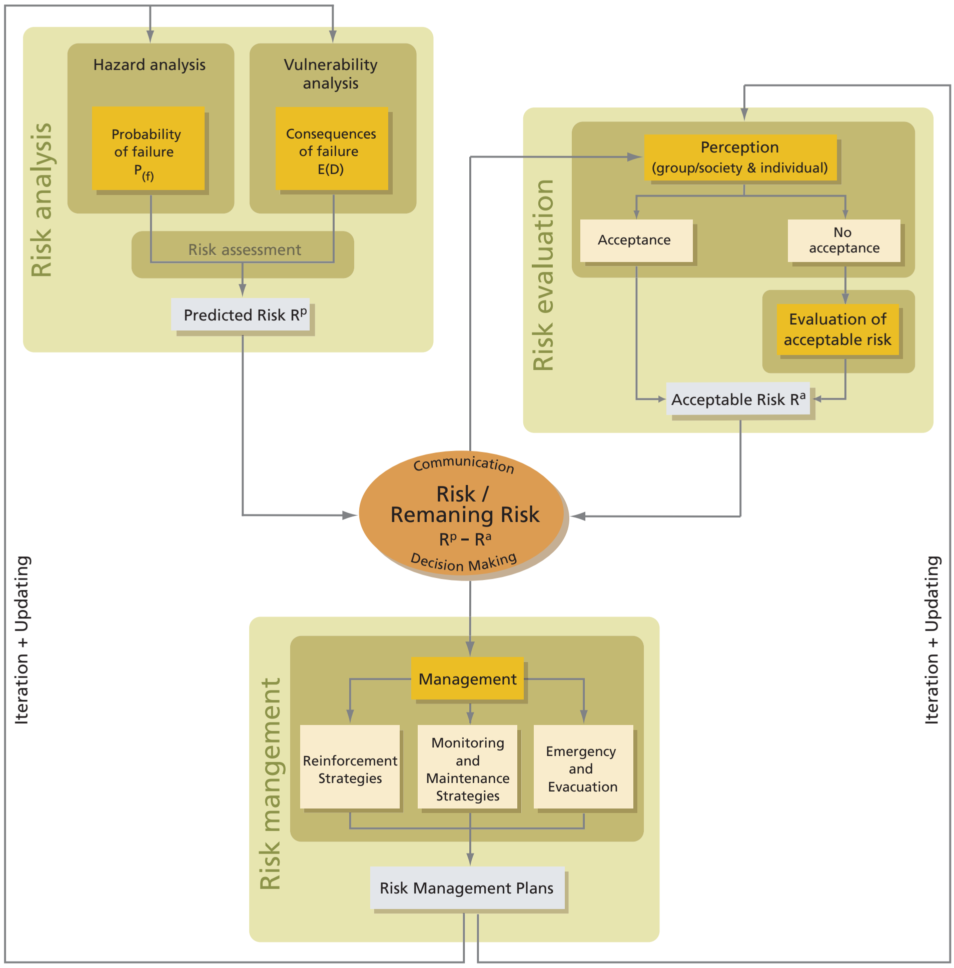

Figure 2-1: Conceptual risk handling structure.

Risk Analysis

By performing a risk analysis, the specific risk of e.g. coastal flooding is determined. Risk analysis involves both hazard assessment and vulnerability assessment. The objective of analysing the hazard is the prediction of the flood probability, which either means a functional failure (e.g. wave overtopping) or a structural failure of the defence system (dike breach). The social-economic consequences of flooding due to e.g. a dike breach are determined by means of a vulnerability analysis. In a vulnerability analysis the potential damage and costs of flooding in a specific area are assessed. In order to determine the potential damage, potential risk elements have to be evaluated. The specific risk is finally calculated through a risk assessment where the probability of flooding is multiplied by the vulnerability figure. The wide variety of uncertainties in calculating the flood risk has to be addressed explicitly in the analysis (Oumeraci & Kortenhaus, 2002). This is further dealt with in Chapter 2.3 together with a more detailed explanation of risk analysis.

This way, risk analysis aims at answering the following questions:

- Which structures in a defence system can fail during a storm surge?
- How will each structure fail?
- What is the probability of failure?
- If the defence system fails, what are the consequences?

Risk Evaluation

The specific risk calculated in the previous analytical approach leads to the subsequent part of risk evaluation. Intuitively it may be assumed that risks with the same numerical value are perceived as being equal, but this is often not the case. In some cases, the significance of a risk is assessed by multiplying the probability by the consequences. In other cases it is important to understand the nature of the risk, distinguishing between rare catastrophic events and more frequent but less severe events (DEFRA, 2002). Moreover, many other factors influence society and individuals in the process of risk perception. When considering the evaluation of flood risk, not only the numerical value of the probability multiplied by the vulnerability is important, but it is also important how the risk will be perceived by society or the individual. Therefore, the first objective of a risk evaluation is to study the perception of a specific risk.

When determining the perception and acceptability of a flood risk it is distinguished between society (or group) risk and individual risk (Vrijling, 1984 in Kortenhaus & Oumeraci, 2002; CUR, 1990; DEFRA, 2002). A hazard can affect whole groups of people or properties, for example all inhabitants and their property in a flood-prone area. The evaluation of a risk in this case includes the judgement of whether the predicted risk is sufficiently low for this group/society. On the other hand, a particular inhabitant in the flood-prone area may be at risk due to his location and other circumstances, as e.g. person A compared to person B (see example in Chapter 2.1). Furthermore, individual interests, experiences, know-how and awareness play an important role in the evaluation of the risk which can either lead to aversion or acceptance. However, the evaluation of both group risks and individual risks can result in different perceptions of the predicted risk.

Aversion arises if the perception of risk crosses an individual or societal risk level, beyond which the risk is deemed unacceptable. Below this level a higher risk is accepted, however, a risk reduction would be desirable (Reese, 2003).

Aversion of flood risk leads to the second objective of a risk evaluation: The determination of an acceptable flood risk for a specific area. According to Oumeraci (2001), the ALARP principle (As Low As Reasonably Practicable) is a widely accepted concept for the evaluation of an acceptable risk across most engineering disciplines. Within the field of flood and coastal defence, decision-making typically takes place based on the ALARP principles (DEFRA, 2002). It includes techniques and tools like Cost-Benefit Analysis, Reliability Analysis and Multi-Criteria Decision Theory (Oumeraci, 2001). Acceptance criteria for the failure probability of the flood system and for the potential damage have to be defined. Comparable to the calculated predicted risk, the acceptable flood risk is defined as the product of the acceptable failure probability and the acceptable damage. Again, as mentioned above, it is noteworthy that the tolerability of a risk may depend on the nature of the event. Normally, frequent events with a low impact are more tolerable than low-frequency catastrophic events.

The evaluation of an acceptable flood risk allows for further consideration of scenarios of e.g. different sea level rises. This way the acceptable risk may not only be calculated for the present moment but also for different future scenarios.

In case of a broadly accepted risk determined by a risk analysis, no further approach for evaluating an acceptable risk is needed. However, the risk management has to ensure that the risk remains at this level by maintaining the flood defence system.

This way, risk evaluation aims at answering the following questions:

- How is the predicted risk perceived individually?
- Is the calculated risk accepted or not – personally and socially?
- Which facts and conditions play an important role in the process of perception and evaluation?
- What criteria are important for defining an acceptable risk?

Risk management

Based on the results derived from risk analysis and risk evaluation, the handling of the risk can be facilitated by means of management procedures. In general, the predicted risk and the acceptable risk will not be equal. Through comparison of the predicted risk and the acceptable risk, the remaining risk is determined. Ideally, the determined remaining risk leads to the definition of tools and strategies in order to manage the remaining risk in practice. However, the definition of management tools and strategies includes not only technical measures but also economic and political measures. Risk management therefore comprises administrative, technical and political strategies which are translated into concrete measures, e.g. reinforcement, monitoring and maintenance, compensation payments or evacuation plans, through risk management plans (see also Oumeraci, 2001).

This way, risk management aims at answering the following questions:

- How great is the remaining risk?
- How can the remaining risk be managed?
- What are the consequences of today's management decisions for future opportunities with regard to efficient flood protection?

Moreover, risk management is one of the key features in risk handling. The risk management can as the integral part make decisions on the methodology of risk analysis and risk evaluation. It includes the iterative process of monitoring and updating risk analysis and/or risk evaluation (see Figure 2-1). Together with the iterative process of monitoring and updating, communication plays an important role, especially in the decision-making phase. Here, the question of a remaining risk will lead the discussion about appropriate management strategies. Figure 2-2 shows the decision-making process regarding the remaining risk at a flood defence system.

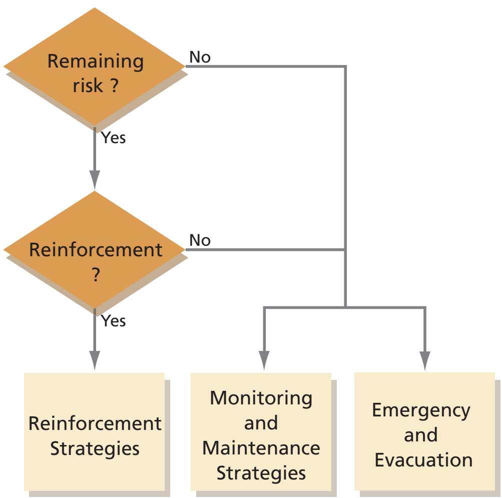

Figure 2-2: Decision-making on the remaining risk regarding a flood defence system.

Furthermore, in the decision-making process insufficient communication can lead to confusion as coastal defence agencies, government and local authorities are promoting or using different descriptions of risk for different purposes. The clear communication to all involved players and stakeholders of a consistent framework for risk handling is therefore indispensable.

The objective of such a conceptual structure is to promote and enable consistent approaches to assess and communicate the risk of flooding. These approaches analyse and describe the defence system as a whole, incorporating the various uncertainties in the assessment of the safety of the defence system. Moreover, it is possible to take explicit account of the cost of damage or loss expectation in the specific area as well as the cost of improving the defence system (CUR, 1990). This way, these approaches enable the politicians to obtain a clearer conception of the defence system and its safety function which should help bridge the gap between technical and non-technical decision-makers (Oumeraci & Kortenhaus, 2002).

On the other hand, Kortenhaus (2003) mentions the disadvantages of probabilistic concepts of risk handling which are e.g. the non-acceptance of these concepts and the often insufficient database. Nevertheless, the application of probabilistic risk concepts has to be recommended in general.

2.3 Risk analysis and risk assessment

In general, the objective of designing a flood defence system is to obtain a construction with a sufficiently low failure probability during its whole service life. In order to achieve the best possible assessment of this probability, a risk analysis can be performed. Reese (2003) defines a risk analysis as a systematic, understandable and formal procedure to quantify the probability and intensity of a certain hazard and the subsequent possible consequences in a specific area in case of failure. Within this definition, the risk analysis is composed of two sub-analyses: the hazard analysis and the vulnerability analysis (see Figures 2-1 and 2-4). Risk assessment is a sub-process of the risk analysis in which the results of the hazard analysis and the vulnerability analysis are tied together. The result of the risk assessment is the predicted risk for a specific area (Reese, 2003).

The following Chapters 2.3.1 and 2.3.2 will explain the hazard analysis and the vulnerability analysis in detail. Figure 2-4 shows the general risk analysis procedure, including the analyses of hazard and vulnerability.

2.3.1 Hazard analysis

As already stated in Chapter 2.1, a hazard analysis is the systematic approach used to identify events, situations or actions with the potential to result in danger to human life and property in a specific area. In the field of coastal flood defence, the dike is an important structure preventing inundation of coastal areas. This fact has led to dike structures quite frequently being the object of hazard analyses during the last years (e.g. CUR, 1990; Meadowcroft et al., 1994; Oumeraci, 2001; Kortenhaus, 2003).

Looking at the design of a dike structure, it is often based on purely deterministic or quasi-deterministic approaches. The design criterion is a water level which is exceeded with a predetermined frequency (e.g. 1/200 years). The specified exceedance frequency of the design water level is normally interpreted as the failure probability of the dike, which again is equated with a flooding probability (Oumeraci, 2001). Moreover, the crest height of the dike is obtained by superimposing the design water level by a maximum wave run-up and a certain extra height in order to compensate especially for sea level rises. The extra height needed to cope with wave run-up and sea level rises is further considered to provide a substantial reserve of safety in the event of the design water level being exceeded. However, this reserve is not quantified (CUR, 1990).

Apart from the hydraulic boundary conditions and the cross-sectional profile, the geotechnical parameters (e.g. cohesion of sand and clay) play an important part in the stability calculation. However, in the present design practice geotechnical calculations are rarely applied.

Furthermore, deterministic approaches do not take account of uncertainties in data values or model functions. Figure 2-3 summarises the main sources of uncertainties.

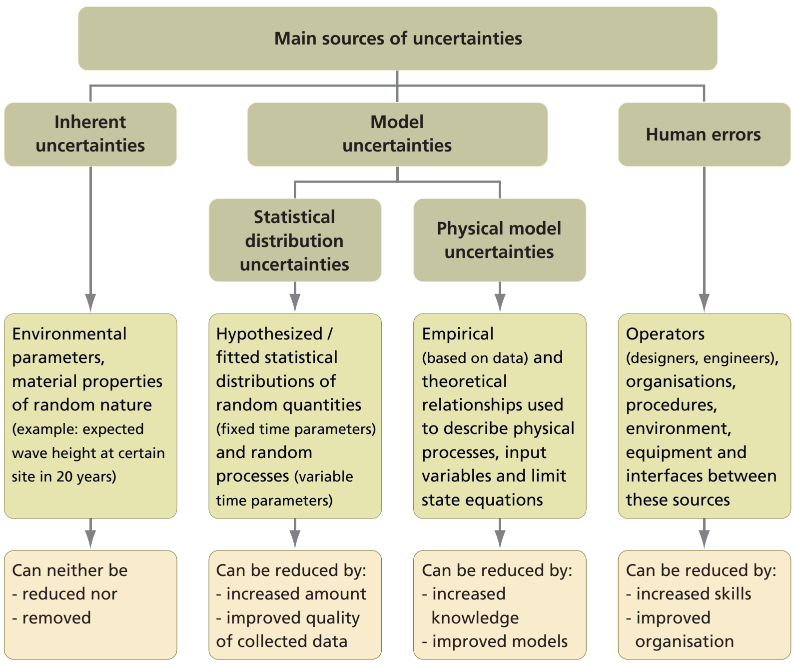

Figure 2-3: Main sources of uncertainties (adopted from Oumeraci, 2001).

Hence, Oumeraci (2001) concludes that deterministic approaches are too simplistic to be used as consistent and transparent design approaches for coastal flood defences, as it may for instance have the following consequences:

- that the water level during a storm surge exceeds the design water level without dike failure, because the dike may not necessarily fail when the design water level is exceeded. Too high and expensive dike constructions can be evaded.
- an incorrect analysis of the hazard because the dike may also fail even if the design water level is not being exceeded, leading to dike breach and subsequent flooding of the protected area.

However, the probabilistic methods embedded in a hazard analysis account for the uncertainties of the input parameters and the models which describe possible failure mechanisms of the dike. They take account of the lack of precise knowledge of the dike properties, the loading, and the response function. This is performed in a systematic and transparent manner.

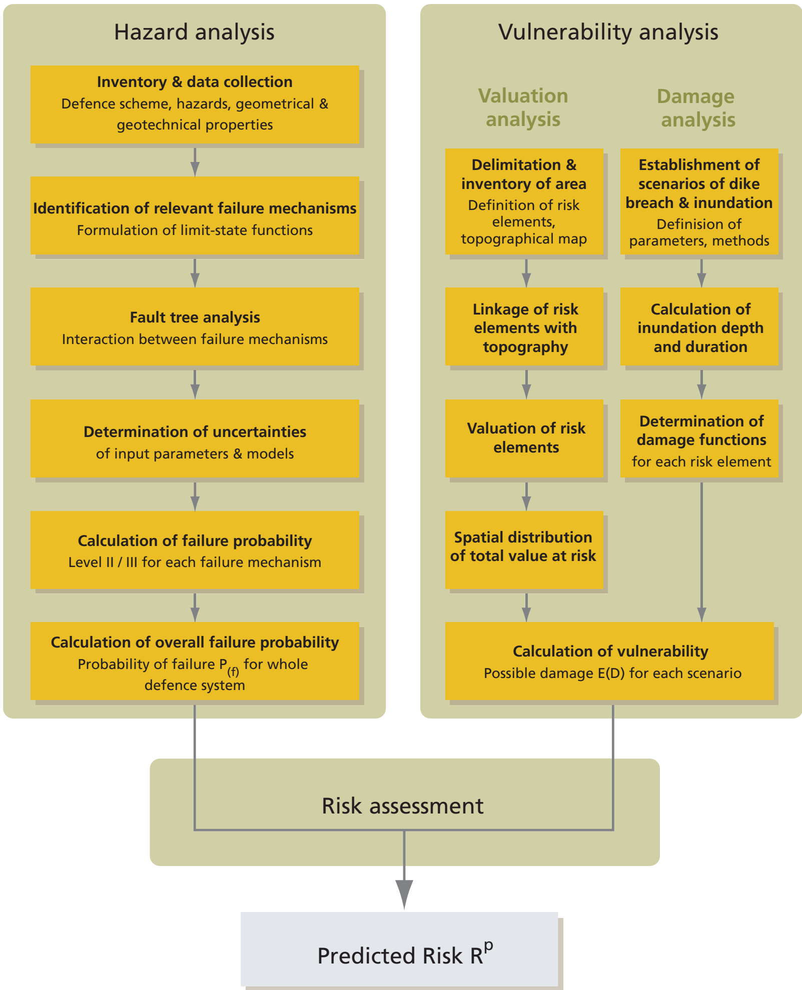

Figure 2-4: Risk analysis, including hazard and vulnerability analyses.

A hazard analysis begins with an inventory of the coastal defence scheme, including hydraulic boundary conditions, foreshore topography as well as geometrical and geotechnical properties (Figure 2-4). The geometrical description of the flood defence system is needed in cross-sectional representation and plan view representation due to the fact that coastal defence systems are composed of many components, e.g. dikes, dunes or sluices. The failure of one component may lead directly to failure of the whole system, as in the case of a serial system. In other cases components may compensate for one another (parallel systems) (CUR, 1990).

The hydraulic boundary conditions must be reliably assessed because small errors in hydraulic input parameters may lead to graver errors in the failure mechanisms' output, such as wave impact and wave overtopping. This comprises water levels and wave conditions in front of the defence structure. Two aspects are important in this connection:

1. The simultaneous occurrence of large waves and a high water level.

2. The transformations of waves propagating over a shallow foreshore.

In case of the first aspect, a number of authors propose a joint probability distribution of the hydraulic load variables (e.g. Oumeraci, 2001; Hawkes et al., 2002; Voortmann, 2003). The choice of variables for description of the joint probability distribution of hydraulic loads normally comprise water level, wave height and wave period due to a strong correlation between them. Over the years a number of methods for describing the joint probability distribution of long-term hydraulic boundary conditions have been introduced, which are listed in Voortman (2003).

Coastal defence systems are generally attacked by waves which have propagated over shallow foreshores with a complex morphology before reaching the main defence line.

The wave conditions just in front of the defence system are, however, important for determination of the system's loading by wave impact, wave run-up or wave overtopping. Therefore, the second aspect considers the wave transformation processes, including depth-limited wave breaking, wave reformation, etc. These processes and the subsequent changes in the wave height distribution have to be simulated in order to obtain the wave loading and its distribution just in front the defence system (Oumeraci, 2001).

Having determined the hydraulic boundary conditions as well as geometrical and geotechnical input parameters, the next step involves the systematic identification of all relevant failure mechanisms, see Figure 2-4. All failure mechanisms which most likely lead to the failure of the defence structure, including a suitable model to describe the failure, have to be defined. In the case of sea and estuary dikes, Schüttrumpf & Oumeraci (2002) have performed a detailed failure analysis, dividing all identified failure mechanisms into either an origin on the seaside, on the shoreward side or inside the sea dike. All failure mechanisms have to be described and arranged in logical order. Figure 2-5 shows an example for the seaward slope.

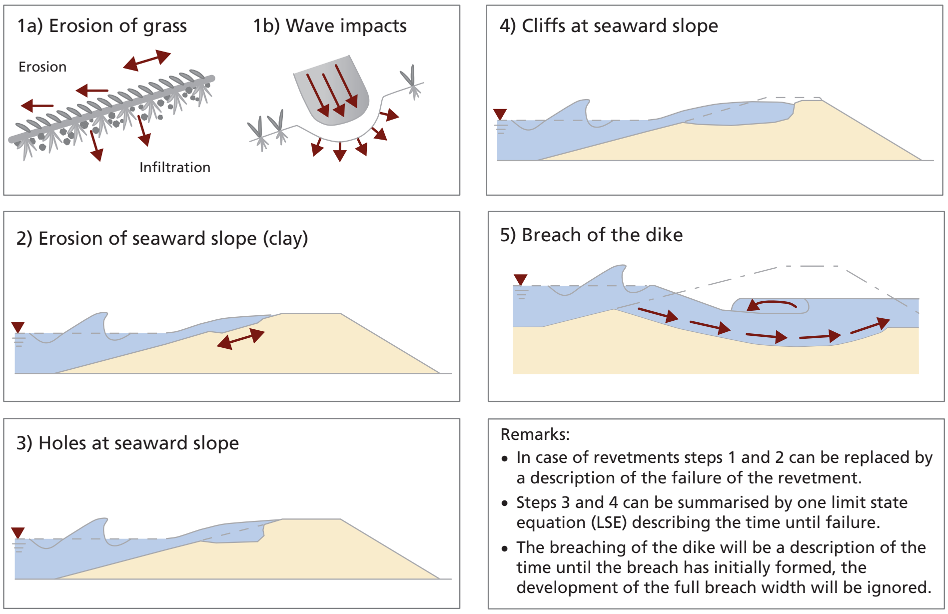

Figure 2-5: Failure mechanisms on the seaward slope (Kortenhaus et al., 2002).

In comparison to deterministic approaches, each failure mechanism needs a definition which can later be used in the probabilistic calculation. The "failure" is therefore expressed by the comparison of two quantities: the resistance term R and the stress term S. The boundary between failure and non-failure is generally called limit state. Thus, each failure mechanism has to be expressed as a limit state function (CUR, 1990; Kortenhaus et al., 2002):

$$Z = R - S \qquad \text{(Eq. 2)}$$

A negative value of Z corresponds to failure and a positive value to non-failure.

When identifying the failure mechanisms which lead to defence system failure, a spatial and temporal order of the failure mechanisms becomes noticeable. It begins with one failure mechanism initiating the next failure mechanism and so on, which eventually results in the overall failure (breach) of the defence system. A useful aid to establish an ordered pattern of all failure mechanisms can be obtained by a fault tree diagram (see Figure 2-6). A fault tree provides a graphic description of complex connections in a defence system, in which failure mechanisms are logically connected and initiated one after the other. The top event of the fault tree is defined as the flooding of the hinterland due to a dike breach or wave overtopping/overflow (CUR, 1990; Kortenhaus, 2003).

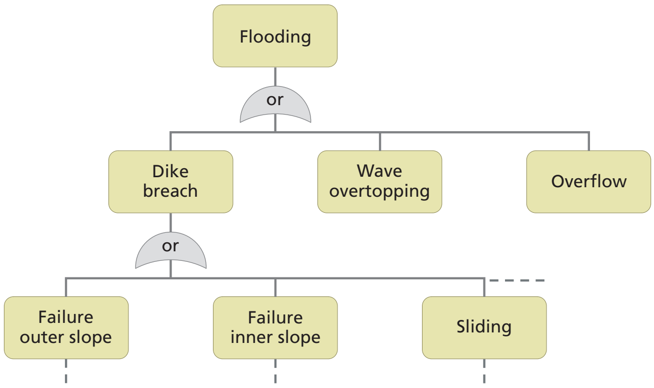

Figure 2-6: Example of a fault tree.

In order to describe the connections between the top event and the subordinated failure mechanisms, symbols such as AND/IF-gates and OR-gates are used in the fault tree (Kortenhaus, 2003). The symbols visualise the correlation between the failure mechanisms and the relative contribution to the overall failure of the defence system. Moreover, they define the mathematical manner in which the probability of a failure mechanism is calculated by subordinated failure probabilities.

The AND-gate corresponds to a parallel system. This means that all mechanisms aiming at this gate must be initiated before the gate is "open" and the failure mechanism ahead is initiated. The probability of initiating the failure mechanism ahead is calculated by multiplying the failure probabilities of all mechanisms at the gate.

In the case of an OR-gate, all mechanisms aiming at the gate are connected in series. This time, only one failure mechanism is needed to initiate the next failure mechanism. The probability for initiating the next failure mechanism is calculated by adding the probability values of the failure mechanisms at the gate. Similar to the OR-gate, Kortenhaus (2003) names an IF-gate. At an IF-gate all failure events are treated as comparable to an OR-gate, it means that only one failure mechanism is needed. However, an additional mechanism/event has to be initiated in order to initiate the next failure mechanism. The failure probability at an IF-gate is calculated in the same manner as for an AND-gate.

Having identified all relevant failure mechanisms, including the associated limit state functions, the uncertainties originated in the sources as shown in figure 2-3, must be quantified in the next step. For the probabilistic calculation, two types of uncertainties must be determined: the uncertainties (scattering) of the input parameters and the model uncertainties. The input parameter uncertainties have to be described by means of statistical distributions. In this connection, the description through the distribution density function is the most accurate way. The probability density function for a parameter provides a complete description of the parameter's probability characteristics. However, the density function is not always known. In this case, the density function of a parameter may be described by its mean (expected) value, standard deviation or coefficient of variation and the type of statistical distribution. Normally, a normal (Gaussian) distribution and a standard deviation based on engineering experiences are chosen as a parameter where no data or references from the literature are available (Kortenhaus et al., 2002).

The model uncertainty may be understood as the accuracy of the model describing a physical process/mechanism and the subsequent limit state function. The model uncertainty is normally quantified by a model factor, correcting the calculated result of the model. Thus, the model factor may be seen as the magnitude of corrections, which may be described by statistical distribution. Different approaches are available for determining the model factor, which are further explained by Kortenhaus (2003).

Finally, the probability calculations for a given failure mechanism defined by a limit state function and the related parameters (e.g. water level, crest height, angle of internal friction, etc.) can be performed. In reality, the calculation of the probability of failure of a flood defence system is a complex matter. For this reason it is necessary to have a computational basis for calculating the failure probability.

There are various methods available, which are classified into the following levels (CUR, 1990):

Level III: Comprises calculations in which the complete probability density functions of each parameter in the limit state function are introduced and a possibly non-linear character of the limit state function is exactly taken into account.

Level II: Comprises a number of approximate methods in which the limit state function is linearized and all probability density functions are replaced by probability density functions of normal distributions.

At level I calculations are based on characteristic values and partial safety factors or safety margins, which do not involve failure probabilities. Level I calculations have not been dealt with in this report. For further information about the different types of calculation, reference is made to Kortenhaus (2003) and CUR (1990).

At the end, the failure probabilities of all failure mechanisms are transferred to the fault tree. Based on the type of relationship (gate) between the failure mechanisms, the overall failure probability of the coastal defence system may be calculated.

A complete fault tree for the Ribe sea defence system and further information about the performance of a hazard analysis is provided in Chapter 4.

2.3.2 Vulnerability analysis

To carry out a risk analysis of flood defence systems it is furthermore necessary to know what consequences the failure of the defence system will have. Therefore, it is desirable to establish the relation between the undesirable event (dike breach) and the consequences.

When a flood defence system fails, water flows into the region which the system was intended to protect. In the great majority of cases, the area behind the defence system will be inundated. Only if the quantity of inflowing water is small (e.g. limited wave overtopping), so that it can be accommodated by pumping or by storage basins, no inundation will occur. If inundation occurs, it may have a variety of consequences. Voortman (2003) lists a few examples:

- casualties,
- fear and anxiety among people,
- loss of economic value due to material damage,
- direct damage at the flood defence system,
- loss of land (reversible/irreversible),
- loss of historical and cultural monuments,
- loss of natural and ecological values.

The variety of consequences prompts a classification of all types of damage. In general, it is distinguished between direct damage and indirect damage. Direct damage is defined as damage caused by contact with the flood water. Indirect damage is a consequence of direct damage. A second level of distinction can be made between monetary and non-monetary damage, also referred to as tangible and intangible damage (Reese, 2003). Smith and Ward (1998, in Reese, 2003) differentiate further between primary and secondary damage, considering causal connections in the categorisation of flood damage. Thus, primary damage results from the flooding itself. Secondary damage, however, is at least one causal step away from the event. The different types of damage due to flooding are presented in Figure 2-7.

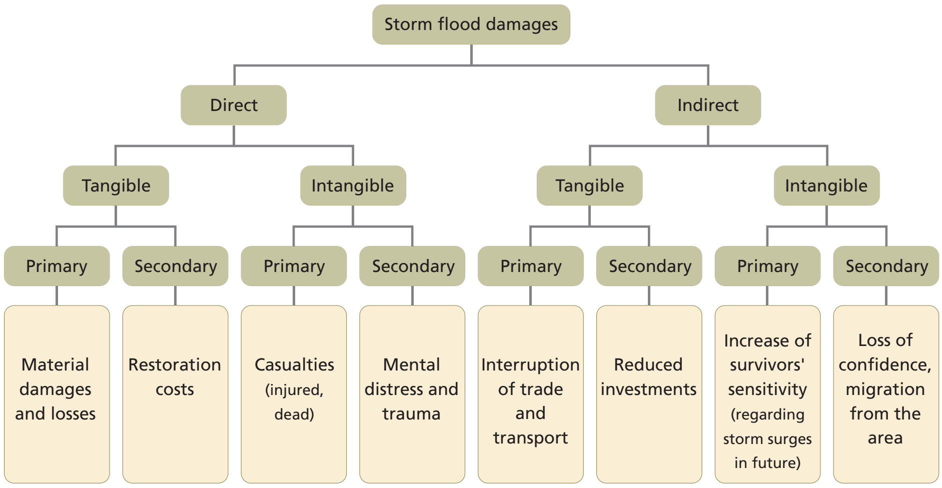

Figure 2-7: Classification of flood damage (adopted from Reese, 2003).

A vulnerability analysis conducted as part of a risk analysis is subdivided into a valuation analysis and a subsequent damage analysis (see Figure 2-4).

The valuation analysis assesses all endangered values which are supposed to be considered in the damage analysis. For this purpose, the valuation analysis starts with delimitation of the flood-prone area. Secondly, an inventory of all possible types of damage based on the classification in Figure 2-7 will define all elements at risk. Due to the complexity of valuating intangible damage, the vulnerability analysis considers usually only direct tangible damage, e.g. damage to buildings, infrastructure or agricultural areas. The valuation of human life has been subject to many discussions in the literature. A number of models have been developed, however, ethical aspects call the valuation of human life in question. Thus, possible casualties are often only qualitatively assessed. The same applies to some types of indirect intangible damage such as fear and distress among survivors or migration from the area due to loss of confidence.

After definition of all risk elements (Reese, 2003), each element has to be linked to the topography of the flood-prone area. The location and elevation of each risk element will be relevant in the subsequent damage analysis. A detailed GIS-supported topographical map of the affected area, including contour lines, is thus indispensable.

Moreover, the spatial distribution of material assets within the potential flooding area leads to the next step of valuating the assets. Frenkel and John (1999, in Reese, 2003) propose valuation of assets based either on initial costs, replacement costs or fixed costs. Initial costs represent the market price at the time of purchase. Replacement costs are defined as the market price on the day of valuation and represent the monetary value of replacement. Fixed costs relate to a basis year.

The valuation analysis ends with the spatial distribution of the total value of all risk elements within the possible flooding area. Information about spatial distribution of the total value is considered input for the following damage analysis.

Based on the results of the valuation analysis as well as the hazard analysis, different breach and flood scenarios are established. The scenarios form the basis for determining the inundation area and inundation behaviour. Very many parameters describe and influence the inundation process and the circumstances during inundation (CUR, 1990; Reese, 2003):

- type of event (e.g. dike breach, sluice failure, overtopping of greater magnitude)
- number and location of failure,
- time-dependent development of the breach (depth and width),
- time of failure,
- outer water level as a function of time,
- inner water level as a function of time,
- inflow volume,
- flow velocity,
- duration of inundation,
- water quality,
- size of the polder.

The purpose of the flood scenarios is to assess as precisely as possible the extension of inundation as well as depth and duration. The correlation of inflow volume and topography in order to determine the inundation depth can either be established by means of numerical modelling or "manual work" supported by GIS. The inundation duration depends chiefly on the water run off. A fast run off is only achievable above the breach threshold. Below the threshold level and especially in topographical hollows, the flood water will remain in the area for a longer period of time depending on the existing drainage and pumping capacity. Reese (2003) mentions an average water level drop rate of 8 cm/d.

Furthermore, the damage analysis comprises the definition of damage functions. A damage function describes the relationship between the inundation depth and the degree of destruction. For each risk element a damage function has to be deduced from data or from expert knowledge. At the end of the vulnerability analysis - combining the results from the valuation analysis and the damage analysis - stands the calculation of the possible damage depending on each scenario.

Chapter 5 deals with the vulnerability analysis for the Ribe sea defence system, including a valuation analysis and a damage analysis.

Finally, the results of the hazard analysis and the vulnerability analysis have to be linked together in order to obtain the predicted flood risk for a specific coastal area. This is performed through a risk assessment, which is the final formal step in the risk analysis.

Reese (2003) points out that the term of risk assessment is not uniformly used in the literature. However, he pleads for a methodical separation of calculating the risk from the previous analyses (hazard and vulnerability analyses).

Within risk assessment, the predicted risk is calculated by multiplying the overall failure probability by the vulnerability (see also Chapter 2.2). The calculated risk value corresponds to an annual expectation value of damage and is expressed as a monetary value per year.

2.4 Methods and models

In the following, an overview of existing methods and models used when performing a hazard analysis and/or a vulnerability analysis will be given. Methods and models have been partly presented at the COMRISK workshops. The overview does not claim completeness.

For the purpose of conducting a hazard analysis and determining the overall failure probability, two computer models are available: ProDeich and PC Ring.

ProDeich

ProDeich has been developed during a research project at the Leichtweiss Institute at the Technical University of Braunschweig (Kortenhaus & Oumeraci, 2002; Kortenhaus, 2003). The model allows the calculation of the failure probability of sea and estuary dikes.

It comprises 25 failure mechanisms and 87 input parameters. The number of failure mechanisms includes structural failure (breach of the dike) and non-structural failure, for example large overtopping without breaching. The description of all failure mechanisms, their interaction and the uncertainties are based on an extensive analysis of historical dike failure events. Missing or incomplete limit state functions of some of the failure mechanisms have been developed further and are integrated in the model.

The correlation in time (duration of a storm surge) has been considered when defining the limit state functions and the fault tree. So far the ProDeich model has been applied at typical non-existing sea and estuary dikes. In this connection, a detailed sensitivity analysis of input parameters, failure mechanisms, and uncertainties has been performed.

However, ProDeich is limited to calculating the overall failure probability by considering cross-sections of the defence system. The length effect and the division of the defence system into a number of sections are not included in the model at this time. Moreover, some of the failure mechanisms are only integrated in the model in a simplistic manner, because further research regarding the particular failure mechanisms has still to be carried out.

PC-Ring

In the Netherlands software called PC-Ring has been developed in order to calculate the failure probability of the Dutch 'dike rings' (Buijs, 2003). PC-Ring only calculates failure mechanisms concerned with structural failure. Buijs (2003) lists the following four failure mechanisms included in PC-Ring:

- Overtopping/running over causing erosion on and saturation of the shoreward slope.
- Instability of the shoreward slope.
- Piping.
- Damage of the revetment on the seaward slope.

The integrated statistical model in PC-Ring comprises a spatial correlation function and a model representing the correlation in time.

Moreover, in PC-Ring a number of models for different situations of hydraulic boundary conditions are incorporated. Further information about these models and PC-Ring in general are, however, not available at this time.

MERK

In the case of performing a vulnerability analysis, the Federal Department of Coastal Defence in Germany assigned to the Research and Technology Center a project to develop a transferable instrument for the handling of storm surge risks and risk assessment. The main focus of the MERK-project was a vulnerability analysis for selected lowlands along the German North Sea and Baltic Sea coasts.

The vulnerable tangible and intangible structures were identified and evaluated within the scope of a micro-scale valuation analysis. The micro-scale, object-orientated, approaches in the analysis has been beneficial because of their high accuracy and preciseness (MERK, 2002).

To determine the possible damage, tangible and intangible risk elements have been defined. Different flood scenarios and dike breach scenarios have been elaborated to realise the simulation of various flooding processes and the different associated scales of possible damage. To record the damage due to flooding at the objects itself, depth-damage models have been derived by expert interviews. The models are still theoretical and need a more profound analysis regarding practicable implementation. However, the methods developed within the scope of the MERK-project are of rational and transparent nature.

Information and decision-making tools

Due to the great demand for having all important data regarding the risk of flooding collected at one place, a number of countries in the North Sea region are working on developing tools to process all information about the probability of flooding as well as the associated damage.

In the United Kingdom operational tools to assess the values in coastal lowlands are under development. In Belgium a special research group called Hydrological Information Centre has been formed in order to secure a systematic approach and develop tools for water level management as well as to provide scientific support to policy-makers in Flanders.

Flood wave propagation

The modelling of flood wave propagation in a flood plain after a breach of the defence system may for example be performed by the MIKE FLOOD flood modelling package. MIKE FLOOD has been developed by DHI, Water & Environment, Denmark. The model consists of components taken from the models called MIKE 11 and MIKE 21. By exchanging simulation results with GIS applications, risk and flood maps can be drawn up.

3. Specification of objectives and methodology

The literature review in Chapter 2 showed that there is increased attention to risk-based design concepts within the field of coastal defence. The first models have been compiled to assist in the assessment of the risk of coastal flooding. The probabilistic methods on which these models are based allow consideration of the uncertainties of input parameters and describe possible failure mechanisms for various types of coastal structures.

General agreement is found in the literature about the definition of risk by multiplying the failure probability by the possible consequences. The structure of risk-based design concepts, however, differs slightly and there is a lack of consistent term definitions. The differences between the models are the number of failure mechanisms taken into consideration and the degree of specification for the set-up of a fault tree. However, the top event of hinterland flooding due to the failure of a defence system is concurrent for all models.

All in all, the literature contains a common pleading for and first approaches to the application of reliability and risk-based methods and models.

3.1 Objectives

As mentioned in Chapter 1.2, the main objective of the study in hand is to assess the risk of an existing sea defence system located at the Danish Wadden Sea coast. Risk is defined by multiplying the failure probability by the consequences, as described in the literature. The risk assessment will be based on the literature review and existing methods and procedures will thus be applied.

The objectives in detail are therefore as follows:

- the selection of appropriate methods and models in order to assess the risk of the Ribe sea defence system;
- the calculation of the overall failure probability of the defence system, including a sensitivity analysis of the overall results;
- the estimation of values and the damage in the protected area behind Ribe dike;

- the calculation of risk by multiplying the overall failure probability by the damage due to flooding.

The objective of performing a risk assessment for the Ribe sea defence system may be regarded as a starting point for the application of a reliability-based risk analysis on a feasibility level. The results will give insight into the high complexity of hydrodynamic and geotechnical processes at sea dikes as well as attract attention to the types of assets, which are located in the flood-prone area. Moreover, the understanding of the damage characteristics of individual assets due to the contact with floodwater will be improved.

3.2 Methodology

In general, the study will be performed in two major steps which comprise a hazard analysis of the flood defence system and a vulnerability analysis of the hinterland.

The hazard analysis aims at the calculation of the flooding probability for the Ribe defence system. For this reason, the ProDeich model has been chosen (see Chapter 2.4) due to the large number of failure mechanisms included, the detailed set-up of the fault tree and the transparent documentation in Kortenhaus (2003). Moreover, a cooperation agreement between the Leichtweiss-Institute and the Danish Coastal Authority has been concluded for the probabilistic calculations to be made by means of the ProDeich model.

Hazard analysis

The detailed procedure of performing the hazard analysis and calculating the overall flooding probability of the Ribe defence system is described in Figure 3-1.

At first, the defence system will be described in detail, including all relevant characteristic features. Due to the fact that the defence system is interrupted by one sluice and three outlets, the hazard analysis will also comprise probabilistic calculations of the sluice and the three outlets. Hence, a larger number of input parameters are needed to describe the defence system and its elements. The input parameters will be grouped into parameters describing (i) the geometry of the structure, (ii) the hydrodynamic boundary conditions and (iii) the geotechnical features of the Ribe defence system.

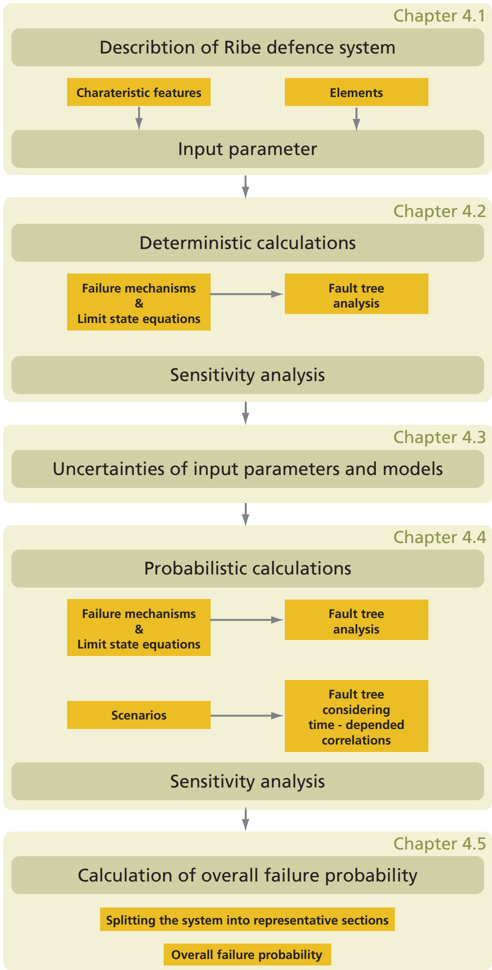

Figure 3-1: Procedure for performing the hazard analysis (according to Oumeraci et al., 2004).

Traditional deterministic design procedures form the basis of the probabilistic calculations in the ProDeich model. A detailed fault tree for the Ribe defence system will be presented comprising relevant failure mechanisms and related limit state equations. Based on the defined fault tree, deterministic computer calculations will be performed. The deterministic results will lead to a first selection of significant limit state functions, and a sensitivity analysis will be performed of the most important input parameters of the limit state function selected.

At the next step, the uncertainties of all input parameters and models embedded in the ProDeich model will be determined and discussed in detail.

After quantification of all uncertainties, probabilistic calculations will be performed based on the same fault tree and failure mechanisms as those used for the deterministic calculations. The calculations will consider at first the failure probability of individual sections. Furthermore, scenarios will be defined to consider the time-dependent correlation between the failure mechanisms at Ribe dike. This will result in a revised fault tree which will consider the time-dependent correlation between the failure mechanisms. Again, a sensitivity analysis will end the probabilistic calculations and make clear the most important input parameters and failure mechanisms for the calculation of the overall flooding probability.

Finally, the failure probabilities of each section of the system will be linked by an overall fault tree in order to determine the overall failure probability of the whole Ribe flood defence system.

Vulnerability analysis

The vulnerability analysis aims at the determination of the damage potential of the hinterland. To achieve this, the sub-division of the vulnerability analysis into a valuation analysis and a subsequent damage analysis is considered (see also Chapter 2.3.2). The detailed procedure of performing the vulnerability analysis is described in Figure 3-2, where the first three steps (Chapters 5.1 to 5.3) may refer to the valuation analysis and the remaining steps (Chapters 5.4 to 5.5) may refer to the damage analysis.

As in the hazard analysis, at first a detailed description and an inventory of the hinterland will be made after the flood-prone area has been delimited. According to Chapter 2.3.2, the inventory will be based on the types of damage – material/nonmaterial, direct/indirect, tangible/intangible damage – which will be selected for the valuation analysis. Due to the practicability of valuation and the available data/information, only direct and tangible flood damage will be considered in this study.

At the next step, data about the risk elements for the Ribe area will be requested at different national registers. A GIS application software will be set-up to handle all input data about the risk elements. In this study, the MapInfo software package will be used. At the same time, data about the topography of the flood-prone area will be input into the GIS program. Furthermore, each risk element will be geocoded. Geocoding is the process that assigns a latitude/longitude coordinate to the address of a risk element.

The following step deals with the actual valuation of the risk elements. For estimation of the different values, expert knowledge or information from the literature will be used. By means of the GIS program, the spatial distribution of the total value of the risk elements in the flood-prone area can be calculated.

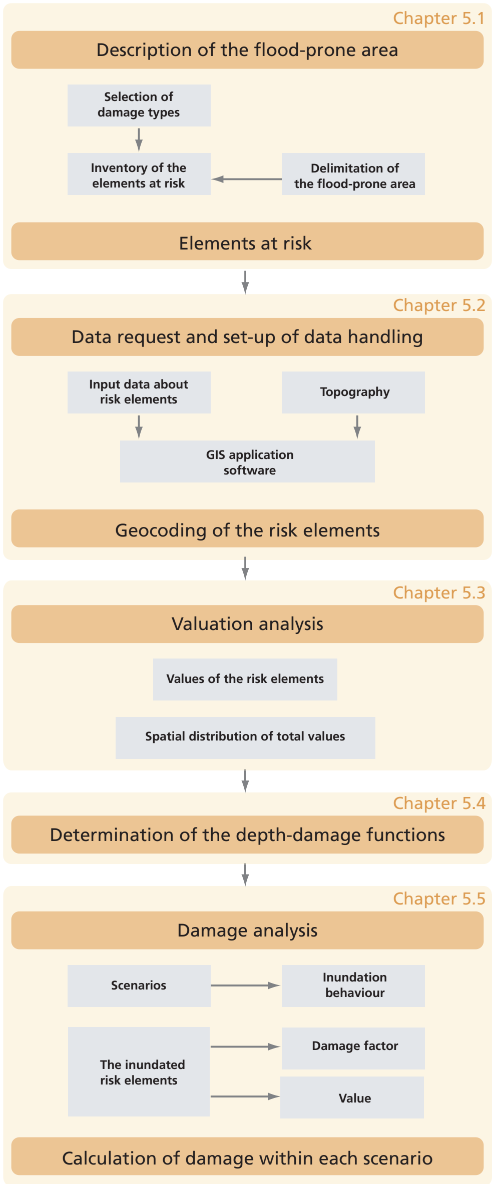

Figure 3-2: Procedure for performing the vulnerability analysis.

After having determined the values of the risk element and its spatial distribution, the question of the extent of the damage affecting each risk element in case of inundation will be dealt with. For this purpose, depth-damage functions will be determined by means of expert knowledge or information from literature. The depth-damage functions describe the damage to inundated risk elements in retation to the inundation depth.

The final step will deal with the assessment of the damage. For this purpose, dike failure scenarios (breaching or wave overtopping) will be defined which will result in different inundation events. The inundation characteristics such as extension, inundation depth and duration are simulated for each scenario. The simulation of inundation will be performed only in a manual way. Due to limited resources in this sub-project, a digital simulation by means of numerical computer software (see e.g. Chapter 2.4) is renounced. The manual assessment is here assumed to be a rough, but sufficient procedure to describe the inundation behaviour based on different breach and overtopping events. Based on the inundation characteristics, the inundated risk elements within each scenario will be selected by means of a GIS program. The results of the valuation (Chapter 5.3) and the depth-damage functions (Chapter 5.4) of each risk element will finally enable the calculation of the damage within each scenario.

Finally, in Chapter 6, the calculated overall flooding probability of the whole Ribe flood defence system will be multiplied by the scenario-dependent damage within a risk assessment in order to determine the risk of the Ribe flood defence system.

4. Hazard analysis and overall failure probability

The following chapter describes the calculation of the failure probability of a number of failure mechanisms as well as the determination of the overall flooding probability of the Ribe flood defence system.

4.1 Description of the Ribe defence system and input parameters for calculation

The Ribe flood defence system protects the town of Ribe which is surrounded by flat marshland against flooding. The dike line of the defence system consists of a 15,3 km long section which is directly exposed to the sea and therefore will be named 'the main dike' in the following. Together with a northern and southern wing dike, the total length of the Ribe dike is 18,6 km. The numbering of the dike stationing line begins at the southern end of the dike line.

Three streams and a large river, Ribe Å, cross the flat marshland on their way towards their mouths. The river flows through the town of Ribe and passes a sluice, named the Kammer sluice, shortly before it reaches its mouth. The three streams pass the dike through their outlets.

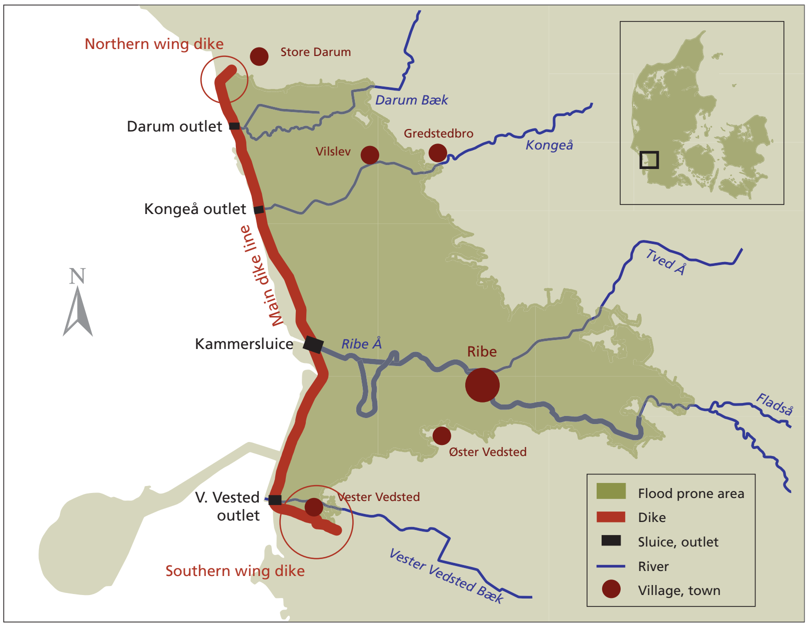

Figure 4-1: Map of the Ribe flood defence system.

The flood-prone area, which is protected by the defence system, comprises an area of about 95 km². Figure 4-1 provides an overview of the Ribe flood defence system and the accompanying flood-prone area.

As already mentioned in Chapter 1.3, Ribe dike was reinforced during the years of 1978 – 1980. The crown height was increased up to 7,0 m DNN[1]. A standard cross-section of Ribe dike and its key geometric parameters are shown in Figure 4-2.

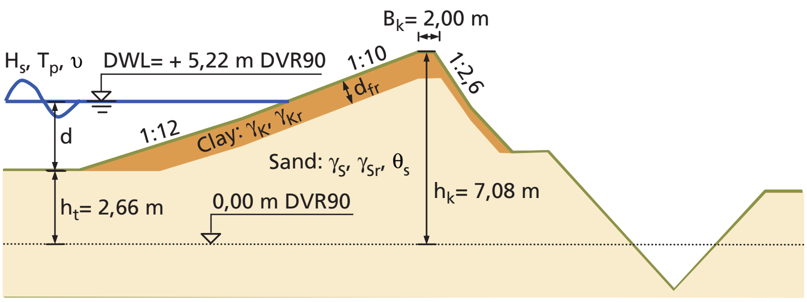

H_s = 1,51 m	d_{fr} = 1,0 m	c_u = 15,0 KN/m²
T_p = 4,89 s	γ_K = 17,0 KN/m³	d_G = 0,05 m
υ = 20 °	γ_{Kr} = 20,0 KN/m³	γ_S = 19,0 KN/m³
t_s = 6,5 h	c_s = 35,0 KN/m²	γ_{Sr} = 22,0 KN/m³
d = 2,65 m	c_{ss} = 10,0 KN/m²	θ_s = 40,0 °

Figure 4-2: Standard cross-section of Ribe dike (km 6,644 as an example).

At the shoreward side of the dike, an emergency road and a drainage channel separate the dike from the marshland. There are 17 ramps in total, and two of them provide access to the Wadden Sea island of Mandø. All other ramps are used for access to the sea area for repair and maintenance work.

The Kammer sluice and the three outlets interrupt the dike line. The Kammer sluice is located in km 8,470. A major outlet for the river called Konge Å (km 13,450) and a smaller outlet at Darum (km 14,800) are located in the northern part of the dike line. In the southern part, the third outlet is located close to Vester Vedsted (km 2,890). These structures are described in more detail in the following.

The Kammer sluice controls the discharge of the river of Ribe and serves as a sluice for small yachts and boats. The sluice was constructed concurrently with the construction of the dike from 1911 to 1914. The sluice walls with a top height of 5,88 m DVR90 are made of bricks. The bottom of the sluice is made of 0,2 m thick bricks and is located in a height of -3,60 m DVR90. The two-winged 5,0 m wide outer sluice gates are made of steel and reach a height of 5,78 m DVR90. Figure 4-3 shows the cross-section of the Kammer sluice.

[1] DNN stands for the old Danish reference level »Dansk Normal Nul«. Since May 2002, the new Danish reference system »DVR90« has been in force. The following applies to DVR90: DVR90 = DNN – 0,12 m. In the following, all heights are based on DVR90.

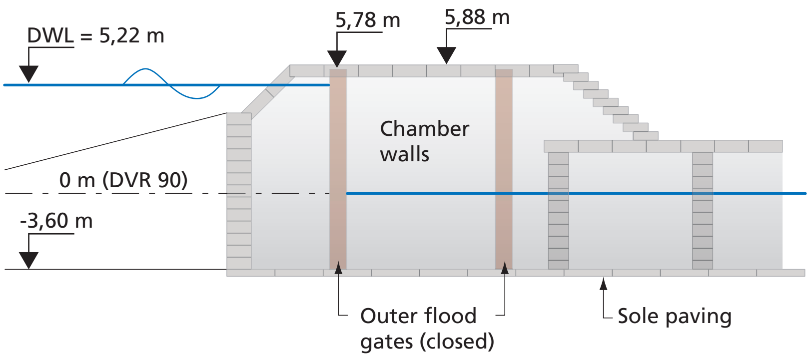

Figure 4-3: The cross-section of the Kammer sluice (according to Oumeraci et al., 2004).

The gates close automatically at a certain outer water level. In case of a power failure (the gate motors are powered by the public power supply), the gates can be operated manually. The inner sluice gates (storm gates) are not motor-operated, but will be closed manually if needed.

At the Konge Å outlet (see Figure 4-4), the Konge Å flows through 5 outlet channels, each having a width of 4,0 m and a height of 4,60 m. The gates of the outlet channels close automatically in case of a raising outer water level. Additionally, an emergency (storm) gate has been provided for each of the channels.

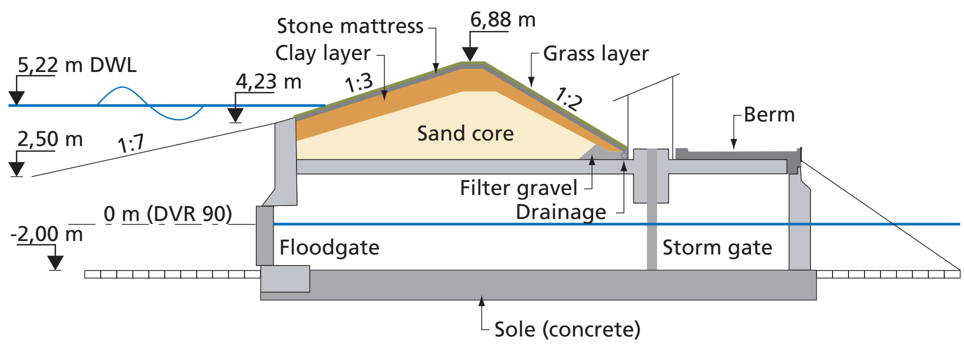

Figure 4-4: The cross-section of the Konge Å outlet (according to Oumeraci et al., 2004).

The outlet channels, including the bottom, are made of concrete. On top of the concrete construction part a dike core is placed which is made of sand. The sand body is covered by a clay layer of 1,0 m on the seaward slope and 0,5 m on the shoreward slope respectively. On top of the clay layer, there is a 0,23 m thick stone mattress lying on a filter textile. At the shoreward toe, the dike is drained by a 110 mm large filter tube embedded in filter gravel. The seaward slope is 1:3, the landward slope is 1:2. The crown height is at 6,88 m DVR90.

The Vester Vedstedt and Darum outlets (see Figure 4-1) generally have similar construction characteristics apart from having only one outlet channel. The outer gates at Vester Vedstedt and Darum consist of automatically closing gates. The dike cross-sections are identical to the description of the Konge Å outlet.

For the deterministic and probabilistic calculations, the method applied by Kortenhaus (2003) is used. For this purpose, an overall number of 87 input parameters are necessary. In order to keep track of it, the input parameters have been grouped into geometrical parameters, hydrodynamic parameters and geotechnical parameters.

Geometrical parameters

Geometrical input parameters are available for six cross-sections along the main dike line. The selection of cross-sections resulted from settlement investigations in 1998 performed by the Danish Coastal Authority (DCA). These investigations were based on measurements of crown heights from different years. In the resulting report, the selected cross-sections were regarded as the weakest points of the main dike.

Thus, it was concluded that analysing these profiles should include the potential weak spots of the dike. In addition, the selection of the cross-sections should represent both the northern and southern parts of the main dike such that the whole dike system would be sufficiently represented. The six selected cross-sections are located at:

km 3,156	km 6,644
km 8,422	km 9,400
km 10,403	km 14,499

In order to use the cross-sections, the measured profiles from surveys need to be assigned to the input parameters of the design formulae. These formulae require idealised cross-sections based on geometric parameters. One of the key simplifications needed is for example the use of a single value for the seaward slope of the dike.

The dimensions and the constructional details of the sluice and the outlets were taken from technical drawings which were made available by the DCA. All six cross-sections are illustrated in more detail in Appendix A, including the cross-sections of the dike, key input parameters as well as two photos of the respective location. All geometrical input parameters required for the calculations are listed in Appendix B.

Geotechnical parameters

All geotechnical parameters, like the shear strength of clay, have been predefined by the DCA. This information is based on geotechnical investigations which were performed close to the six cross-sections during reinforcement works from 1978 to1980. For the Ribe sluice and the outlets, the geotechnical parameters of the nearby dike cross-sections are used. All geotechnical input parameters are listed in Appendix B.

Hydrodynamic parameters

The design water level for all cross-sections, the sluice and the outlets at the Ribe defence system has been determined by extreme water level statistics for a pre-described 200-year return period. The design water level is defined as h_W = 5,22 m DVR90.

The input parameters for wave height and wave period result from a study performed by DHI, Water & Environment, Denmark (DHI). In 1998, the DCA commissioned DHI to undertake a detailed numerical study in which the hydrodynamic parameters along the Danish Wadden Sea coastline were simulated. The offshore input parameters for this study were given by the DCA. Altogether, 21 simulations with different input parameters were performed. The results of the numerical study are stated as the wave height H_{m0} and the wave period T_m for specific points with a distance of 100 m in between the points along the coastline as well as a distance to the toe of the dike of 50 m and 300 m respectively.

Angles of wave attack are based on instructions given by the DCA and correspond to the angles of wave attack used in the numerical study by DHI. The angles of wave attack represent the most unfavourable conditions for the specific cross-sections. The duration of storm surge is defined as constant for the defence system through calculations where t_s = 6,5 h. All hydrodynamic input parameters required are presented in Appendix B.

The range of selected parameters for all six cross-sections is presented in Table 4-1. The first column contains a description of the parameter, the second column states the units, the third column contains the parameter abbreviation used in this document and in the software, and the last two columns provide information on the minimum and maximum values of the parameters which are input into the software regarding all six cross-sections.

It can be seen from Table 4-1 that the geometric parameters vary the most, e.g. the crown height h_k and the foreland height h_t, which consequently results in large variations in the water depth d at the dike toe and the freeboard R_c. The wave height H_s differs up to 0,2 m over the total length of the main dike line. The wave period Tp varies within a range of 0,80 s. On the other hand, most of the values of the geotechnical parameters are of the same magnitude.

The most important input parameters for the Kammer sluice and the outlets are stated in Table 4-2. The table structure of Table 4-2 is identical to Table 4-1. In addition, some lines of Table 4-2 are shaded in grey indicating that these values are only required for the outlets but not for the sluice.

Description	Dim.	Parameter	Min.	Max.
Geometrical parameter				
Height of water level in front of dike	[m]	hw	5,22	5,22
Height of toe protection in front of dike	[m]	ht	1,92	2,66
Seaward slope below berm	[-]	mo	9,30	20,00
Seaward slope above berm	[-]	mb	8,00	12,00
Height of crown	[m]	hk	6,65	7,08
Freeboard	[m]	Rc	1,43	1,86
Width of crown	[m]	Bk	2,00	10,50
Shoreward slope above berm	[-]	mbb	2,30	3,10
Shoreward slope below berm	[-]	mbo	2,70	9,70
Wave parameter				
Water level in front of dike	[m]	d	2,56	3,30
significant wave height at toe of dike	[m]	Hs	1,45	1,65
Peak wave period	[s]	Tp	4,07	4,89
Angle of wave attack at toe of dike (0° = perpendicular)	[°]	theta	0,00	20,00
Storm surge duration	[h]	ts	6,50	6,50
Geotechnical parameter				
Thickness of clay cover seaward slope	[m]	dfr	1,00	1,00
Thickness of clay cover shoreward slope	[m]	db	0,50	0,50
Thickness of clay cover at crown	[m]	dcr	1,00	1,00
Specific weight of clay at crown	[kN/m³]	gK	17,00	17,00
Specific weight of saturated clay at crown	[kN/m³]	gKr	20,00	20,00
Cohesion	[kN/m²]	c_s	35,00	35,00
Virtual cohesion in sand	[kN/m²]	c_ss	10,00	10,00
undrained shear strength	[kN/m²]	c_u	15,00	15,00
Clay part in sand (results in cohesion of sand)	[%]	pK	18,00	18,00
Clay quality (0 = poor clay; 1 = good clay)	[-]	qc	0,40	0,80
Thickness of grass cover	[m]	dG	0,05	0,05
Grass quality (0 = poor grass; 1 = good grass)	[-]	qG	0,70	0,70
Specific weight of sand	[kN/m³]	gS	19,00	19,00
Specific weight of saturated sand	[kN/m³]	gSr	22,00	22,00
inner friction angle of sand	[°]	phi_s	40,00	40,00

Table 4-1: Range of values for selected input parameters of all cross-sections.

Table 4-2 shows that the crown heights of the sluice and outlets together with the water depth in front of the structures vary the most. A total overview of all input parameters for sluice and outlets is presented in Appendix B.

Description	Dim.	Parameter	Min.	Max.
Geometrische Parameter				
Height of water level in front of structure	[m]	hw	5,22	5,22
Height of river bottom in front of structure	[m]	ht	-2,60	-2,27
Seaward slope	[-]	mo	3,00	3,00
Height of dike toe	[m]	hbfr	4,18	4,35
Water depth at toe of dike	[m]	dh	0,87	1,04
Height of crown / of sluice gates	[m]	hk	5,78	6,88
Freeboard	[m]	Rc	0,56	1,66
Width of crown	[m]	Bk	1,00	1,50
Shoreward slope above berm	[-]	mbb	2,00	2,40
Width of shoreward berm	[m]	Bbb	0,00	0,00
Height of shoreward berm	[m]	hbb	4,87	5,01
Shoreward slope below berm	[-]	mbo	2,00	2,40
Wave parameter				
Water level in front of structure	[m]	d	7,49	7,82
significant wave height at toe of structure	[m]	Hs	1,59	1,65
Angle of wave attack at toe of dike (0° = perpendicular)	[°]	theta	0,00	20,00
Storm surge duration	[h]	ts	6,50	6,50
Geotechnical parameter				
Thickness of clay cover seaward slope	[m]	dfr	1,00	1,00
Thickness of clay cover shoreward slope	[m]	db	0,50	0,50
Thickness of clay cover at crown	[m]	dcr	1,00	1,00
Specific weight of clay at crown	[kN/m^3]	gK	17,00	17,00
Specific weight of saturated clay at crown	[kN/m^3]	gKr	20,00	20,00
Cohesion	[kN/m^2]	c_s	35,00	35,00
Virtual cohesion in sand	[kN/m^2]	c_ss	10,00	10,00
undrained shear strength	[kN/m^2]	c_u	15,00	15,00
Clay part in sand (results in cohesion of sand)	[%]	pK	18,00	18,00
Clay quality (0 = poor clay; 1 = good clay)	[-]	qc	0,60	0,80
Thickness of grass cover	[m]	dG	0,05	0,05
Grass quality (0 = poor grass; 1 = good grass)	[-]	qG	0,70	0,70
Specific weight of sand	[kN/m^3]	gS	19,00	19,00
Specific weight of saturated sand	[kN/m^3]	gSr	22,00	22,00
inner friction angle of sand	[°]	phi_s	40,00	40,00

grey shaded lines only for outlets

Table 4-2: Range of values for selected input parameters of the Kammer sluice and outlets.

4.2 Deterministic calculations

Traditional deterministic calculations are based on a comparison of the resistance R of the construction and the stress S working on the construction. Failure in a deterministic way takes place if the stress S exceeds the resistance R of the construction.

In the case of failure: $R - S < 0$ (Eq. 3)

The extent of safety in deterministic approaches is normally expressed by a safety coefficient $\eta = R/S$.

However, as already mentioned in Chapter 2.3.1, for probabilistic calculations the boundary between failure and non-failure has to be described by the following limit state equation:

$$Z = R - S \qquad \text{(see Eq. 2)}$$

This has to be done for each failure mechanism.

4.2.1 Limit state equations and fault tree analysis

The deterministic calculations comprise 25 failure mechanisms with an overall number of 87 input parameters (see Kortenhaus, 2003). Figure 4-5 presents an overview of the failure mechanisms of a sea dike which are considered in the ProDeich model.

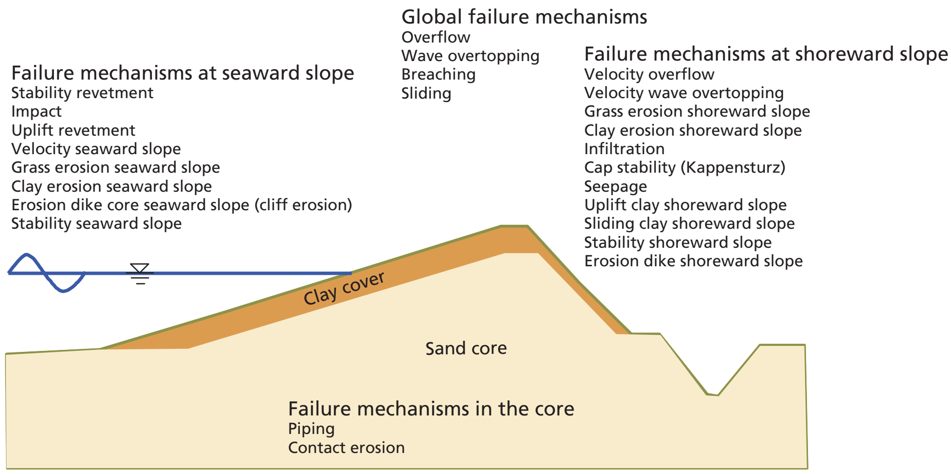

Figure 4-5: Overview of failure mechanisms of a sea dike considered in the ProDeich model (Oumeraci et al., 2004).

The failure mechanisms are divided into the following four groups:

- Global failure mechanisms result in a direct failure of the cross-section;
- Failure mechanisms on the seaward slope lead to failure of the seaward slope and subsequently to breaching;
- Failure mechanisms on the shoreward slope lead to failure of the shoreward slope and then to breaching ('Kappensturz' is not included since it is a separate branch in the fault tree);
- Failure mechanisms in the dike core describe mechanisms which lead to inner erosion of the core and thus provide the basis for breaching of the dike.

For limit state equations and more detailed descriptions of the failure mechanisms, see Kortenhaus (2003). The connections between each failure mechanism are considered by means of a fault tree (see Figure 4-6). In the fault tree, additional possible failure mechanisms are provided which are not considered in this study due to lack of models, shortage of data or an estimated extremely low failure probability. These failure mechanisms are e.g. vandalism, explosion, sabotage, ship collision, liquefaction and damage by debris.

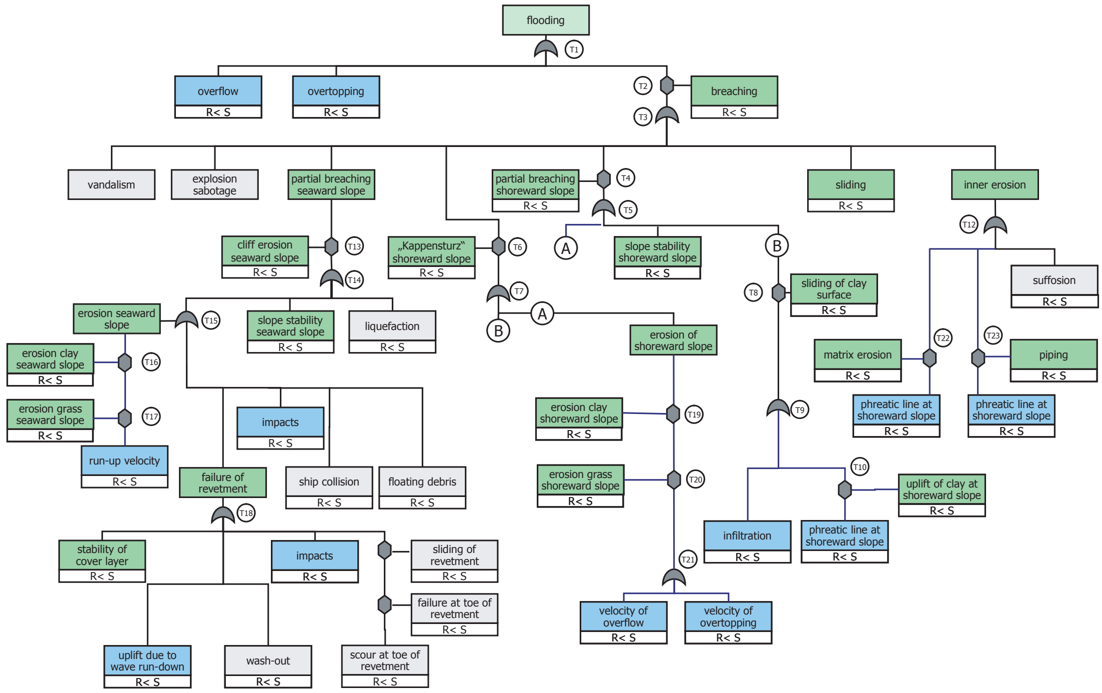

Figure 4-6: Fault tree for a sea dike (Kortenhaus, 2003).

Due to the lack of a revetment at the Ribe dike, all failure mechanisms for revetments are not considered in the calculations either. The total number of input parameters is therefore reduced to 80. All gates in the fault tree will be calculated according to Kortenhaus (2003) and are schematically shown in Figure 4-7.

The calculations of the limit state equations and the failure probabilities have been performed by software programmed in 'Pascal'. MS Excel extended with VBA routines[2] has been used to check the calculation results of the limit state equations, to calculate the limit state equations in the fault tree as well as to display the results. The software has been developed at the Leichtweiss Institute and details are provided in Kortenhaus (2003).

[2] VBA = Visual Basic for Applications

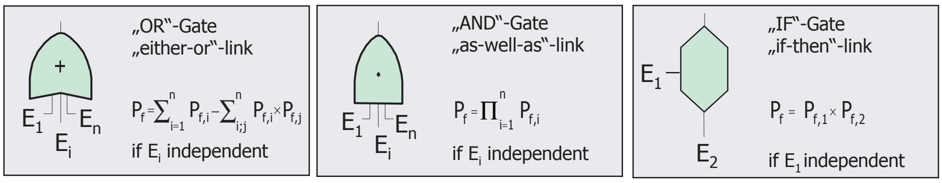

Figure 4-7: Gates in the fault tree for a sea dike (Kortenhaus, 2003).

The failure mechanisms of a sluice cannot be described using the aforementioned procedure. Therefore, further limit state equations have to be formulated. Figure 4-8 presents an overview of relevant failure mechanisms of the Kammer sluice (see also Vrouwenvelder (1993), TAW (1997), TAW (2000)).

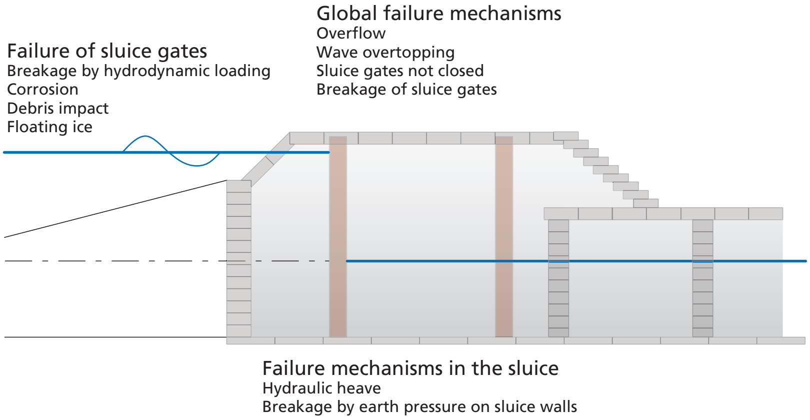

Figure 4-8: Overview of failure mechanisms of the Ribe Kammer sluice (Oumeraci et al., 2004).

All failure mechanisms are summarised within a simple fault tree, shown in Figure 4-9 (see e.g. CUR (1990)).

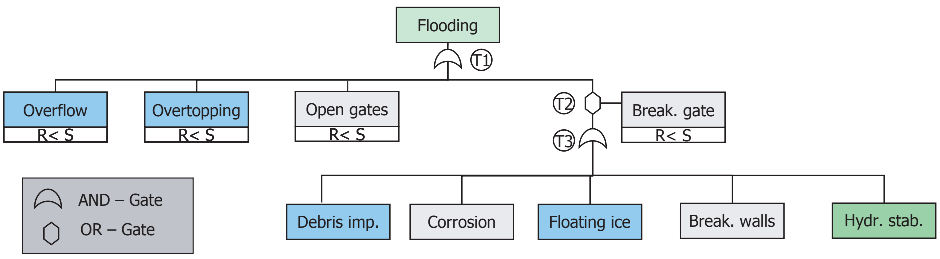

Figure 4-9: Fault tree for Ribe Kammer sluice (Oumeraci et al., 2004).

For the following failure mechanisms

- breaching due to hydrostatic and hydrodynamic loading,
- breaching due to earth pressure on the walls of the sluice,
- corrosion,
- debris impact,

- floating ice,
- ship collision

no proper calculation models are available or the amount of data is not sufficient. These failure mechanisms will therefore not be considered in the further determination of the overall failure probability of the sluice.

For the “sluice gate not closed” failure mechanism an overall failure probability for storm surge protection gates in the harbour of Hamburg is stated by Napp (1999) which is $P_f = 1{,}2 \cdot 10^{-3}$. This value will be used for the fault tree calculations shown in Figure 4-9.

The limit state equations for the “hydraulic uplift”, “overflow” and “wave overtopping” failure mechanisms will be described in more detail in the following. These limit state equations will be implemented in the software and used in the following for calculation of the overall failure probability of the sluice and the outlets.

Limit state equation for wave overtopping

For economic reasons, the freeboard of a structure cannot be chosen arbitrary. Therefore, failure due to wave overtopping is defined as the event in which the overtopping rate of water q_{vorh} exceeds the tolerable overtopping rate q_{zul}. Thus, the limit state equation for wave overtopping can be written as:

$$z = q_{zul} - q_{vorh} \tag{Eq. 4}$$

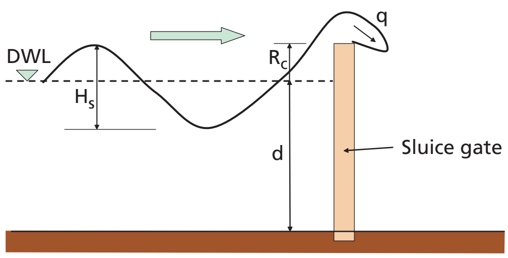

Figure 4-10: Principal sketch of wave overtopping over the sluice gate (Oumeraci et al., 2004).

If the sluice gate is considered a vertical wall (see Figure 4-10), the following equation according to EAK (2002) can be used to calculate the overtopping rate:

$$Q_x = a \cdot \exp\left[b \cdot \frac{R_x}{\gamma}\right] \tag{Eq. 5}$$

where:

$$Q_x = \frac{q_{vorh}}{\sqrt{g \cdot H_s^3}}$$ = dimensionless wave overtopping rate

$R_X = R_C/H_S$ = relative freeboard [-]

R_C = freeboard [m]

q = mean wave overtopping rate [m³/(sm)]

a = 0,082 (dimensionless wave overtopping rate for zero free board for vertical walls according to EAK (2002) [-]

b = -3,0 (factor for vertical walls according to EAK (2002)) [-]

γ = correction factor for oblique wave attack [-]

Following Kortenhaus (2003), the limit state equation needs to be reformulated and stated in terms of available and tolerable freeboards to avoid instability in the probabilistic calculations. For a given maximal tolerable overtopping rate q_{zul}, the required freeboard $R_{C,erf}$ is determined and afterwards compared to the available freeboard $R_{C,vorh}$. The limit state equation then reads:

$$z = R_{C,erf} - R_{C,vorh} \qquad \text{(Eq. 6)}$$

Using Eq. 5, the required freeboard $R_{C,erf}$ results in:

$$R_{c,\,erf} = \ln\left(\frac{q_{zul}}{\sqrt{g \cdot H_s^3} \cdot a}\right) \cdot \frac{1}{b} \cdot H_s \cdot \gamma \qquad \text{(Eq. 7)}$$

Limit state equation for overflow

Overflow is defined as the flow of water over the sluice gate in case of a higher water level on the seaward side of the gate than the height of the gate (see Figure 4-11).

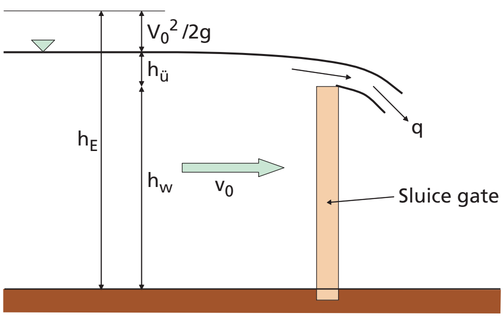

Figure 4-11: Principal sketch for overflow over the sluice gate (Oumeraci et al., 2004).

For a given tolerable overflow rate $q_{Üs,zul}$ and an existing overflow rate $q_{Üs,vorh}$, the limit state equation for this failure mechanism can be determined as follows:

$$z = R - S = q_{Üs,zul} - q_{Üs,vorh} \qquad \text{(Eq. 8)}$$

According to Napp (1999), the gate of the Ribe sluice can be regarded as a sharp weir with respect to its hydrodynamic efficiency. Therefore, the overflow rate can be determined as follows:

$$q_{Us,\,vorh} = \frac{2}{3} \cdot \mu \cdot \sqrt{2g} \cdot h_E^{3/2} \qquad \text{(Eq. 9)}$$

where: g = gravitational constant [m/s2]

μ = overflow parameter; for sharp weir crowns with aerated overflow: $\mu \approx 0.64$ [-]

and where h_E is the energy height with respect to the ground. The energy height (see Figure 4-11) is calculated as follows:

$$h_E = h_W + h_u + \frac{v_0^2}{2g} \qquad \text{(Eq. 10)}$$

where: h_W = weir height (height of the upper end of the sluice gate) [m]

$h_Ü$ = energy height at the weir (at the sluice gate) [m]

v_0 = velocity at the gate [m/s]

Limit state equation for hydraulic uplift

Hydraulic uplift is when a vertical upward flow force is greater than the weight force of the soil under water (see principal sketch in Figure 4-12).

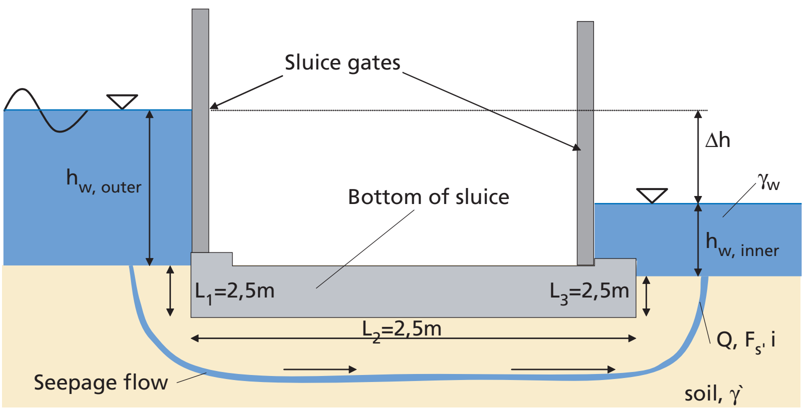

Figure 4-12: Principal sketch for hydraulic uplift at the Ribe Kammer sluice (Oumeraci et al., 2004).

The flow force F_S on the inner side of the sluice is larger than the weight force of the soil under water. This is a result of the hydraulic difference Δh which results in erosion of the soil and a loss of stability behind the sluice.

The structure may fail under these conditions. The limit state equation can be written according to Lang et al. (2003):

$$z = R - S = \gamma' - F_S \qquad \text{(Eq. 11)}$$

where: γ' = weight of soil under uplift [kN/m³]

F_S = flow force of the upward flow with a gradient i [kN/m³]

An approximate calculation of the flow gradient i according to Figure 4-12 can be made as follows:

$$i = \frac{\Delta h}{L1 + L2 + L3} \cdot f \qquad \text{(Eq. 12)}$$

where: Δh = difference of water levels outside $h_{w,außen}$ and inside $h_{w,innen}$

L1, L2, L3 = length of different flow parts around the structure

f = factor for consideration of flow potential at the considered point (using a manually constructed flow grid).

The failure mechanisms for the three outlets are a combination of the failure mechanisms for the sluice and the failure mechanisms for the main dike. Figure 4-13 provides an overview of relevant failure mechanisms for the three outlets.

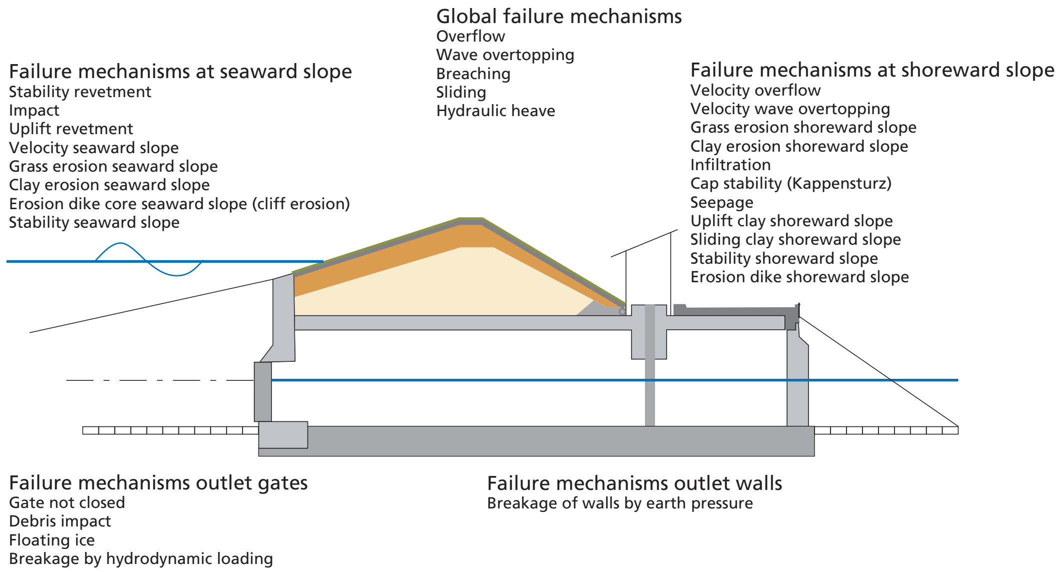

Figure 4-13: Overview of failure mechanisms for outlets (Oumeraci et al., 2004).

The combination of failure mechanisms for both the sluice and the main dike has been selected because the outlets are partly sluices (walls, gates, etc.) but also show characteristics of a dike (slope, grass cover, crown, etc.) The cross-section, however, deviates from the standard profile quite significantly and cannot be described by the fault tree in Figure 4-6.

This fault tree is therefore extended to include failure mechanisms for the outlet gates and the main body of the outlet (see Figure 4-14).

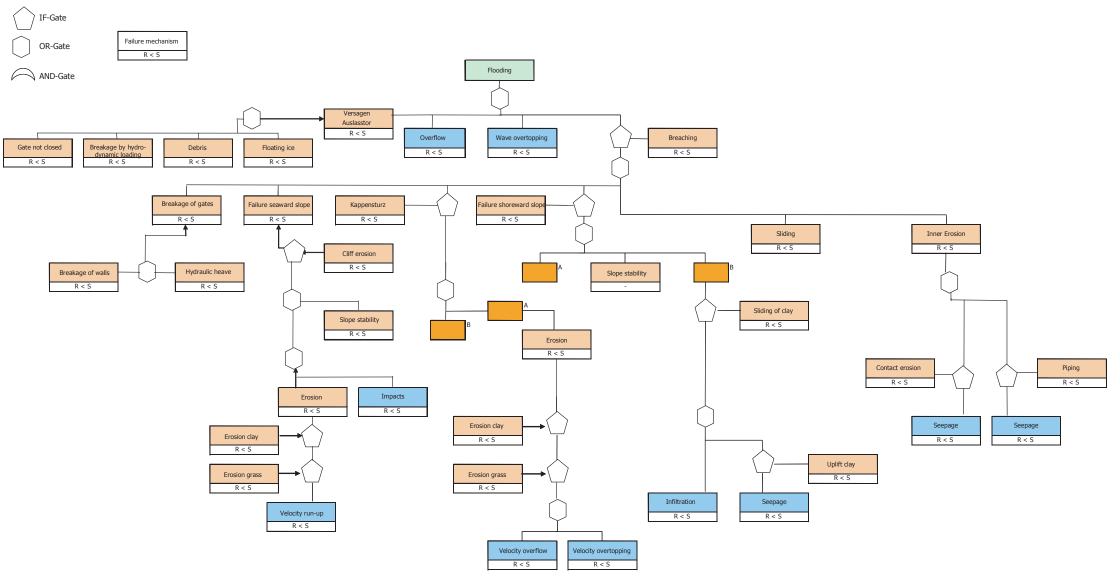

Figure 4-14: Fault tree for the three outlets within the Ribe defence system (Oumeraci et al., 2004).

To all mechanisms, which describe the failure of the outlet gates in particular, it applies that no models are available or that there is no sufficient information to quantify the input parameters. For the "outlet gate not closed" failure mechanism, the same failure probability as used for the sluice gate can be used as a first assumption ($P_f = 1{,}2 \cdot 10^{-3}$). It can be expected that the failure probability of the outlet gates is much lower than for the sluice gates because the outlet gates close automatically with a raising outer water level which is, however, not the case for the sluice gates. Therefore, the failure probability can be assumed to be $P_f = 1 \cdot 10^{-4}$. This assumption will be discussed later in the report.

The failure of the main body of the outlet, which might be caused by a failure of the walls due to earth pressure, cannot be described by a model due to insufficient information about the soil input parameters. Therefore, this failure mechanism will not be considered for calculations within this study[3].

The stone mattresses between grass cover and clay layer will change the erosion processes significantly. There are no investigations available for this type of strengthened dike covers so it is assumed (according to Westrich et al. (2003)) that the seaward and shoreward slopes are very stable. Thus, it can be expected that the erosion of the seaward and the shoreward slopes is negligible as compared to cases without stone mattresses (failure probabilities of an order of magnitude that is lower than without mattresses). Consequently, the "erosion of the seaward slope" and "erosion of the shoreward slope" branches can be neglected in the

3 Ignoring the failure mechanism in a fault tree automatically means that the failure probability of this mechanism is set to $P_f = 1{,}0$. This implicit assumption results in a higher overall failure probability of the whole cross-section and is therefore on the "safe side".

fault tree. Furthermore, the stones will increase the weight of the soil so that there is no hazard due to soil uplift and the "partial breaching at shoreward slope" branch can be ignored as well. These considerations result in no initial conditions for a dike breach. Therefore, the probability of "breaching" failure is supposed to be less than $P_f = 1 \cdot 10^{-10}$ and can hence be ignored in the fault tree.

4.2.2 Results of the deterministic calculations of all cross-sections

A deterministic calculation for all failure mechanisms summarised in Chapter 4.2.1 is performed for all six cross-sections. An overview of the results is presented in Table 4-3.

A safety coefficient of $\eta = 999$ is automatically selected in the software if the loading S in the limit state equation is zero. This is required to avoid a division by zero ($\eta = R/S$) in the software code.

It can be seen from Table 4-3 that the "erosion of grass cover on the seaward slope" failure mechanism will lead to failure at all cross sections. This means that in case of a design water level of $h_W = 5{,}22$ m and a storm surge duration of $t_S = 6{,}5$ h the grass cover on the seaward slopes of all cross-sections will fail.

No	Failure mechanism	Dike section 3156 R/S	6644 R/S	8422 R/S	9400 R/S	10403 R/S	14499 R/S
	Global failure mechanisms						
1	Overflow	999	999	999	999	999	999
2	Wave overtopping	6,8	8,8	6,3	7,2	4,8	8,1
3	Breaching	999	999	999	999	999	999
4	Sliding	69,5	64,1	45,6	65,7	64,6	60,1
	Failure mechanisms at the seaward slope of the dike						
6	Impact	35,0	36,2	31,5	35,8	34,1	34,8
8	Velocity seaward slope	1,6	1,7	1,6	1,6	1,7	1,6
9	Grass erosion seaward slope	0,43	0,47	0,35	0,46	0,41	0,43
10	Clay erosion seaward slope	8,3	7,0	4,5	6,1	5,3	4,5
11	Erosion dike core seaward slope	999	999	999	999	999	999
12	Stability seaward slope	1,6	1,6	1,8	1,6	1,8	1,6
	Failure mechanisms at the shoreward slope of the dike						
13	Velocity overflow	999	999	999	999	999	999
14	Velocity wave overtopping	999	999	999	999	999	999
15	Grass erosion shoreward slope	999	999	999	999	999	999
16	Clay erosion shoreward slope	999	999	999	999	999	999
17	Infiltration	999	999	999	999	999	999
18	Kappensturz	1,9	1,6	1,9	1,7	2,1	999
19	Seepage	466,1	415,4	370,0	455,0	512,6	532,1
20	Uplift clay on shoreward slope	4,3	4,8	6,3	3,3	5,7	5,7
21	Sliding clay shoreward slope	4,6	4,4	5,1	4,0	5,1	4,8
22	Stability shoreward slope	2,7	2,3	3,1	2,3	2,1	2,1
23	Erosion dike shoreward slope	999	999	999	999	999	999
	Failure mechanisms in the dike						
24	Piping	11,3	999	999	23,5	10,9	17,1
25	Matrix erosion	1,7	1,4	1,9	1,9	2,4	3,6

Table 4-3: Results of the deterministic calculations for all dike cross-sections.

Failure mechanisms such as "velocity wave run-up", "slope stability seaward slope", "Kappensturz" and "matrix erosion" result in safety coefficients within the range of $1,0 \leq \eta < 2,0$. These coefficients are rather low and hardly contain any "safety margin" under design conditions. More details about the safety margin of such failure mechanisms will be given in the sensitivity analysis in Chapter 4.2.3.

The results of the deterministic calculations of the Kammer sluice and the outlets of Vester Vedsted, Darum and Konge Å are summarised in Table 4-4. All values for the input parameters used for the deterministic calculations are presented in Appendix B.

			Outlets		
		Kammer-sluice	V.Vedsted	Konge-Å	Darum
No	**Failure mechanism**	R/S	R/S	R/S	R/S
1	Overflow	1,3	999	999	999
2	Wave overtopping	0,3	0,7	0,6	0,6
3	Hydraulic uplift	20,8	21,4	19,5	21,4

Table 4-4: *Results of the deterministic calculations of the Kammer sluice and the three outlets.*

The results show that there is wave overtopping failure at the Kammer sluice and the three outlets. Due to the fact that wave overtopping belongs to the group of global failure mechanisms – the hinterland is inundated by the overtopping water – the sluice and the outlets totally fail, considering the fault trees shown in Figures 4-9 and 4-14. The safety coefficients for wave overtopping and overflow are significantly lower compared to the dike cross-sections. A reason for this observation is that the seaward slope of the outlets is much shorter and steeper compared to the main dike. Furthermore, the water depth in front of the structures is significantly larger than in front of the main dike. Since the breaker criterion according to Oumeraci & Muttray (2001) is used for the determination of the wave height, which strongly depends on the water depth, the heights of incoming waves will be less reduced in front of the sluice/outlets than in front of the sea dikes. Consequently, higher wave run-up and overtopping may be expected.

Furthermore, the wave heights at the Kammer sluice are increased due to wave reflection from the gates. This effect is implicitly considered in the limit state equation for wave overtopping.

The safety coefficient for hydraulic uplift is sufficiently high for both the Kammer sluice and the three outlets.

4.2.3 Sensitivity analysis

The overall aim of performing a sensitivity analysis is to evaluate the importance of all input parameters for the failure mechanisms in a way that allow the following investigations with respect to uncertainties (see Chapter 4.3) to concentrate only on the most important parameters. The sensitivity analysis can be considered a step between deterministic and probabilistic calculations since it already considers the variations of the input parameters and their influence on the results of the limit state equations.

Within the sensitivity analysis, all input parameters will be varied at certain steps one after another within physically meaningful boundaries. The variation of the re-calculated safety coefficient is the measure of the importance of each input parameter in the respective limit state equation.

A pre-selection of the parameters to be varied is taken from Kortenhaus (2003). The sensitivity analysis is performed for all mechanisms which have led to failure during the deterministic calculations (grass erosion on seaward slope) and for all failure mechanisms which have been close to failure (see Chapter 4.2.2). For this purpose, only one dike section with the lowest safety coefficient will be used for the sensitivity analysis, whereas the others will be used to verify the results.

In Table 4-5 an overview of all parameters are given showing the biggest influence on the failure mechanisms investigated in the study. The 'plus' signs in the 'influence' column indicate that higher input values result in higher safety coefficients. The opposite is indicated by the 'minus' signs. The number of signs shows the importance of the parameters as more signs indicate greater importance.

Failure mode analysed	Parameter		influence
Grass erosion outer slope	quality of gras	qG	++
	water level	hw	---
	wave height	Hs	--
	storm surge duration	ts	-
Velocity wave run-up	material constant surface outer slope	qM	+++
	wave period	Tp	--
Bishop outer slope	cohesion of clay	cu	+++
	saturated volume weight of sand	gSr	---
Kappensturz	undrained shear strength of clay	cu	++
	percentage of sand in clay	pk	++
	volume weight of clay	gK	---
Wave overtopping	admissible overtopping rate	qzul	++
	water level	hw	---
	wave height	Hs	---
	wave period	Tp	-
	reduction factor seaward slope	rrfr	-

Table 4-5: The influence of the most important parameters on the investigated failure mechanisms.

The importance of the input parameters for the investigated failure mechanisms are also illustrated by figures, which are provided in Oumeraci et al. (2004), Appendix E.

4.3 Input parameter uncertainty

Uncertainties are defined as the variation of parameters from their mean values. As already mentioned in Chapter 2.3.1, the uncertainties may be described using either the statistical distribution or the mean value together with the standard deviation (or the coefficient of variation respectively) of a specific input parameter. In this study, the uncertainties for specific input parameters given by Kortenhaus (2003) will be used, if no other information is available.

For some parameters, which are considered to be important for the failure mechanisms (see sensitivity analysis in Chapter 4.2.3), the uncertainties have been evaluated in more detail, as the following chapters will describe.

4.3.1 Water level uncertainty

The height of the water level h_W has a significant influence on many of the failure mechanisms of the dike cross-sections. As described above, the design water level of h_W = 5,22 m DVR90 has been calculated by the DCA by means of extreme water statistics using a peak-over-threshold method, a 200-year return period and a LogNormal distribution. These results were re-calculated by the Leichtweiss Institute using the same data set. These calculations have led to slightly different results.

The application of different distribution functions (Pearson-III, Log Pearson, Gumbel, Weibull, Pareto) for the re-calculation of the design water level using information according to Plate (1993), Jensen (1985) and Maniak (2004) have shown that Weibull and Pareto distributions result in the worst fit and that the maximum variation of the design water level goes up to 0,37 m.

The influence of the number of considered data points in the re-calculation has been investigated by varying the threshold value, too. Depending on the selected threshold value, changes of the design water level could reach up to 90 cm.

Also the return period of 200 years has been changed to 50, 100, and 500 years respectively in the re-calculation by the Leichtweiss Institute. A maximum variation by using a return period of 500 years shows differences in the design water levels of up to 80 cm for the Gumbel distribution and about 60 cm for all other distributions.

All variations used for determining the uncertainties of the water level have led to deviations of several decimetres. Unfavourable combinations of different methods to determine the uncertainty may therefore lead to large variations of the design water level which underlines the importance of mean values and full statistical distributions rather than extrapolated values in the sense of a deterministic approach.

In the following, the values predefined by the DCA will, however, be used for the probabilistic calculations in Chapter 4.4. Thus, the LogNormal distribution is used together with a mean value of μ = 4,02 m and a standard deviation of σ = 0,47 m using a threshold of 3,38 m DVR90.

4.3.2 Dike height uncertainty

The dike crown height is one of the most important parameters for designing a dike. In many failure mechanisms, the crown height is considered by using the freeboard $R_c = h_k - h_w$ and therefore it has a significant influence on the failure probability of a sea dike.

For the Ribe dike, a number of surveys of the crown height are available from different years. After a quality check of the data, only data from two of the surveys could be used for estimating the uncertainties of the measurements. The analysis has shown that there is a standard deviation of 3 cm. Since the DCA estimates the uncertainty of GPS measurements to be within the range of 5 – 6 cm, the latter value will be used for uncertainty evaluation. This applies to the dike cross-sections and the outlets. Due to lack of information about the sluice gates, a simple estimation of 10 cm is used for the sluice gates. For reasons of simplification, a uniform standard deviation of 10 cm is finally used for all elements (main dike, sluice, outlets) for the probabilistic calculations.

4.3.3 Uncertainty of wave height and period

As described in Chapter 4.1, the wave heights result from numerical simulations performed by DHI. The uncertainties linked to these numerical simulations need to consider the correlation between the hydrodynamic input parameters. For example, the wave heights may depend on the angle of wave attack and the local water depth.

As a first step, the influence of the angle of wave attack has been investigated for all six dike cross-sections. The variation of the angle of wave attack of about 40° shows a variation of the wave height H_{m0} of only 3 - 4 mm. Therefore, it is concluded that the angle of wave attack has no influence and a uniform angle of 250° is thus chosen for all subsequent calculations.

At the next step, the relationship between the wave heights and the water levels given by DHI are investigated. A strong linear relation can be observed between the wave height H_{m0} and the water level d in front of the dike. However, no uniform factor can be determined for the different cross-sections (H_{m0}/d varied from 0,56 to 0,79). Therefore, it is decided to use the breaker criterion of $H_{m0}/d = 0{,}55$ following the principal investigations of Oumeraci & Muttray (2001).

To find a relation between wave periods and wave heights, the wave period T_m and the wave height H_{m0} are plotted against each other. A linear relationship is found which is assumed to result from a constant wave steepness $s_0 = H_{m0}/L_{0m}$. A verification of all types of wave steepness gives $s_0 = 0{,}07$ for km 14,449 in the northern end and $s_0 = 0{,}06$ for km 3,156 in the southern end of the dike line. It is decided to use $s_0 = 0{,}06$

for all subsequent calculations resulting in the following reduction of the wave period:

$$T_p = \sqrt{\frac{H_s \cdot g \cdot 0,06}{2\pi}} \quad \text{for} \quad H_s > 0,06 \cdot \frac{g \cdot T_p^2}{2\pi} \qquad \text{(Eq. 13)}$$

Due to the fact that no local wave measurements at the dike toe are available, no information can be derived regarding the statistical distribution of wave parameters. To consider the related uncertainties of the wave parameters, the investigations conducted by Kortenhaus (2003) is used. He assumes a normal distribution for wave height and wave period with a coefficient of variation of $\sigma' = 20$ % for the wave period and $\sigma' = 13$ % for the wave height respectively.

4.3.4 Geotechnical parameters

The shear strength c_S partly shows a strong influence on the geotechnical failure mechanisms (see Chapter 4.2.3). Therefore, the uncertainties of these parameters need to be considered as accurately as possible. During the dike reinforcement from 1978 to 1980, detailed in situ investigations measured several geotechnical parameters. However, an assessment of the uncertainty of the values is not practicable. Kortenhaus (2003) has used a coefficient of variation of $\sigma' = 0,76$ which is considered too high for Ribe. Thus, a coefficient of variation of $\sigma' = 0,2$ is used for e.g. the drained shear strength of sand c_S and the undrained shear strength of clay c_U in the subsequent calculations.

Detailed analysis of the internal friction angle of the non-cohesive soil φ_S has shown that this value should be restricted to input parameters for sand ($15° \leq \varphi_S \leq 40°$) since the results of some failure mechanisms using this value will otherwise lead to unreliable results.

4.3.5 Model uncertainties

Besides the uncertainties of the input parameters, the models describing the failure mechanisms based on the limit state equations are also subject to uncertainty. Kortenhaus (2003) provides details on how to determine these uncertainties and their importance on the overall failure probabilities. Since the cross-sections in this study have very similar characteristics, it can be assumed that the values mentioned in Kortenhaus (2003) can be applied. Hence, model factors with a mean value of $M_f = 1,0$ and a coefficient of variation of 20 % is used for all probabilistic calculations.

Table 4-6 summarises the assessed uncertainties of the input parameters discussed in the previous chapters. The remaining input parameters, including their uncertainties, used in the probabilistic calculations are presented in Appendix B.

Parameter	Uncertainty	Restriction	Remarks
Crown height hk	Sdev = 0,10 m	-	Uncertainty in measurements
Water level hw	Sdev = 0,47 m	-	Extreme statistics from available measurements
Wave height Hs	CoV = 0,13	Hs = 0,55*d	Breaker criterion, d = local water depth
Wave period Tp	CoV = 0,20	Tp = (Hs / 0,0938)^0.5	Restriction by wave steepness
Cohesion of clay c	CoV = 0,20		Available soil investigation, CoV usually higher
Undrained shear strength cu	CoV = 0,20		Available soil investigation, CoV usually slightly higher in average
Virtual cohesion	CoV = 0,20		Available soil investigation, CoV usually higher
Internal angle of friction phis	CoV = 0,58	15° ≤ phis < 40°	restriction to values for sand

Sdev = standard deviation
CoV = coefficient of variation

Table 4-6: Overview of uncertainties and limitations of selected parameters.

4.4 Probabilistic calculations

It is the overall aim of probabilistic calculations to explicitly consider uncertainties in the calculation of the overall failure probability of an engineering structure. The theoretical background and details about probabilistic calculations are presented in Kortenhaus (2003).

As a first step, the failure probability P_f of each mechanism is determined. Afterwards, level II or level III calculations are performed depending on the complexity of the limit state equations. A level II analysis is performed using FORM (first order reliability method) and a level III analysis is conducted by means of Monte-Carlo simulations. The calculated failure probability is expressed as P_f/year. Failure probabilities smaller than $P_f = 1 \cdot 10^{-10}$ are assumed as $P_f = 0$ and are ignored for subsequent calculations.

For the overall flooding probability of a dike section, the individual failure probabilities related to the limit state equations are linked to each other as already indicated in the fault tree analysis for deterministic calculations (see Chapter 4.2).

To calculate the temporal dependencies of the failure mechanisms, a scenario approach is used. The scenarios comprise several individual failure mechanisms which are put in a logical and temporal order. A simple example can be the grass and clay erosion on the seaward slope where the latter only starts when the former has finished. At the same time, the grass erosion takes some time from the overall storm surge duration so that the loading S for the clay erosion is already reduced. Kortenhaus (2003) has defined 11 scenarios. These 11 scenarios are divided into four groups which describe seaward slope failure, shoreward slope failure, the "Kappensturz" and failure due to inner erosion. The groups are linked together by means of a second fault tree. This second fault tree also considers individual failure mechanisms which are not time-dependent and therefore remain stand-alone failure mechanisms, like wave overtopping. The results of the scenario-based approach will be presented in Chapter 4.4.2.

4.4.1 Results of dike cross-sections

Table 4-7 provides an overview of the results of the probabilistic calculations of all dike cross-sections and all individual failure mechanisms.

		Dike section					
No.	Failure mechanism	3156	6644	8422	9400	10403	14499
	Global failure mechanisms						
1	Overflow	1,0E-06	2,0E-07	2,3E-06	1,0E-06	3,4E-06	5,0E-07
2	Wave overtopping	3,0E-05	9,0E-06	4,1E-05	3,5E-05	6,6E-05	9,0E-06
3	Breaching	4,3E-02	1,8E-02	7,4E-02	4,2E-02	8,9E-02	3,6E-02
4	Sliding	3,4E-07	3,3E-07	4,1E-07	3,3E-07	3,5E-07	3,4E-07
	Failure mechanisms at the seaward slope of the dike						
6	Impact	8,0E-06	5,0E-06	2,0E-05	4,0E-06	7,0E-06	8,0E-06
8	Velocity seaward slope	2,2E-02	1,8E-02	3,4E-02	1,9E-02	3,4E-02	3,2E-02
9	Grass erosion seaward slope	2,9E-01	2,4E-01	6,8E-01	2,6E-01	3,3E-01	3,0E-01
10	Clay erosion seaward slope	1,3E-05	5,6E-05	3,6E-03	1,3E-05	3,7E-04	4,6E-04
11	Erosion dike core seaward slope	1,7E-05	7,6E-05	4,8E-04	1,1E-04	3,2E-04	5,6E-04
12	Stability seaward slope	0,0	0,0	0,0	0,0	0,0	0,0
	Failure mechanisms at the shoreward slope of the dike						
13	Velocity overflow	2,0E-06	3,0E-06	3,0E-06	2,0E-06	2,0E-06	0,0E+00
14	Velocity wave overtopping	2,6E-05	3,3E-05	1,4E-04	1,2E-05	1,9E-04	2,2E-05
15	Grass erosion shoreward slope	1,6E-04	1,0E-04	5,7E-04	8,5E-05	6,9E-04	1,2E-04
16	Clay erosion shoreward slope	6,3E-05	1,6E-05	6,6E-05	2,3E-05	7,6E-05	1,7E-05
17	Infiltration	0,0	8,0E-06	2,1E-04	1,0E-06	0,0E+00	1,6E-04
18	Kappensturz	1,4E-02	1,1E-02	7,6E-03	2,3E-02	4,1E-03	1,4E-02
19	Seepage	1,0E-06	1,0E-06	1,0E-06	2,0E-06	0,0E+00	1,0E-06
20	Uplift clay on shoreward slope	1,0E-06	2,0E-06	1,0E-06	1,0E-06	0,0E+00	0,0E+00
21	Sliding clay shoreward slope	4,1E-04	5,4E-04	1,4E-04	1,3E-03	1,4E-04	2,4E-04
22	Stability shoreward slope	0,0	0,0	9,6E-05	0,0	0,0	0,0
23	Erosion dike shoreward slope	0,0	0,0	3,2E-05	3,0E-06	7,0E-06	0,0
	Failure mechanisms in the dike						
24	Piping	9,6E-07	2,0E-06	2,0E-06	6,8E-07	1,1E-06	5,4E-07
25	Matrix erosion	2,5E-01	1,4E-01	2,7E-02	2,6E-02	3,8E-03	2,8E-04
	Overall failure	3,1E-05	9,2E-06	4,3E-05	3,6E-05	6,9E-05	9,5E-06

Table 4-7: Overview of failure probabilities for all failure mechanisms of all dike cross-sections (calculated by Monte-Carlo simulation).

The overall failure probability of the cross-sections is also stated in Table 4-7 based on the fault tree defined for the previous deterministic calculations. The overall failure probability of each cross-section is therefore only understandable by considering the fault trees illustrated in Appendix C.

Within all global failure mechanisms, the 'breaching' failure mechanism has a failure probability of $P_f = 10^{-2}$. This very high probability is a result of not taking into account the temporal relation between the failure mechanisms. This way, the full storm surge duration is used to calculate the loading S of the limit state equation. Hence, this failure probability is too high and needs to be re-calculated using the scenario approach (see Chapter 4.4.2).

The failure probability of wave overtopping represents the second highest values of $P_f = 10^{-5}$ - 10^{-6}. This implies a tolerable wave overtopping rate of q_{zul} = 20 l/sm. The difference of the order of magnitude results from the difference in freeboard heights of the six cross-sections. The failure probability of sliding of the whole dike body is $P_f = 10^{-7}$. However, it can be assumed to be even lower since the Monte-Carlo simulation was stopped in order to avoid a simulation run that was too long.

For the seaward slope, the failure probabilities of grass erosion ($P_f = 10^{-1}$) and run-up velocity ($P_f = 10^{-2}$) present the highest values. Especially for grass erosion, this type of failure will occur in almost all cases. The failure probability of clay erosion is on the other hand much lower ($P_f = 10^{-4}$ – 10^{-5}) due to the fact that the clay cover is very thick on the seaward side.

Failure probabilities for mechanisms on the shoreward slope of the dike are relatively high for 'Kappensturz' and 'sliding of the clay cover'. Both mechanisms are essentially governed by the undrained shear strength c_u of the clay. A general failure of the sliding of the clay cover will occur when the shear strength is lower than c_u = 3 kN/m². This value corresponds to a mushy, almost liquid consistency. The second most important input parameter is the relatively steep shoreward slope of the dike (see Table 4-1) which implies that failure may occur on the shoreward slope.

In Figure 4-15, the fault tree for the dike cross-section km 8,422 is shown. The fault tree illustrates the influence of the individual failure mechanisms on the overall failure probability. The fault tree is at its root branched out and converges at its top into the top-event of flooding. In order to determine the overall failure probability, the failure probabilities of the individual failure mechanisms are calculated - starting at the tree root - according to the type of gate (see Figure 4-7) they are pointing at. For this, each failure mechanism is represented by a box, stating the failure mechanism, the calculated failure probability P_f and the reliability index β. Furthermore, each gate is represented by a box, stating the type of gate (OR, AND, IF) and the calculated failure probability of the failure mechanisms pointing at the particular gate. The figures/numbers, which are stated above each box, are designations being used for calculation reasons. Looking at the IF-gate T17 (branch 'seaward slope'), for example, the failure probability in this gate is calculated by multiplying the failure probability of 'erosion grass, seaward slope' ($6{,}8 \cdot 10^{-1}$) by the failure probability of 'velocity run-up' ($3{,}4 \cdot 10^{-2}$). This failure probability is afterwards passed on to the next IF-gate, where the value is multiplied by the probability of 'erosion clay, seaward slope' ($3{,}6 \cdot 10^{-3}$).

The blue failure mechanisms indicate initial (stress) failure mechanisms at the bottom of each branch. The branches being called 'A' and 'B' (orange boxes) have to be each considered twice: Once in the branch regarding 'Kappensturz, shoreward slope' and once in the branch 'failure shoreward slope'. The fault trees for all six cross-sections comprising the results of the probabilistic calculations are presented in Appendix C.

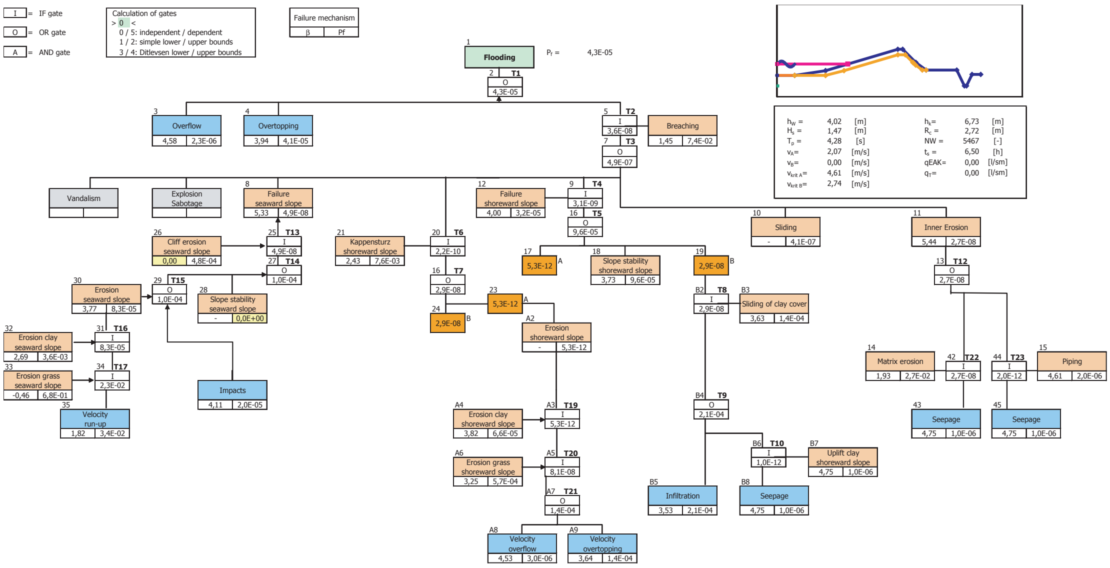

Figure 4-15: Fault tree with failure mechanisms for the cross-section km 8,422.

It can be seen from Figure 4-15 that the overall failure probability of the cross-section km 8,422 mainly depends on the failure probability of 'wave overtopping' and 'overflow'. The very high failure probability of 'grass erosion' is not of major importance to the overall failure probability. It only represents the beginning of the erosion process on the seaward slope which eventually adds up to a failure probability of $P_f = 4{,}9 \cdot 10^{-8}$ for the seaward slope. The failure probability of 'breaching' is of a similar order of magnitude ($P_f = 3{,}6 \cdot 10^{-8}$) and both are therefore 10^3 times lower than the failure probability of wave overtopping and a factor of 64 lower than the failure probability of overflow. These factors are similar for all six cross-sections.

The fault tree does, however, not consider the temporal correlation between the failure mechanisms. Therefore, the following chapter will present the results of the scenario approach calculation and the related fault tree analysis.

4.4.2 Results of the scenario approach

The failure probabilities of the scenarios are calculated by using the level III approach (Monte-Carlo simulation). The results are summarised in Table 4-8. The overall failure probability, which also is stated in the table, is calculated based on the scenario fault tree. The overall failure probability of each cross-section is therefore only understandable by considering the simplified scenario fault tree illustrated in Appendix D.

	Individual mechanisms	Dike cross section					
No	(see Tab. 4-7 for def.)	3156	6644	8422	9400	10403	14499
Sc 1	9+10+11+3	3,0E-06	6,0E-06	3,5E-05	1,4E-05	3,4E-05	7,0E-06
Sc 2	11+3	3,0E-05	2,6E-04	1,1E-03	6,9E-05	4,9E-04	7,7E-04
Sc 3	15+16+18+3	0	0	0	0	0	0
Sc 4	17+21+18+3	0	0	0	0	0	0
Sc 5	19+20+21+18+3	0	0	0	0	0	0
Sc 6	15+16+23+3	0	0	1,5E-05	0	4,0E-06	0
Sc 7	17+21+23+3	0	0	0	0	0	0
Sc 8	19+20+21+23+3	0	0	0	0	0	0
Sc 9	23+3	0	0	3,8E-05	0	9,0E-06	0
Sc 10	19+24+23+3	0	0	0	0	0	0
Sc 11	19+25+23+3	0	0	0	0	0	0
	Overall failure	3,10E-05	9,60E-06	4,50E-05	3,70E-05	7,10E-05	1,00E-05

Table 4-8: Failure probability of scenarios for all cross-sections.

For several scenarios the overall failure probability results in $P_f = 0$ and $P_f < 10^{-10}$ respectively. Scenario I which comprises grass erosion, clay erosion, cliff erosion and breaching of the dike results in failure probabilities larger than $P_f = 10^{-10}$. The same applies to scenario II (cliff erosion and breaching). For the cross-section km 8,422, scenario I results in $P_f = 3{,}5 \cdot 10^{-5}$. In comparison to the fault tree approach discussed in the previous chapter, the failure probability of the seaward slope of the dike was $P_f = 4{,}9 \cdot 10^{-8}$ and thus three orders of magnitude smaller.

Furthermore, for two cross-sections (km 8,422 and km 10,403) two additional scenarios describing the erosion of the shoreward slope result in failure probabilities of $P_f = 10^{-5}$ and $P_f = 10^{-6}$.

In the fault tree using the scenarios (see Figure 4-16), wave overtopping and overflow have the same failure probabilities as in the standard fault tree due to the fact that the limit state equations for wave overtopping and overflow do not contain any time dependency. Again, the failure probability of wave overtopping is dominant for the overall flooding probability. The increased failure probability of the erosion process on the seaward slope now comes much closer to the failure probability of wave overtopping by using the scenario fault tree. Hence, the erosion process seems to become increasingly important for the overall flooding probability of the Ribe dike.

The overall flooding probabilities of five cross-sections (6644, 8422, 9400, 10409 and 14499) result in 3–5 % higher values when the scenario approach is used. The cross-section km 3,156 does not seem to be affected by the use of the scenario approach.

Using these results, the scenario fault tree can be simplified ignoring all branches in the tree which have failure probabilities of $P_f < 10^{-10}$. Such a simplified fault tree is shown in Figure 4-16 for the cross-section km 8,422. The overall flooding probability results in $P_f = 4{,}5 \cdot 10^{-5}$. The calculation of the overall failure probability within the simplified scenario fault tree is identical to the procedure described in the previous Chapter 4.4.1. All simplified scenario fault trees for the six cross-sections are presented in Appendix D.

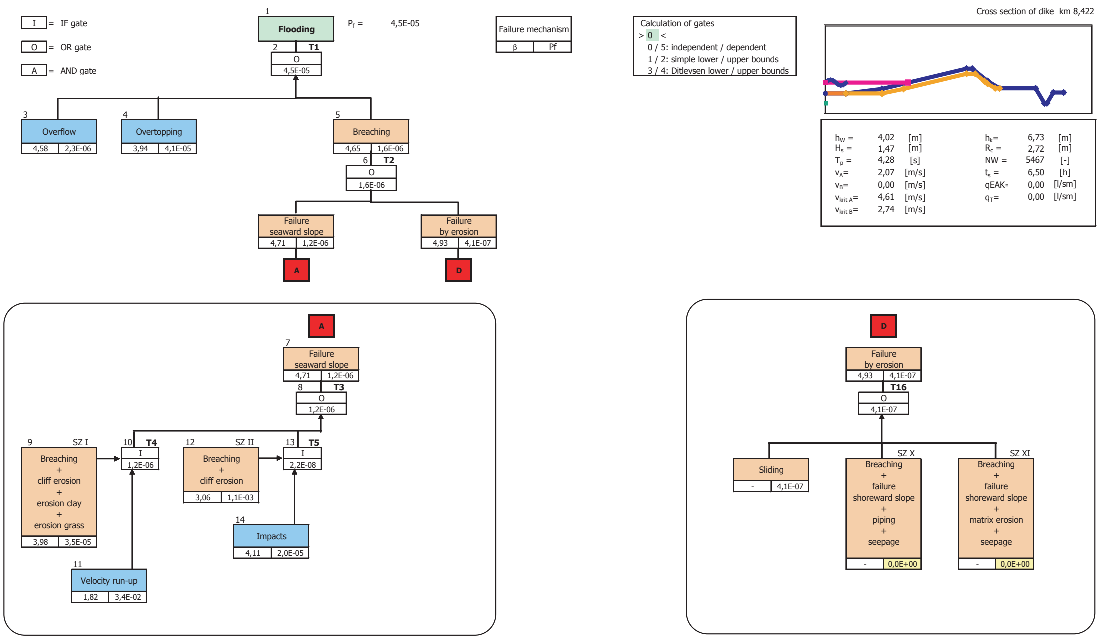

Figure 4-16: Simplified scenario fault tree for the dike cross-section km 8,422.

To study the influence of the uncertainties of the input parameters on the overall flooding probability in more detail, a sensitivity analysis is performed on the basis of the dominant scenarios. The results of the sensitivity analysis will be discussed in the following.

4.4.3 Sensitivity analysis of scenarios

A pre-selection of parameters with the most significant influence on the overall failure probability is performed based on the sensitivity analysis in Chapter 4.2.3. Following this, the water level h_W, the wave period T_p, the storm surge duration t_s, and the wave height H_s are considered. The simplified scenario fault tree is used for all calculations and the variations performed within the sensitivity analysis are presented in Table 4-9.

To calculate the failure probabilities of the individual failure mechanisms used in the simplified scenario fault tree, the FORM analysis is used because the calculation effort is significantly lower than for the Monte-Carlo simulation. However, the scenarios are calculated using the Monte-Carlo simulations due to their complexity.

Parameter	Variation 1	Variation 2
hw [m]	Reference value*) – 0,5 m	Reference value + 0,5 m
Tp [s]	Reference value – 1,0 s	Reference value + 1,0 s
ts [h]	Reference value – 2 h	Reference value + 2 h
Hs [m]	Reference value – 0,5 m	Reference value + 0,5 m
Statistical distribution for hw	Gumbel – distribution	Normal distribution

*) the reference value is defined as the mean value used for the probabilistic calculations

Table 4-9: Variation of key parameters for the sensitivity analysis of all scenarios.

The influence of the mean value of a number of key input parameters on the failure probability of individual mechanisms, scenarios and the overall flooding probability is investigated. For example, the mean water level h_W is changed by 0,5 m upwards and downwards respectively. The results for the cross-section km 10,403 are exemplarily shown in Figure 4-17.

Figure 4-17: The effect of variation of the mean water level h_W on the failure probability of individual mechanisms, scenarios and overall flooding probability of the cross-section km 10,403 (Oumeraci et al., 2004).

The increase of the mean water level h_W by 0,5 m yields an increase of the failure probability of wave overtopping by a factor of 10,0 and a reduction by 0,5 m results in a lower failure probability by a factor of 10,0. The overall flooding probability and the failure probability of scenario II are changed by the same order of magnitude. For both the 'sliding' and the ‘velocity wave run-up’ failure mechanisms the variation does not have a significant influence. However, scenario I does not show a consistent behaviour which may be due to an insufficient number of simulations for the lower mean value of the water level.

At the next step, the influence of the mean values of further parameters on the failure probability of wave overtopping is investigated in more detail. Wave overtopping is selected since it has the greatest influence on the overall flooding probability. In Figure 4-18 the results of the variation of the mean values are presented for the cross-section km 10,403.

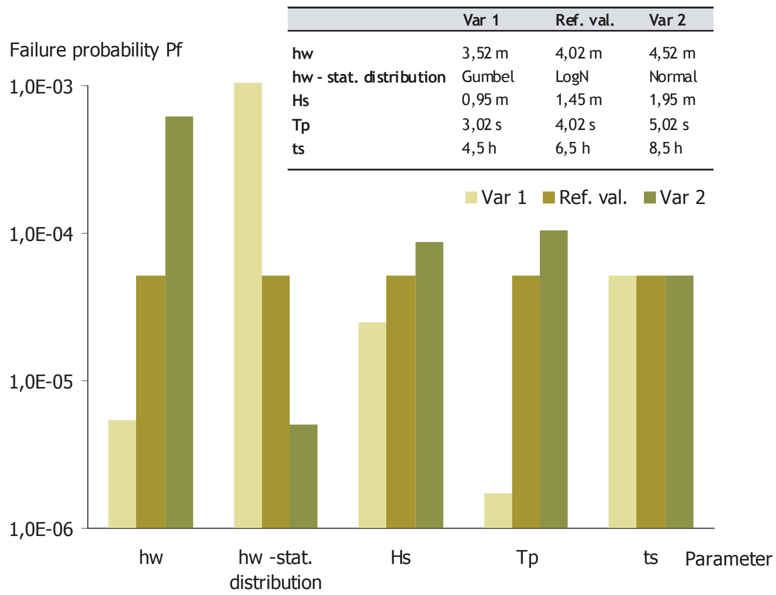

	Var 1	Ref. val.	Var 2
hw	3,52 m	4,02 m	4,52 m
hw - stat. distribution	Gumbel	LogN	Normal
Hs	0,95 m	1,45 m	1,95 m
Tp	3,02 s	4,02 s	5,02 s
ts	4,5 h	6,5 h	8,5 h

Figure 4-18: Failure probability of wave overtopping depending on variation of mean values of key input parameters (Oumeraci et al., 2004).

The increase of the water level h_W and the variation of the type of statistical distribution leads to significant changes of the failure probabilities (order of magnitude of about 10,0). On the other hand, an increase of the wave height H_S and wave period T_p has less influence as the variations lead to a factor of about 2,0. However, the decrease of the wave period T_p does not show a consistent behaviour, which requires further verification of the plausibility of the result. The inconsistent behaviour may be due to an insufficent number of simluations and/or a missing consistency between the reference wave height and the reduced wave period. As expected, the storm duration does not have any influence on wave overtopping because it is not an input parameter for the wave overtopping formula and the water level is assumed to be constant during the storm surge. Therefore, the key parameters to influence the failure probability of wave overtopping and the overall flooding probability are the water level and the wave period. The uncertainties of both parameters should therefore be evaluated very carefully.

4.4.4 Results for the Ribe sluice and the outlets

The failure probability of the Kammer sluice and the outlets is calculated using the Monte-Carlo method. The results are shown in Table 4-10.

No	Failure mechanism	Kammer sluice	Outlets: V.Vedsted	Outlets: Konge Å	Outlets: Darum
1	Overflow	5,3E-02	1,5E-04	2,5E-04	7,9E-05
2	Wave overtopping	6,1E-01	5,6E-01	4,7E-01	4,9E-01
3	Hydraulic heave	1,0E-10	1,0E-10	1,0E-10	1,0E-10
4	Gates not closed	1,2E-03	1,0E-04	1,0E-04	1,0E-04
	Overall failure	6,3E-01	5,6E-01	4,7E-01	4,9E-01

Table 4-10: Results of probabilistic calculations for the Kammer sluice and the three outlets.

The overall flooding probability of the Kammer sluice and the three outlets is calculated using the fault tree in Figure 4-9 and Figure 4-14 respectively. The failure probabilities for the outlets are all within the range of $P_f \approx 5{\cdot}10^{-1}$, which means that flooding occurs approximately every second year. The key failure mechanism for all structures is wave overtopping comprising a tolerable wave overtopping rate of q_{zul} = 20 l/(sm). Variations of the tolerable overtopping rates (q_{zul} = 100 l/(sm), 200 l/(sm) and 515 l/(sm) – 515 l/(sm) corresponds to the overtopping rate for a zero freeboard as a maximum possible value) are performed to study their influence on the results. The results of these variations are shown in Table 4-11.

Increasing the tolerable wave overtopping rate to 100 l/(sm) and 200 l/(sm) results in a decrease of the failure probability of wave overtopping by a factor of about 10,0 and 100,0 for all outlets and the sluice respectively. If the tolerable wave overtopping rate is set to 515 l/(sm), the failure probability of wave overtopping comes within the range of $P_f = 10^{-4}$ for the sluice and $P_f = 10^{-5}$ or $P_f = 10^{-6}$ for the outlets.

Therefore, the selection of the tolerable wave overtopping rate is very important for calculating the overall failure probability and may change the result by several factors. Consequently, the choice of these values for the sluice and the outlets has to be made very carefully.

No	Failure mechanism	q_{zul} [l/(sm)]	Kammer sluice	Outlets V.Vedsted	Konge-Å	Darum
1	Overflow	20	5,3E-02	1,5E-04	2,5E-04	7,9E-05
		100	1,0E-10	4,8E-07	4,8E-07	4,8E-07
		200	1,0E-10	4,8E-07	6,3E-08	4,8E-07
		515	1,0E-10	4,8E-07	4,8E-07	4,8E-07
2	Wave overtopping	20	6,1E-01	5,6E-01	4,7E-01	4,9E-01
		100	2,4E-02	1,0E-01	8,3E-02	8,3E-02
		200	6,1E-03	1,6E-02	6,1E-03	6,1E-03
		515	8,0E-04	7,4E-05	4,1E-06	3,0E-05

Table 4-11: Failure probabilities of wave overtopping and overflow at the Kammer sluice and the outlets for variations of the tolerable wave overtopping rate.

Keeping in mind the fault trees for the sluice and the outlets (Figure 4-9 and Figure 4-14 respectively), the failure probability of wave overtopping may become lower than what has been assumed for the 'gates not closed' scenario in which case the latter is relevant for the overall failure probability. Failure probabilities for this scenario have been set to $P_f = 2{,}1 \cdot 10^{-3}$ and $1 \cdot 10^{-4}$ respectively, as already discussed in Chapter 4.2.1.

4.5 Calculation of the overall failure probability of the total defence system

As a last step, the overall flooding probability of the whole flood defence system is calculated. As already mentioned in Chapter 2.3, the risk assessment, as a sub-process of the risk analysis, combines the results of the hazard analysis and the vulnerability analysis. The principal result of the hazard analysis needed for the risk assessment is the overall flooding probability of the whole defence system. So far, only the failure probability of the six cross-sections, the Kammer sluice and the three outlets has been calculated.

4.5.1 Representative sections for the main part of the defence system

To determine the overall flooding probability of the Ribe defence system, the dike stretches between the six cross-sections, the sluice and the outlets have to be considered. This is done by dividing the defence system into representative sections. A rough division can be made following the two criteria below (the division of the Ribe defence system comprises only the main dike):

1. structure type, e.g. dike, outlet, sluice,
2. variation of input parameter for either the stress (S) or the resistance (R) of the limit state equations (only applicable for the dike structure).

A further, more detailed division of the second criteria can be chosen for the following aspects:

a) geometry of the structures, e.g. crown height, angle of slopes
b) principal composition of the dike cross-section, e.g. existence of a revetment
c) properties of the used material, e.g. soil parameters
d) differences in the loading of the structures, e.g. wave heights, angle of wave attack.

While the rough division is easily made by letting dikes, outlets and the sluice be different sections, the more detailed division based on the four aspects requires some assumptions. First, the material properties of the dikes are assumed to be similar. Second, the principal cross-sections of the dikes can be assumed to be similar. Furthermore, the sensitivity analysis has shown that wave overtopping is one of the key failure mechanisms. Wave overtopping is essentially governed by the wave period T_p and the water level h_W in front of the structure or the freeboard R_C. Since h_W is assumed to be constant for the whole dike length, the crown height plays a major role for the determination of the freeboard R_C. Therefore, both the crown height h_k of the dike and the peak wave period T_p are the key selection criteria for the division of the defence system into representative dike sections.

In addition, it is decided that the mean crown height of a dike section should be the same as the crown height of one of the six calculated cross-sections. Further, the variation of the wave period should maximum be T_p = 0,5 s.

The aforementioned criteria are shown in Figure 4-19, where the crown height h_k and the wave period T_p are drawn at a distance of 50 m in front of the dike line (taken from the DHI simulation). Additionally, the location of the cross-sections of the dike, the sluice and the outlets are marked according to the stationing line of the defence system.

Following the selected criteria, 15 sections are defined as shown in Figure 4-19. Four sections are defined as close to the cross-section km 6,644, two sections close to the cross-section km 14,499, whereas all other sections differ from each other. Section 4 in Figure 4-19 cannot be assigned to one of the cross-sections due to a crown height of h_k = 7,53 m which is significantly higher than for the other sections. This section will be ignored for the subsequent probabilistic calculation[4].

To calculate the overall flooding probability of the whole defence system, the overall failure probabilities of the individual sections are structured in

[4] Due to the much larger crown height, the failure probability of wave overtopping of this section will be much lower than for all other sections. Thus, the section will not have any influence when the overall failure probability of the system is calculated using an OR gate in the fault tree approach.

a fault tree, which will be discussed in more detail in the following chapter.

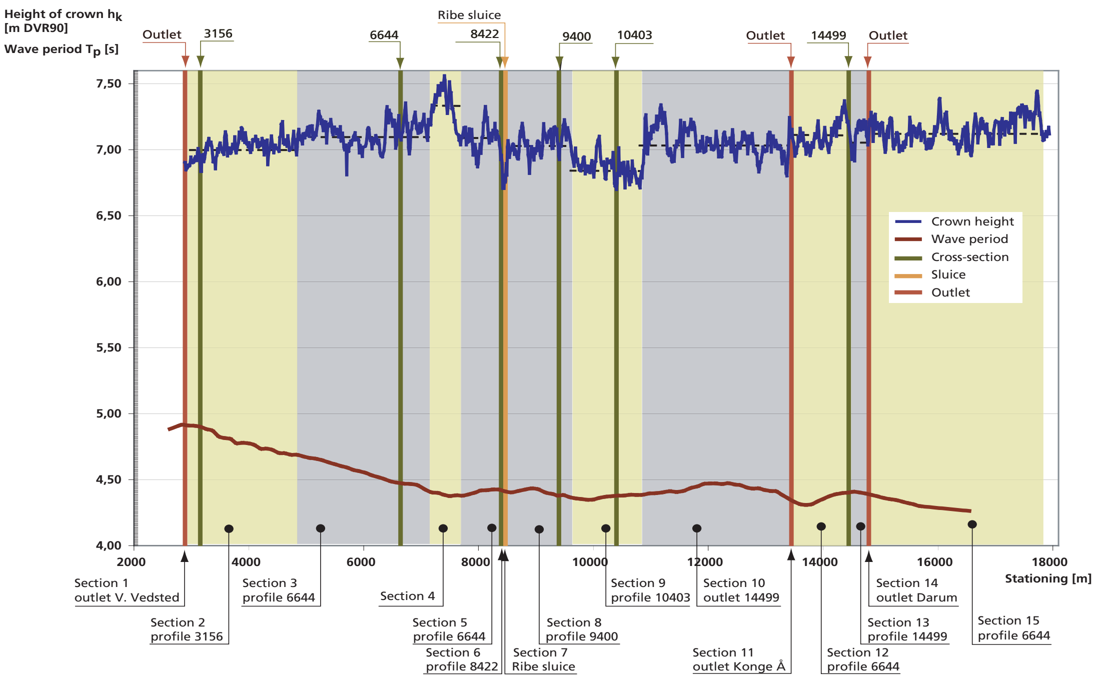

Figure 4-19: Division of the Ribe flood defence system into representative sections (Oumeraci et al., 2004).

4.5.2 Failure probability of the defence system and evaluation of the results

For most of the dike sections which have been discussed in Chapter 4.5.1, the failure probabilities have been calculated already (see Chapter 4.4). For section 3 (corresponds to the cross-section km 6,644) and section 10 (corresponds to the cross-section km 14,499) the failure probabilities are re-calculated with an increased wave period T_p. To determine the failure probability of these sections, only the failure probability of wave overtopping is calculated since this will be the main contribution to the overall flooding probability as shown in Chapter 4.4. Variations of the wave period in section 2 (corresponds to the cross-section km 3,156) are not considered because the original cross-section km 3,156 has been calculated using the highest wave period and hence resulting in the highest failure probability.

The failure probabilities of the dike sections are linked to each other by means of a fault tree, including only one OR gate. This gate is used to calculate the overall probability of flooding of the hinterland. The result is shown in Figure 4-20.

Taking into consideration the aforementioned assumptions in Chapter 4.5.1, the overall flooding probability of the defence system in Ribe can be calculated to be $P_f = 9{,}5 \cdot 10^{-1}$. This very high failure probability is essentially dominated by the failure probability of the sluice and the outlets (see Table 4-10). Reasons for these results have already been stated in Chapter 4.4.4. All sections comprising a dike structure resulted in much lower failure probabilities within the range of $P_f = 10^{-6}$ to 10^{-5} (see Chapter 4.4.2).

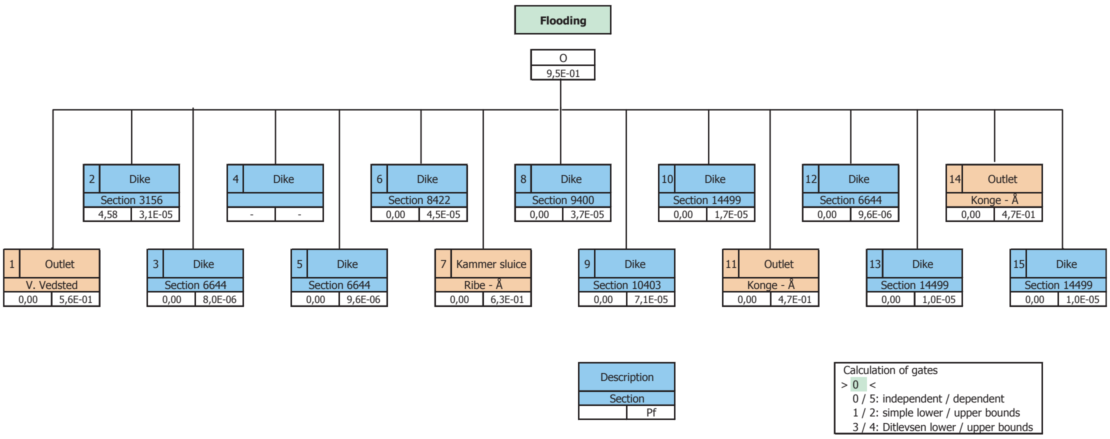

Figure 4-20: Fault tree for calculating the overall flooding probability of the whole defence system in Ribe (including the sluice and the outlets) (Oumeraci et al, 2004).

It has to be considered though that the weakest elements of the defence line (sluice and outlets) are only very narrow sections and therefore only constitute a very short stretch in the whole defence line. A calculation of the expected wave overtopping volume can provide a criterion for the evaluation of the failure probabilities.

The wave overtopping volume per running meter length of the structure can be calculated using Eq. 5 in Chapter 4.2.1. Using the input values of $H_s = 1{,}65$ m, $h_k = 5{,}78$ m and $h_w = 5{,}22$ m, the wave overtopping rate results in q = 159 l/(sm) for short-crested waves and an angle of wave attack of $\theta = 20°$. Assuming that this overtopping rate is constant during the storm surge duration of 6,5 hours, the overall volume for the approximately 10,0 m wide sluice gate may be estimated to $Q \approx 37200$ m³. This corresponds to a water level in the flood-prone area of less than 1,0 mm. Therefore, flooding of the hinterland will only occur if the sluice or one of the outlets will structurally fail.

Hence, a simple method used to calculate the lowest possible failure probability is to leave out the sluice and the outlets in the fault tree of Figure 4-20. The reduced fault tree is shown in Figure 4-21. The overall flooding probability now results in $P_f = 2{,}5 \cdot 10^{-4}$.

Alternatively, the outlets and the sluice can be calculated using the failure probability of the 'gate not closed' failure mechanism. This will then result in an overall flooding probability of $P_f = 1{,}7 \cdot 10^{-3}$. It is therefore essential to investigate the sluice and the outlets in more detail to finally determine their overall failure probability. For the time being, it is recommended to use a flooding probability of $P_f = 2{,}5 \cdot 10^{-4}$ for the risk assessment in Chapter 6.

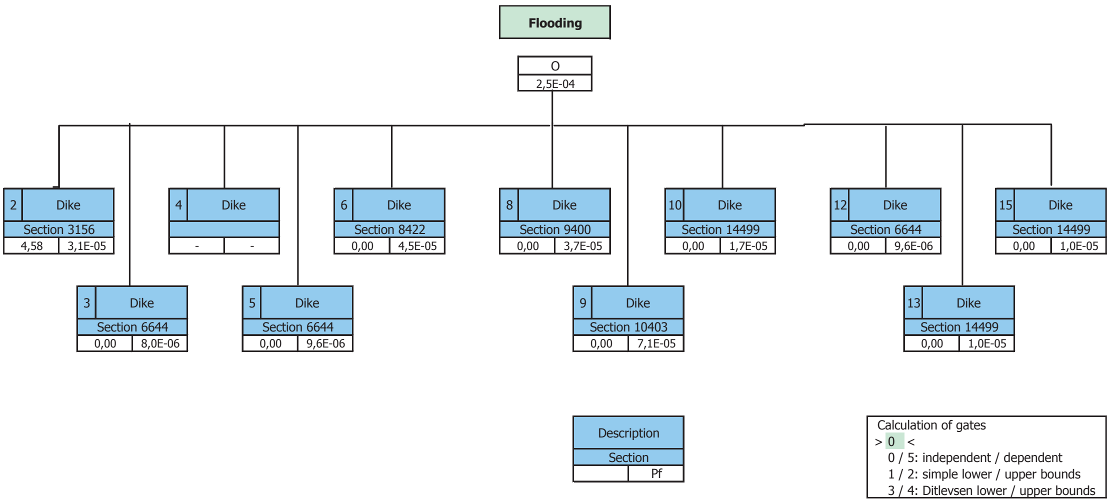

Figure 4-21: Reduced fault tree for the coastal defence system in Ribe (without sluice and outlets) (Oumeraci et al., 2004).

4.5.3 Remarks on the results

As already mentioned in Chapter 3, the main objective of the hazard analysis has been the calculation of the overall flooding probability of the Ribe defence system based on the ProDeich model (Kortenhaus, 2003). When calculating the overall failure probability, a total of 25 failure mechanisms have been applied at the main dike. At the Kammer sluice and the three outlets, a small number of failure mechanisms regarding overflow, wave overtopping and hydraulic uplift have been developed. However, these failure mechanisms have to be further evaluated in coming studies and the missing limit state equations e.g. concerning the sluice gates have to be defined in the future. Also the approach concerned with dividing the Ribe defence system into representative sections will be further investigated during the coming two years.

Therefore, the aforementioned results in Chapter 4.5.2 have to be seen as results of this study applying probabilistic calculations to the Ribe defence system. The results may, however, not be seen as the final overall flooding probability of the Ribe flood defence system.

5. Vulnerability analysis and damage potential

To carry out the risk analysis of the Ribe flood defence system it is necessary to know what consequences the failure of the main dike, the sluice or the outlets will have. Therefore, it is desirable to establish the relation between the effect (e.g. failure of the dike) and the consequences. This relation is established within the framework of a vulnerability analysis. The following chapters describe the vulnerability analysis of the Ribe flood defence system, which will be sub-divided into a valuation analysis and a subsequent damage analysis.

5.1 Description of the flood-prone area

The vulnerability analysis begins with the description and inventorying of the flood-prone hinterland. In order to limit the analysis to the elements most at risk, the flood-prone hinterland is delimited.

In Chapter 1.3 the present situation and the history of the hinterland have already been described briefly. The hinterland is mainly characterised by a flat rural area of former marshland and by an urban area, Ribe town. The urban area of Ribe town goes back to the period before the year 800, where the first settlements were established on high sandy land. However, an effective and protected (against regular flooding) exploitation of the rural area around Ribe town was not possible before the building of the Ribe dike from 1911 till 1914. The utilization of the hinterland may therefore be described as a two-part land utilization, which is historically conditioned.

5.1.1 Delimitation of the flood-prone area

The subsequent selection of the risk elements requires a delimitation of the area. The delimitation is further needed for the presentation of the land utilization and the spatial distribution of the assets within the valuation analysis. This way, the delimitation of the flood-prone area determines the geographical framework of the vulnerability analysis and thus represents the specific area within the risk analysis.

The delimitation orientates itself in relation to the existing flood defence system, topographical and hydrodynamic features as well as historical flood events. In the western direction, towards the North Sea, the flood-prone area is marked off by the main dike, which is described in detail in Chapter 4.1. At the northern and southern ends of the defence system two wing dikes delimit the Ribe hinterland towards the neighbouring flood-prone areas, which are protected by the Darum-Tjæreborg defence system in the North and by the Rejsby defence system in the South respectively. In case of failure at one of the neighbouring flood defence systems, the objective of the wing dikes is to prevent the intrusion of flood water into the Ribe hinterland.

The southern wing dike expands approximately 2,6 km into the hinterland in a south-east direction. The crown height of the wing dike varies between 5,7 m DVR90 and 6,0 m DVR90. The northern wing dike expands about 650 m into the hinterland in a north-east direction. The crown height varies between 5,4 m DVR90 and 6,4 m DVR90. Both ends of the southern and northern wing dikes lead into a topographical elevation at an altitude of 5,0 m DVR90.

For the purpose of further delimitation of the Ribe area towards the remaining hinterland, the altitude line of 5,0 m DVR90 is chosen for three reasons:

- The southern and northern wing dikes lead into a topographical elevation of 5,0 m DVR90. This way, the 5,0 m DVR90 altitude line is assumed to prevent the expansion of severe inundations.
- Through the ages, several storm surges have caused flooding of parts of Ribe town which presupposes flood levels of 4,0 m DVR90 or higher. These flood events occurred before the Ribe flood defence system came into existence. However, the worst assumable dike breach scenario, including an increase of the inundation volume by backwatering of the Ribe river discharge due to closed gates during a storm surge, justifies consideration of all risk elements up to a maximum inundation height of 5,0 m DVR90.
- Storm surge levels of 5,0 m DVR90 or higher have already been registered, e.g. during the storm surge on December 3-4, 1999.

The delimitation by the 5,0 m DVR90 altitude line, however, does not preclude that inhabitants and assets located in areas at an altitude higher than 5,0 m DVR90 may be affected in a very extreme case.

The delimitation of the flood-prone area by the 5,0 m DVR90 altitude line is presented in Figure 5-1.

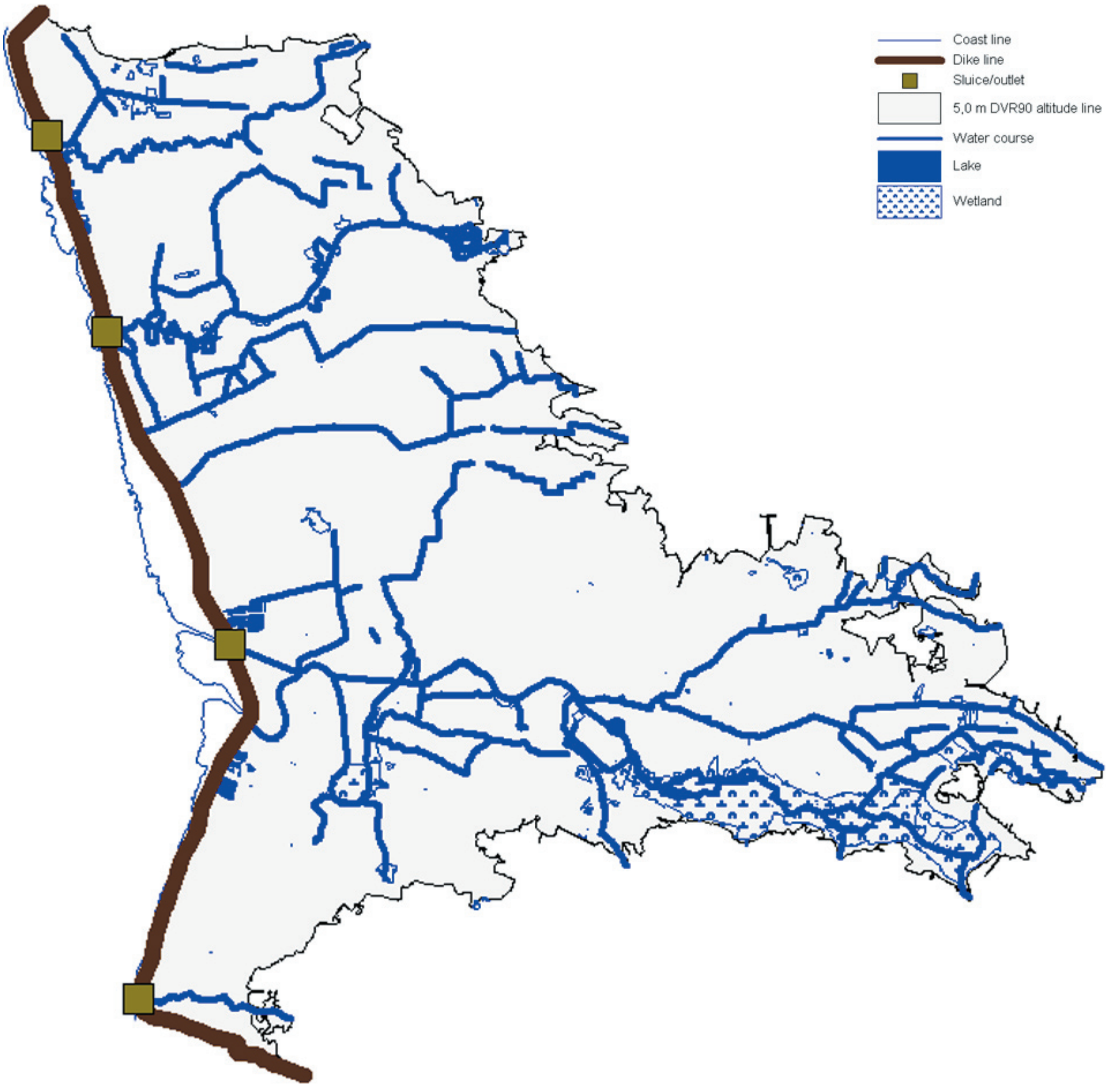

Figure 5-1: Delimitation of the flood-prone area.

Looking at the delimited flood-prone area in Figure 5-1, a major extension of the flood-prone area into the hinterland can be seen where the course of the dike line bends and changes direction. A more or less parallel course of the 5,0 m DVR90 altitude line to the course of the defence line can only be tracked for the northern part of the defence line. In the southern part of the defence line, the 5,0 m DVR90 altitude line runs eastwards into the hinterland. The reason for this can be found in the existence of the Ribe river and its connected streams (see Figure 5-1). The low-lying delta area around the watercourses extends about 12,5 km into the hinterland and thus also the course of the 5,0 m DVR90 altitude line surrounding the delta area.

Figure 5-2: Ribe river and its tributaries west of Ribe town.

5.1.2 Selection of risk elements

According to Figure 2-7 the different types of damage are classified as direct and indirect damage, tangible and intangible damage as well as primary and secondary damage. Direct damage is caused by contact with the flood water whereas indirect damage is a consequence of direct damage, such as interruption of transportation and communication or reduced investments in a specific area after flooding. The second level of classification distinguishes between tangible and intangible damage.

The aforementioned damage classification represents the basis for the selection of the risk elements. When selecting the risk elements not only the objectives of the valuation analysis have to be considered, but also the analysis of the damage potential has to be kept in mind. Both analyses require a quantitative description in a monetary way. Some types of damage can only be described by their number or in a descriptive way (intangible damage categories). This may also be valid for tangible damage types due to missing data and models or complex circumstances which are difficult to grasp. Here especially indirect damage types have to be mentioned.

It is therefore nearly impossible to consider all types of damage and consequences within a vulnerability analysis. The objective is, however, to register the dominant damage caused by flooding. Thus, the major part of the damage considered in a vulnerability analysis may comprise direct, tangible damage. Within the framework of this study, focus has therefore been laid on a number of elements at risk, which may be sorted into direct, tangible damage categories. Additionally, a few intangible, direct/indirect risk elements have been considered.

Within this study the following risk elements of direct, tangible damage have been chosen:

- Buildings, including residential buildings, agricultural buildings and industrial buildings;
- Movable property, including movable property in residential, agricultural and industrial buildings;
- Agricultural acreage, crops;
- Livestock;
- Electric installations (pumps, windmills);
- Traffic system (roads, railways).

As intangible, direct/indirect damage categories, the following risk elements are only considered in a descriptive form in Chapter 5.3:

- Inhabitants;
- Employees;
- Vehicles;
- Tourism.

Figure 5-3 presents an overview of the applied risk elements in this vulnerability analysis where most of the risk elements are classified as direct, tangible damage. These risk elements will be valuated within the valuation analysis and depth-damage functions will be derived for each of those risk elements within the damage analysis.

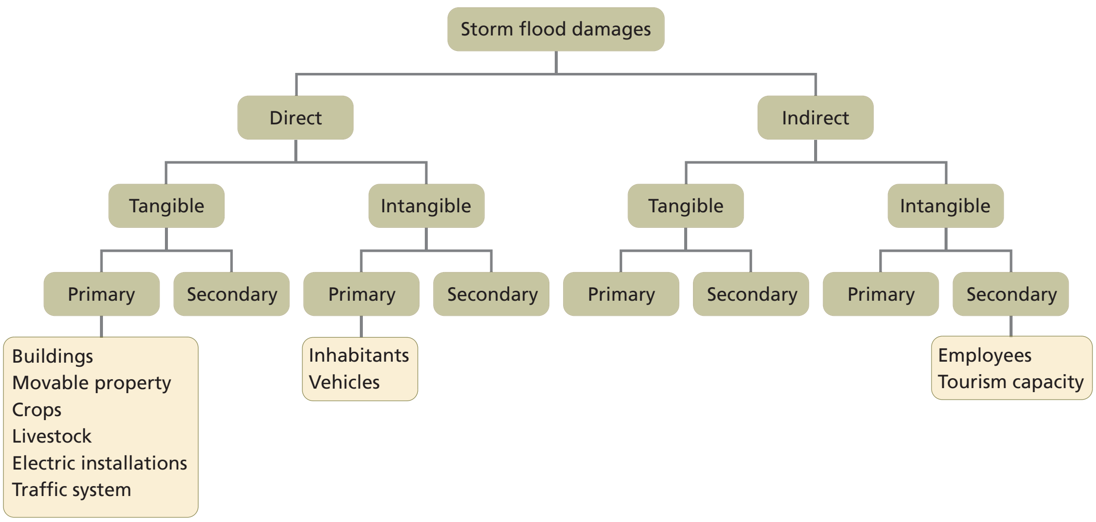

Figure 5-3: Risk elements considered in the vulnerability analysis.

A quite considerable number of scientific publications have discussed the valuation of human life. However, the valuation of a human life turns out to be quite difficult mostly due to ethical questions. This study therefore refrains from monetizing the value of the inhabitants or the damage potential in case of victims/casualties during a storm surge. This point is supported by the fact that evacuation plans exist for the Ribe area, which secure the evacuation of the inhabitants away from the place of danger in good time before storm surge culmination. It can therefore be assumed that in case of failure of the defence system only very few people, who have disobeyed the evacuation order, will be at risk.

In the category of industrial plants and large businesses, production breakdown or reduced investment may be the consequences of the flooding of industrial estates. It is, however, difficult to determine the tangible damage of production breakdown or reduced investments. Furthermore, the Ribe area is characterised by only few industrial plants or large businesses. It is therefore decided not to consider the indirect industrial damage potential in the vulnerability analysis. A description of the number of employees and their distribution by different industrial branches will, however, be presented.

Furthermore, vehicles are placed in the direct, intangible damage category based on the assumption that vehicles at risk will be either removed to safer areas by the owners or used in connection with evacuation measures. Vehicles are therefore only considered in a descriptive form.

The tourism capacity may count as direct as well as indirect damage. Indirect damage occurs if the number of tourists decreases as a consequence of an inundation event. Direct damage regarding the tourism capacity is in many cases difficult to quantify. Seasonal variations in overnight stays and the number of visitors have to be considered. For reasons of simplification, the tourism capacity is grouped into the indirect, intangible damage category and only valuated in a descriptive form.

5.2 Data request and set-up of data handling

The performance of a valuation analysis and a damage analysis requires a great amount of input data. The data basis should reflect a high level of detailed information to secure a sufficient representation of the assets and the damage potential in a flood-prone area (Reese, 2003).

The same applies to the cartographic basis used in the analyses. Especially in the damage analysis where the inundation extension and its depth are simulated, a precise topography of the flood-prone area is essential (see also Chapter 5.5.1).

Within this study, altitude data in a grid net of 25x25 metres is used to generate a topographical map of the flood-prone area within the 5,0 m DVR90 altitude line. Topographical data is available in Denmark at Kort

& Matrikelstyrelsen, Copenhagen. In order to supplement the altitude information of the grid net, altitude data from road surveys performed by the private survey company I/S Bramming is combined with the data from Kort & Matrikelstyrelsen. Based on both data sources, a digital altitude model is generated. Altitude data comprising a narrower grid net has not been available for the study area, which means that the generated digital model stands for the most accurate topographic information available for the Ribe area.

In a next step, altitude lines at regular intervals of 0,5 m, starting at 0 m DVR90 till 5,0 m DVR90, are interpolated. For each interval between two altitude lines the mean value of the altitude is calculated, which is further needed within the damage analysis. Figure 5-4 presents the topography of the Ribe flood-prone area within the 5,0 m DVR90 altitude line.

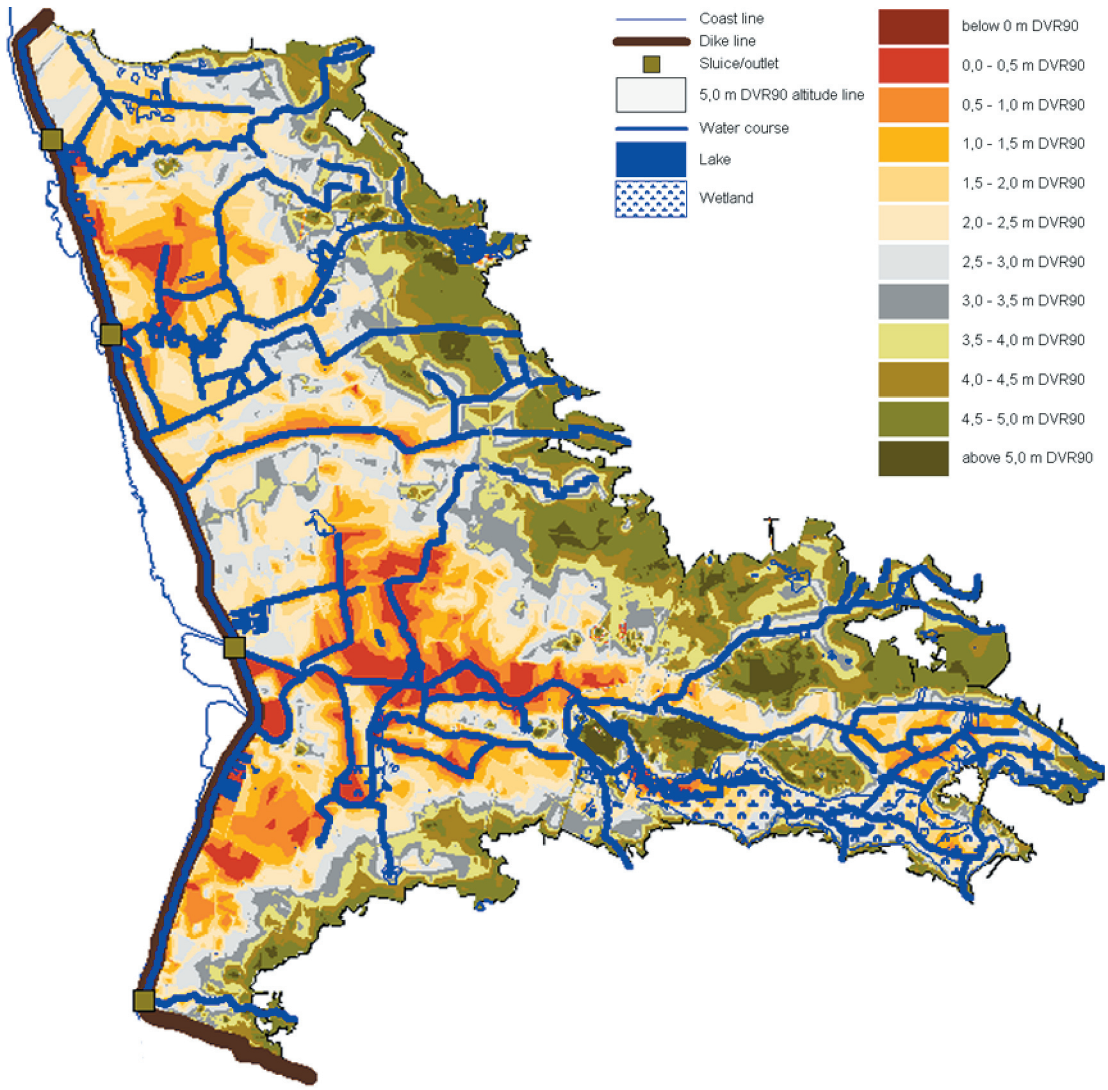

Figure 5-4: Topography of the Ribe flood-prone area.

Again, the influence of the Ribe river and its neighbouring streams on the characteristics of the flood-prone area can be clearly seen. The low-lying delta areas surrounding the watercourses (red areas) expand far into the hinterland (> 5 km). North of Ribe river and its low-lying areas, a topographic elevation stretches from West to East and divides the flood-prone area into a northern area and a southern area. This separation counts up to 2,5 m DVR90, which will be decisive in connection with the inundation scenarios in Chapter 5.5.3.

The size of the delimited flood-prone area is 96,7 km². Table 5-1 shows a distribution of the altitude intervals in the flood-prone hinterland of Ribe.

Altitude interval [m DVR90]	Mean altitude [m DVR90]	Area [km²]	[%]	Acc. [%]
< 0		0,02	0,02	0,02
0,0 - 0,5	0,25	5,91	6,11	6,13
0,5 - 1,0	0,75	6,62	6,84	12,97
1,0 - 1,5	1,25	9,59	9,91	22,88
1,5 - 2,0	1,75	12,77	13,20	36,08
2,0 - 2,5	2,25	16,06	16,60	52,68
2,5 - 3,0	2,75	11,46	11,85	64,53
3,0 - 3,5	3,25	8,04	8,31	72,84
3,5 - 4,0	3,75	7,65	7,91	80,75
4,0 - 4,5	4,25	7,52	7,78	88,53
4,5 - 5,0	4,75	11,10	11,47	100,00
Total		**96,73**	**100,00**	

Table 5-1: Distribution of altitude of the flood prone area.

A high level of accuracy is also desirable regarding the data and information about the risk elements in the flood prone area. However, this has been rather difficult for some of the risk elements. Despite the fact that a large number of registers exist in Denmark, the data acquisition and the data format of the registers differ. Some data has not been at our disposal due to data protection of the inhabitants' personal information. In other cases, a lower level of detail has been chosen in relation to what would have been possible in order to reduce the work load with respect to the available resources of the SP7 project.

The data basis and the data source, the reference data/period, and the procedure of geocoding will be described for each risk element in the following. The intangible risk elements will be dealt with at first, followed by the tangible risk elements.

Inhabitants

In general, the number of inhabitants at risk can be determined based on a residents' register. These registers are available for each municipality and comprise information about each registered person at a specific address. Due to the high level of personal information of each resident, the use of such data in this study is not allowed for data protection reasons. Thus, a direct description of the number of inhabitants for all addresses in the delimited area through data from the residents' register has not been possible.

A different approach is therefore applied. Statistics about the number of persons living in each household within Ribe Municipality are downloaded from Statistics Denmark. Furthermore, a mean value for the number of persons per household is calculated. The mean value of persons per household is afterwards assigned to each residential building and is thus geocoded by means of the risk element 'buildings'. The reference year of the statistical resident data is 2003.

Employees

To describe the number and distribution of employees for different branches in the Ribe Municipality, data is downloaded from Statistics Denmark. The reference year of the statistical data is 2002. In order to obtain an overview of the number of employees working in the flood-prone area, each branch is linked to the input data of the risk element 'buildings'. By comparing synonymous definitions of the branches and the application of buildings, the number of employees is geocoded in the flood-prone area. Depending on the altitude information of each building used for commercial purposes, the sorting of the employees into the altitude intervals is carried out.

Vehicles

The risk element 'vehicles' is only considered in a descriptive form, because most of the cars will be used in case of evacuation. It is further assumed that most car owners will move their cars into higher and protected areas during a flood event. The damage potential of vehicles will therefore be small in the case of flooding compared with more stationary risk elements. However, Chapter 5.3 will show the distribution of the car value by altitude. To do so, data is downloaded from Statistics Denmark which lists the number of households in Ribe Municipality as having no car, one car or two and more cars. The reference year of the data is 2002.

In a next step, a mean value of the number of cars per household is calculated and geocoded for each residential building in the flood-prone area. Furthermore, a mean value per car of 300.000 DKr. (€ 40.200) is defined.

Tourism

Statistics or registrations concerning the occupation of bed spaces in the Ribe area could not be found. The Ribe tourist office has, however, provided some attendance figures for the major attractions in Ribe town and in the surrounding area. These figures are stated for the period 2001 till 2003.

A valuation of tourism turns out to be quite difficult because tourism in Ribe is seasonal. This means that the largest numbers of visitors are seen during the months from May till October. The probability of a storm surge is, however, higher in the remaining months. Furthermore, a valuation of tourism based solely on the number of bed spaces would not take the many day-visitors into account, which constitute about 1 million day-visitors every year (personal communication with Ribe Tourist Office, 2003). The risk element 'tourism' will therefore only be qualitatively described in Chapter 5.3.

Buildings

One of the most important tangible risk elements are buildings. The risk element 'buildings' comprises residential buildings, agricultural buildings and industrial buildings. All data about buildings and apartments are registered in Bygnings- og Boligregistret (building and housing register) in Denmark. Here, information about ownership, built-up area, type of the building, use of the building, number of floors, the existence of a basement, road number and house number of the building, type of heating and further remarks on the building can be found. Data extracts from Bygnings- og Boligregistret are available through agencies which have permission to extract data from the register.

The data needed for the valuation analysis and the damage analysis for all buildings within the 5,0 m DVR90 altitude line has been provided by Gilling Communications & Consulting ApS, Copenhagen, Denmark. The reference year of the data is 2002. Each building or apartment is marked by only one geocode within Bygnings- og Boligregistret. A geographical description of the precise position of the surface area of each building is not available in this register. This is, however, anticipated to be negligible because the effect of possible differences in altitude around a building is considered to be very small with respect to the subsequent analysis of the damage due to flooding.

Movable property

The valuation and the analysis of damage to movable property are linked to the buildings. Based on the statistics of the Flood Compensation Council (Stormrådet), Copenhagen, a mean value of the movable property for different building types has been derived. Each building in the flood-prone area is provided with a mean value for movable property depending on its definition of use. This way, the value of the movable property is geocoded by means of the risk element 'buildings' and classified according to the building type. The data basis of the Flood Compensation Council refers to the year 2002.

Agricultural acreage

The agricultural acreage has been derived from cadastral maps, which were provided in geocoded form by Kort & Matrikelstyrelsen. Each cadastral map is sub-divided by one or more block numbers, which represent the smallest area, on which one sort of crop is cultivated.

In the next step, the most recent data about the cultivated crop sort on each block number has to be found. This information has been provided by the Danish Centre of Agricultural Research in Foulum. For each block number, the sort of crop is stated referring to the period 2001/2002.

Livestock

Data about the livestock of the farms within the flood-prone area is taken from the Central Livestock register. All relevant data about the animal species, number of animals as well as information about the farm are registered. However, the data do not include information about the block number on which e.g. cattle stock normally graze. Thus, some of the stocks may be several kilometres away from their home farm in case of a disastrous flood, which may result in the farm and the accompanying stock suffering different damage as a result of flooding. It is not possible to consider this differentiation regarding the actual location of the stock within the damage analysis with the data basis in hand.

As in the case of Bygnings- og Boligregistret, only authorised agencies are allowed to extract data from the Central Livestock register. For this reason, Maersk Data Public, Copenhagen, has been contacted. The received data refers to the year 2002 and is geocoded by means of the addresses of the farm buildings.

Electric installations

Within this study electric installations comprise windmills and pumps for public supply of drinking water as well as pumps used for sewage disposal. Data about windmills is taken from the digital topographical map TOP10DK in the scale of 1:10.000. The reference year used in this study is the year 2000. The TOP10DK map is provided by Kort & Matrikelstyrelsen and is constructed as a vector map comprising 7 object classes and 47 topics as well as altitude information. The map is updated every 5 years.

Data about pumps within the public supply network in Ribe has been delivered by Ribe Municipality. The data was taken from the municipality's own GIS application, which made another geocoding of the pumps unnecessary. The input data about public pumps refers to the year 2002.

Traffic system

The risk element 'traffic system' comprises the network of roads and railway tracks in the flood-prone area. Data about the road network has been provided by Ribe County, including a division into the following road classifications: path, second road, 3-6 meter wide road, road over 6 meter wide, and expressway. Again, the data had already been geocoded which simplifies the entering of the data into the GIS application used in this study. The county's data refer to the year 1997.

The location and length of railway tracks in the Ribe area are taken from the TOP10DK map.

For the purpose of processing all data concerning the risk elements, the data is input into the GIS application software MapInfo Professional Version 7.5. The analysis work for determining the spatial distribution of the damage potential as well as the damage within inundation scenarios have been performed by means of the aforementioned GIS software and MS Excel calculations.

5.3 Valuation analysis

This chapter describes the valuation of the tangible risk elements. By valuating the tangible risk elements, the damage potential of the flood-prone area is determined and quantified. The chapter will, however, begin with a short description of the intangible elements (inhabitants, employees, vehicles, tourism).

Inhabitants

The statistics of the number of persons living in each household within Ribe Municipality show that 60 % of all households consist of either 1 person, 2 persons or 3 persons (see Figure 5-5). 16 % of all households consist of 4 persons, and households of more than 4 persons make up 17 %. Based on this distribution of the number of occupants per household, a mean value of persons per household is calculated to 2,3 persons.

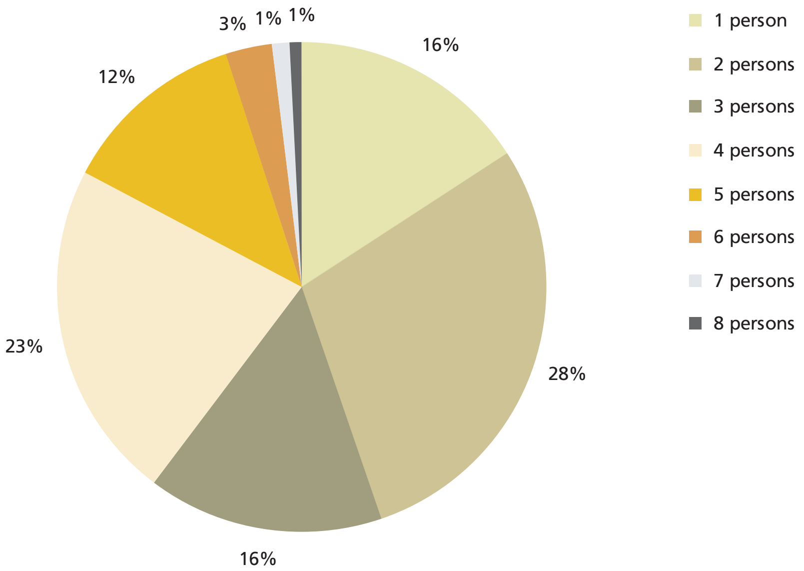

Figure 5-5: Distribution of the type of household by number of occupants.

By assigning the mean value of 2,3 occupants per household to each residential building in the flood-prone area, the distribution of the number of inhabitants over the altitude intervals can be determined. This is illustrated in Figure 5-6.

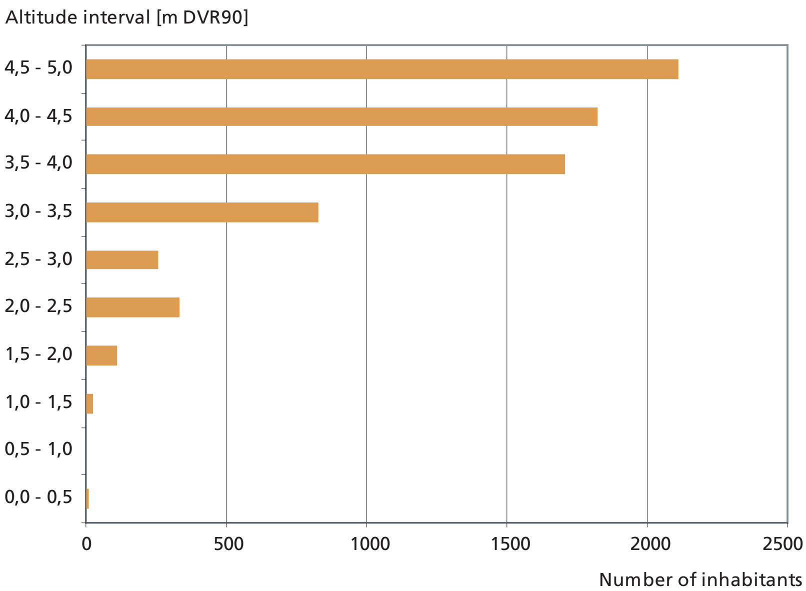

Figure 5-6: The number of inhabitants within each altitude interval.

Figure 5-6 shows that the majority of all inhabitants live in areas above 3,5 m DVR90, which again may be explained by the historical development of the area. Altogether, approximately 7.500 persons live within the delimited flood-prone area.

Employees

As mentioned before the Ribe area is characterised by few industrial plants and service companies, whereas tourism is a major economic sector. This is confirmed by considering the numbers employed. Figure 5-7 illustrates the proportional distribution of the number of employees in the Ribe Municipality.

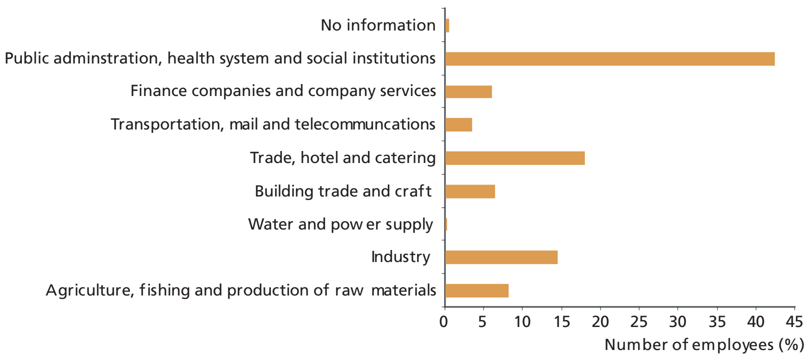

Figure 5-7: Proportional distribution of the number of employees.

Figure 5-7 clearly shows that the largest portion of employees is working within public administration and in health/social institutions. The second largest group consists of employees working within trade and the hotel and catering industry. Employment in industry only makes up about 15 % of total employment.

Comparing the employees' branches with the description of geocoded commercial buildings, most workplaces are located within Ribe town on ground above 3,5 m DVR90.

Vehicles

Based on the statistics of private cars, a mean value of the number of cars per household within Ribe Municipality is calculated to 1,3 cars per household. The mean value is afterwards multiplied by the number of households within each altitude interval. Each car is valued at an average initial price of 300.000 DKK. Figure 5-8 illustrates the car value within each altitude interval.

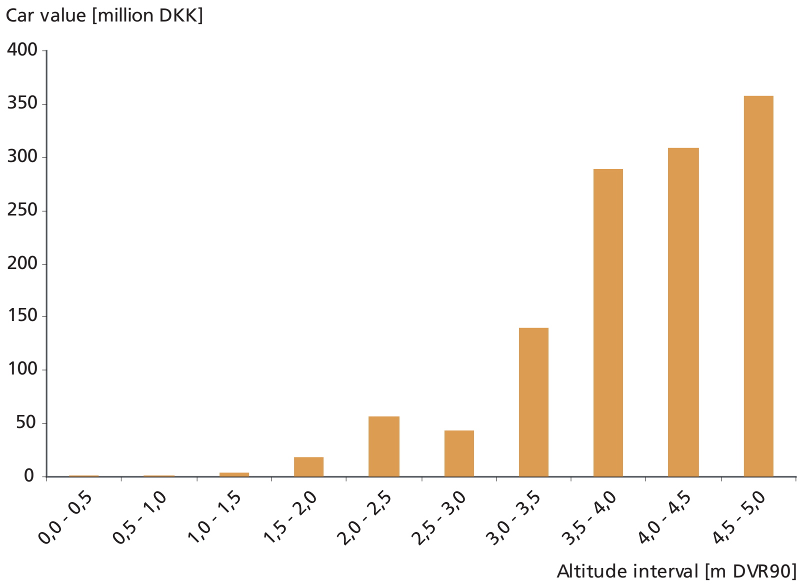

Figure 5-8: Total car value within each altitude interval.

Tourism

The Ribe tourist office has provided the attendance figures of six major tourist attractions, e.g. Ribe cathedral, the old town hall and the Viking museum. By adding up the individual attendance figures, it turns out that about 230.000 visitors have been registered in total at the six attractions per year. The attendance figures further show an increase of visitors during the period 2001 – 2003. Together with the about 1 million day-visitors of Ribe town per year, the figures show the importance of tourism for Ribe town and the surrounding area. A major flooding catastrophe affecting Ribe town and its major tourist attractions will therefore cause immense direct and indirect damage to the tourist trade in the Ribe area.

Buildings

Buildings are important assets to be considered within the valuation analysis because of their high value in most cases. Table 5-2 lists the number of buildings for different fields of application within each altitude interval of the flood-prone area.

Key	Field of application	Altitude interval [m DVR90] 0,0 - 0,5	0,5 - 1,0	1,0 - 1,5	1,5 - 2,0	2,0 - 2,5	2,5 - 3,0	3,0 - 3,5	3,5 - 4,0	4,0 - 4,5	4,5 - 5,0	SUM
110	Residential building to agricultural estate				2	4	22	27	36	39	53	**183**
120	Detached house	3	3	2	22	59	67	203	382	544	610	**1895**
130	Terrace house			5	12	11	8	98	285	169	206	**794**
140	Apartment building	1		4	8	4	8	13	31	36	41	**146**
150	Student hostel						1		2	1	5	**9**
160	Home for children, old people's home				5	4	1	18	2	1	1	**32**
190	Other building for all-year living							1		1		**2**
210	Farm building (agriculture, gardin-ing, forestry)				9	24	95	140	156	204	238	**866**
220	Factory, workshop (industry, craft)			3	1	3	7	10	35	25	73	**157**
230	Buildings for public water and power supply			3		3	10	2	5	7	9	**39**
290	Other building for agriculture of industry						3	3	1		2	**9**
310	Transport- and garagebuilding (freight)				2	1	3	4	6	11	19	**46**
320	Office, trade, warehouse, public administration			1	6	9	23	23	49	54	104	**269**
330	Hotel, restaurant, laundary, service company			1		1	1	24	7	7	5	**46**
390	Other building for trade and service						5	3	1	2	4	**15**
410	Cinema, teather, library, church, museum				4			3	5	6	8	**26**
420	Teaching and research work			1	2	5	7	2	8	8	3	**36**
430	Hospital, outpatients' department				2					1	6	**9**
440	Kindergarten, day nursery							4	3	5	1	**13**
510	Summer house					63	4		4	2	2	**75**
520	Youth hostel, holiday camp						1		1		5	**7**
530	Gym, indoor pool, clubhouse					4	1	3	3	2	3	**16**
540	Allotment graden house	1	6	14	35	7	10	4	2	3		**82**
590	Other building for leisure activities					4	1	2	3	1	6	**17**
910	Garage (1-2 vehicles)	1		3	6	29	30	98	169	228	251	**815**
920	Carport	2	3	1	6	15	29	110	280	268	323	**1037**
930	Outhouse	1	1	6	26	44	47	120	151	249	310	**955**
	SUM	**9**	**13**	**44**	**148**	**294**	**384**	**915**	**1627**	**1874**	**2288**	**7596**

Table 5-2: Number of buildings for different fields of application.

The fields of application key-coded from 110 to 190 are defined as residential buildings within this study. Fields of application numbered from 210 to 290 stand for agricultural and industrial buildings. The key-codes from 310 to 440 are arranged in one group as buildings for public administration, trade and service. Fields of application numbered from 510 till 590 are finally combined as buildings for leisure activities. Appendix E comprises a map showing the location of the buildings in the flood-prone area differentiated by the four groups. Garages (910), carports (920) and outhouses (930) are not included in the map in Appendix E.

The valuation of the building asset in the flood-prone area is based on the public property value[5] of the building. Figure 5-9 illustrates the total property value of buildings distributed over the altitude intervals.

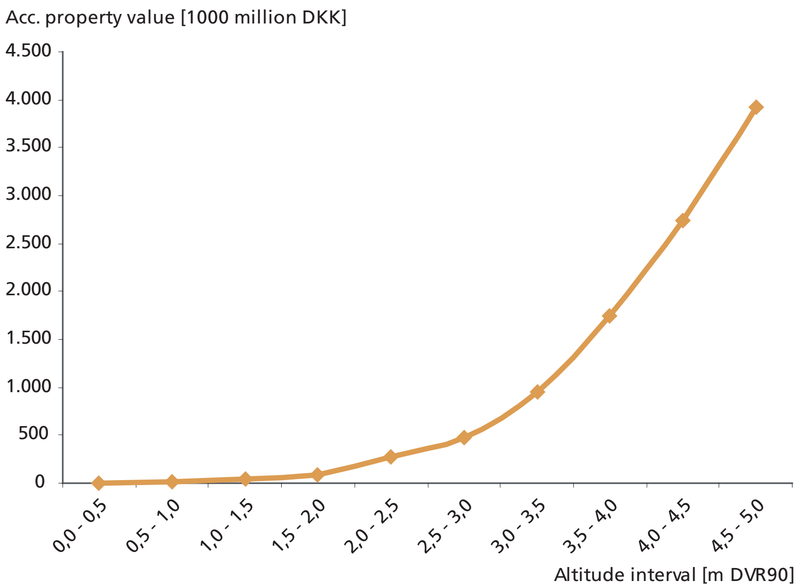

Figure 5-9: Total property value distributed over the altitude intervals.

It is noteworthy that approximately 7 % of the property value is located below 2,5 m DVR90. About 45 % of the property value is placed at altitudes of up to 4,0 m DVR90 and about 30 % of the total property value is located within the altitude interval of 4,5 – 5,0 m DVR90. It may therefore be expected that the damage to buildings due to flooding will only be great during flooding disasters with inundation heights above 2,5 m DVR90.

Movable property

For movable property, no valuation has been performed. The damage to movable property is derived on the basis of data about compensation payments for movable property, which will be described in the following Chapter 5.4.

Agricultural acreage

The valuation of agricultural acreage and crops has been performed by external experts from the DSH Centre in Løgumkloster, Denmark. The

[5] All buildings in Denmark are regularly valued by the Danish tax authority for taxation of property. The property value of each building represents the approximate selling price of the building. The property values are accessible at public registers.

valuation analysis conducted by the DSH Centre has considered the cultivated crops in the delimited flood-prone area. The results of the valuation are presented in Table 5-3. The profit per hectare for the most common crops referring to the price level of 2003 is stated as well as the acreage (see also Appendix E).

Crop	Area [ha]	Profit per ha. [DKK]	Sum value [DKK]
Winter wheat	1.086	6.300	6.839.904
Winter grain	324	4.400	1.424.174
Spring grain	2.463	4.950	12.191.158
Arable grass	2.054	4.550	9.345.658
Permanent grass	520	3.150	1.637.926
Fallow land	567	0	0
Forest	5	0	0
No farm land	1.150	0	0
No information	1.806	0	0
SUM	9.974		31.438.820

Table 5-3: Profit per hectare for representative crops within the flood-prone area.

A differentiation of the total profit of all crops over the altitude intervals is shown in Figure 5-10. An almost linear distribution can be seen, which differs remarkably from the other risk elements.

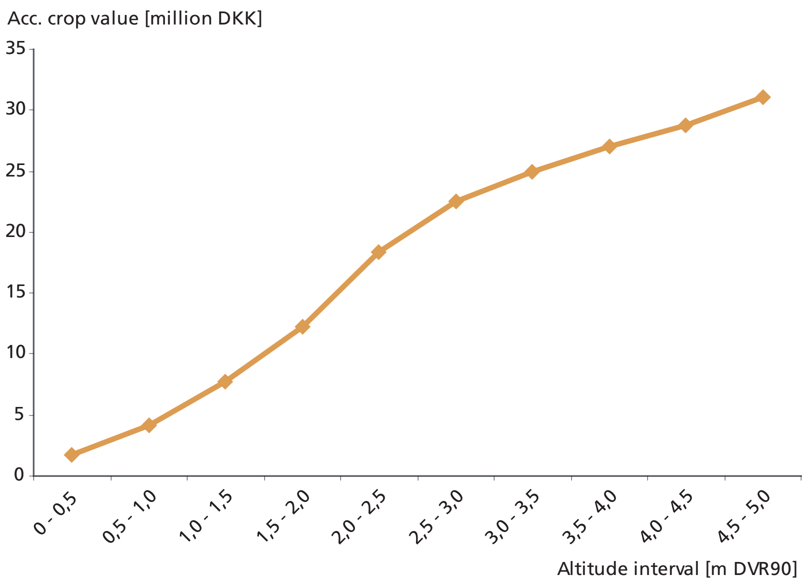

Figure 5-10: Total profit distributed over the altitude intervals.

Livestock

Based on the individual purchase price of each animal species (data by the DCH Centre), the value of livestock is calculated to be approximately

48,6 million DKK (€ 6,5 million). Adding the profit of the livestock, the total value of livestock within the flood-prone area amounts to about 86,8 million DKK. (€ 11,7 million). A map of the geocoded livestock is included in Appendix E.

Electric installations

Within the delimited area, six windmills and eight pumps are located. The eight pumps, which function within the public water supply network, are distributed evenly over the eight altitude intervals. With respect to the six windmills, an even distribution over the altitude intervals also exist within the six highest intervals.

The purchase price of a supply pump is assumed to be 60.000 DKK (€ 8.050), whereas the price of one windmill is set to 7.000.000 DKK (€ 939.600).

Traffic system

Data about construction costs for different road classifications have been provided by Ribe County. Table 5-4 gives an overview of the construction costs as well as the total value of all road classifications within the flood-prone area.

Road	Length [km]	Price per km [DKK]	Sum value [DKK]
Path	24,3	1.100.000	26.730.000
Second road	191,5	1.000.000	191.500.000
Road 3-6 m	120,1	3.700.000	780.650.000
Road over 6 m	13,5	6.500.000	87.750.000
Expressway	0,1	6.500.000	650.000
SUM	349,5		1.087.280.000

Table 5-4: Construction costs and value of different road classifications.

5.4 Derivation of the depth-damage functions

In a next step, functions have to be derived, which describe the damage to an inundated risk element in relation to the inundation depth. For other risk elements, the damage potential will be independent of the inundation depth. Here, the damage of the risk element is described by a damage factor. For buildings, movable property, agricultural acreage, livestock, electric installations and roads the particular depth-damage functions or damage factors will be described in the following.

Buildings

For the risk element 'buildings' comprising residential buildings, agricultural buildings and industrial buildings, one common depth-damage function is derived. The damage function considers damage to the building itself, e.g. damage requiring repair work on masonry and woodwork (doors, windows), cleaning and dehumidification of the building, or painting and restoration.

In Denmark the Flood Compensation Council (FCC) is responsible for compensation payments in the case of flooding caused by storm surges. Compensation is paid to private persons, companies and farms, who have suffered damage due to coastal flooding. All claims for compensation payments are registered at the FCC. Data about compensation payments regarding flood damage to buildings in the Ribe area is therefore available for the reference years 1999 and 2000. Based on this data, a depth-damage function for damage to buildings is set up. For this purpose, two models, one model considering the inundation depth outside the affected building, the other model considering the public property value of the building (see Chapter 5.3), are derived by best-fitting based on the FCC data on flood damage to buildings. Next, both models are combined within one depth-damage model. The concurrence of the depth-damage model with the available FCC data is illustrated in Figure 5-11.

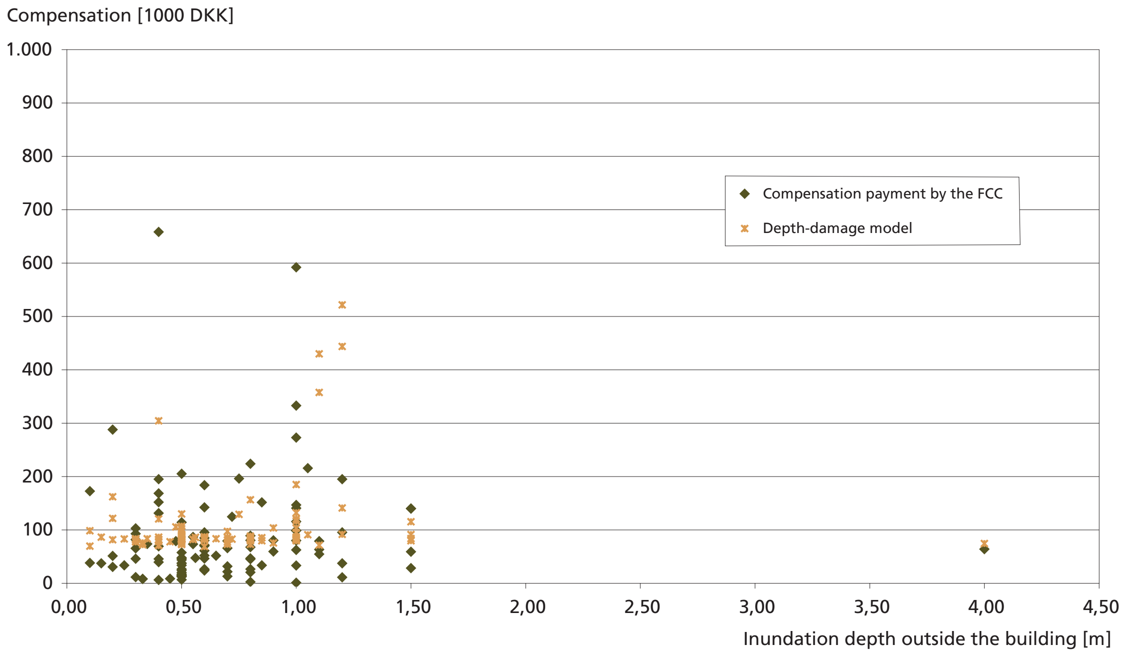

Figure 5-11: Depth-damage model for buildings vs. compensation payments by means of FCC data.

Figure 5-11 shows no clear relationship between the amount of compensation and the outer water level for compensation payments below 60.000 DKK (€ 8050). In a way, higher water levels outside the building should result in higher compensation payments. However, the compensation amount is determined by insurance agents, who must consider further aspects besides the outer water level and the property value when assessing the flood compensation. The derived model therefore only represents an average description of compensation payments for flood damage to buildings.

Movable property

For movable property, two depth-damage models have been derived. One considers damage in residential buildings (private sector) to e.g. household effects, and the other one considers flood damage in agricultural/industrial buildings (economic sector) to e.g. production equipment. This division is made because the FCC data on movable property showed a clear distinction between the private sector and the economic sector. For both sectors the approach used to define the depth-damage models has been identical to the approach used for buildings. For each sector (private and economic), two models, one model considering the inundation depth outside the affected building, the other model considering the buildings public property value, are derived by best-fitting based on the FCC data on compensation payments regarding movable property. For both sectors, the models are again combined to one depth-damage model. The depth-damage model for the private sector is illustrated in Figure 5-12.

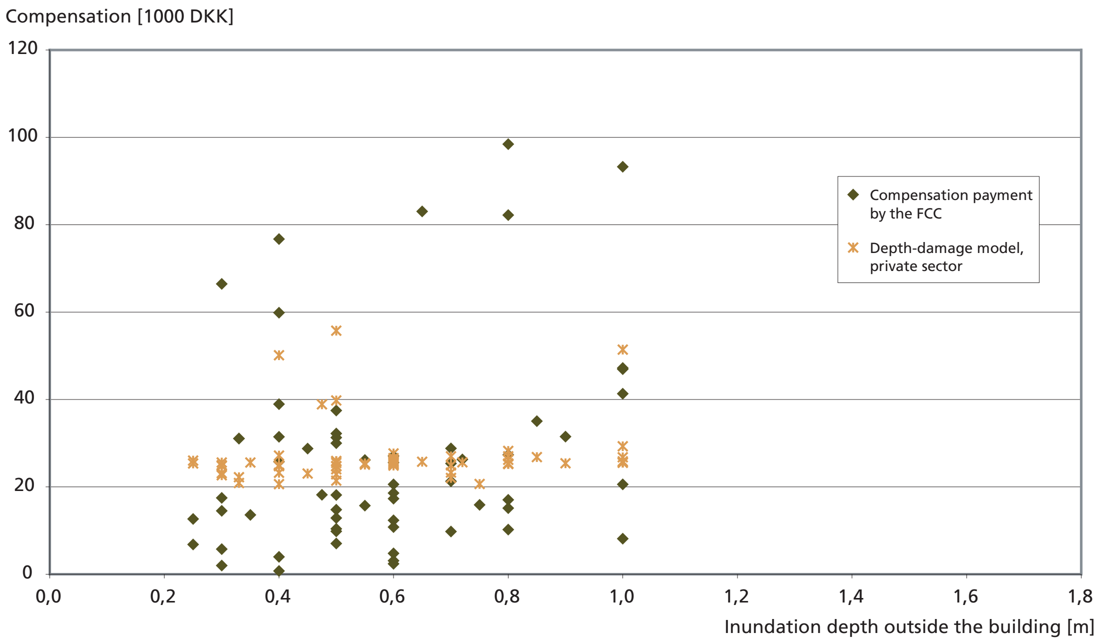

Figure 5-12: Depth-damage model for private movable property compared to the FCC compensation payments.

The same remarks as those described for the building model are valid for the depth-damage models on movable property. The compensation payments differ significantly due to the individual assessments of the insurance agents, which required the derivation of models representing an average description of compensation payments for damage to movable property.

Agricultural acreage

An assessment of the flood damage at agricultural acreage and crops has been performed by the external experts from the DSH Centre. The assessment comprises the damage factors for different crops and inundation periods of 5, 14 and 28 days. Furthermore, direct damage due to oxygen starvation as well as indirect damage due to salt intrusion into the soil have been considered. Additionally, the damage factors are differentiated according to the time of the flood event, since an inundation in October causes less damage compared to an inundation in March where the damage is greater.

The water depth is estimated to have very little influence on crop failure, whereas the duration of the inundation is important for the damage extent. Winter crops will be totally damaged after an inundation period of 14 days, while grass may survive up to 28 days of flooding. Salt intrusion will occur in hollows where the flood water stays throughout the inundation's retreat. The area of hollows within the flood-prone area where salt intrusion into the soil may take place is included in the assumption by a mean value of 15%.

Table 5-5 shows mean values of the damage to crops differentiated by the month of occurrence and the inundation duration.

Mean damage [DKK/ha]						
	October	November	December	January	Febraury	March
5 days	170	232	425	557	775	1097
14 days	303	411	595	823	1020	1337
28 days	1013	1281	1617	1952	2120	3030

Table 5-5: Mean value of the damage to crops differentiated by the month of occurrence and the inundation duration.

Livestock

The DSH Centre has also provided damage factors for livestock. Damage to livestock is normally defined as the number of animals killed due to drowning or stress multiplied by their market price. Furthermore, the production loss, which is suffered in the period after the inundation event due to reduced production capacity, is considered. The production loss continues until total production capacity is regained.

Death due to drowning or stress depends on the inundation depth. The DSH Centre has calculated water depths for all relevant animal species. Cattle stock and cow stock are being killed at water depths of 1 m or higher. Pigs and poultry stock are, however, already at risk at water depths of 0,1 m.

Electric installations and traffic system

Damage functions for pumps within the public supply network and for windmills are derived through expert interviews or literature research, respectively. For pumps, it is assumed that flood water and suspended sediment will damage all electronic parts inside the pump. This requires replacement of the flooded pump by a new pump.

For windmills, Reese (2003) states a damage function where the damage percentage is calculated as 2,3 times the inundation depth referring to the initial costs of a windmill. For inundation depths of more than 2 m the damage percentage remains constant at 4,6 %.

Normally, severe damage to roads and railway tracks occurs only in the area close to the dike breach because of the high current velocity of the inflowing flood water. Outside a 300 m distance from the gap, the current velocity decreases significantly, which means that e.g. scour damage under the carriageway surfacing will only be local. However, major costs arise due to the required cleaning of the roads and the road ditches from sediment depositions and drifted fragments.

Within a 100 m wide current cone, Reese (2003) states a damage factor of 80 % for cleaning and repair work referring to the initial building costs. Within a distance of 300 m or more, the damage factor is set to 10 %. Within the subsequent damage analysis a damage factor of 10 % is applied.

5.5 Damage analysis

As already described in Chapter 4, the top event of the fault tree is defined as the flooding of the hinterland. This can either take place in the case of collapse of the structure where water enters the protected area through a gap, or in case of wave overtopping/overflow where a large water volume flows over the dike crest.

For determination of the damage due to inflowing water in case of dike breach or wave overtopping, scenarios have to be defined comprising different breach and overtopping situations. It is only by means of scenarios that the inundation behaviour (e.g. inundation depth, inundation duration) can be simulated and the assessment of the related damage becomes feasible.

5.5.1 Criteria for definition of inundation scenarios

An investigation of the inundation behaviour begins with the definition of scenarios comprising different inundation events. For this purpose, four criteria are considered while defining relevant scenarios:

- the topography of the hinterland (Chapter 5.2)
- type of flood defence structure,
- the failure probability of each section (Chapter 4.5)
- spatial distribution of the risk elements in the flood-prone area (Chapter 5.3).

The topography of the hinterland (sub-areas)

The topography of the hinterland is most important for simulating the inundation behaviour. As mentioned in Chapter 5.1 the area behind Ribe dike is characterised by flat topography. However, a topographic elevation stretches from West to East. This elevation influences the inundation process in a way which first requires the total filling of one sub-area before the inundation spreads to the adjoining sub-area. On the other hand, the low-lying areas surrounding Ribe river and the other watercourses as well as the watercourses themselves will support a fast intrusion of flood water into the hinterland.

Based on a closer inspection of the topography behind Ribe dike, the flood-prone area is divided into two sub-areas, a northern area and a southern area. Figure 5-13 shows the position and size of the two sub-areas.

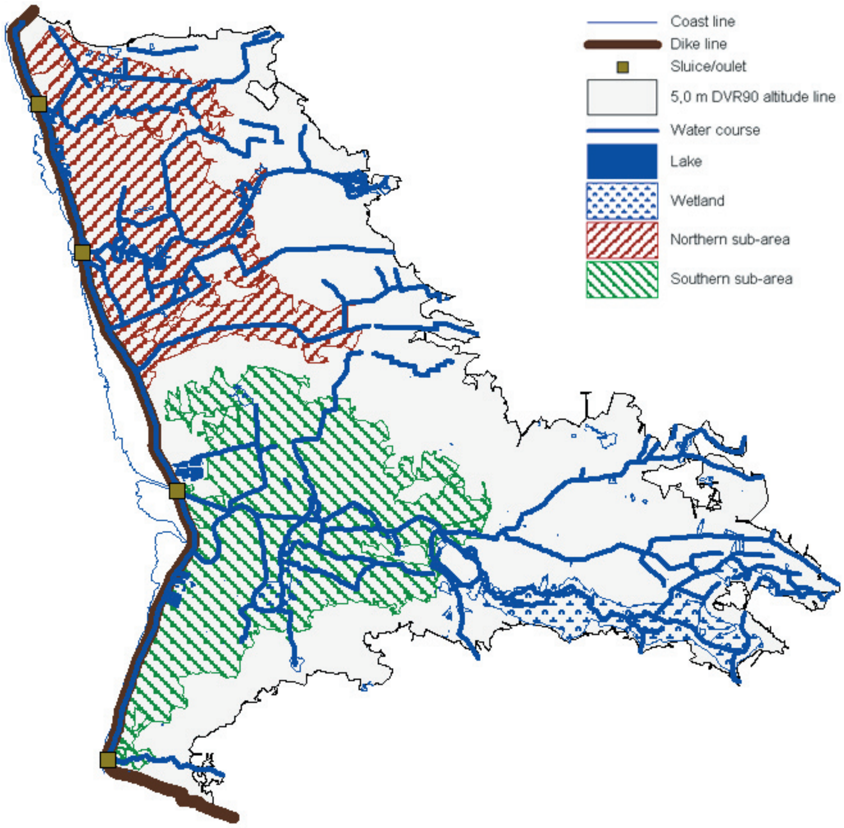

Figure 5-13: Position and size of the two sub-areas.

The division into a northern area and a southern area applies up to 2,5 m DVR90. Thus, further extension of the inundation into the adjoining sub-area presupposes an inundation level above 2,5 m DVR90. This way, the location of failure (dike breach or wave overtopping) is important in relation to the delimitation of the two sub-areas.

Type of flood defence structure

A second criterion for the definition of scenarios is the type of defence structure where a possible failure may occur. At the Ribe defence system a failure may either occur at the Kammer sluice, at the outlets or at the dike structure itself.

Probability of failure

When defining relevant breach and overtopping scenarios, the results of the probabilistic calculations are considered by taking into account the failure probabilities of each section (see Chapter 4.5).

Spatial distribution of the risk elements in the flood-prone area

Furthermore, the spatial distribution of the risk elements is considered in the set-up of scenarios. The location of the major portion of assets on high ground around the low-lying delta area of Ribe river promotes a larger safety reserve in a flood event – or explained differently: Only major failure events at the defence system, including a certain inflow volume, will cause severe damage in areas with more assets, e.g. in Ribe town.

5.5.2 Input parameters of inundation scenarios

The failure scenarios must be described by a number of parameters in order to simulate the inundation depth and extension:

- leading failure mechanisms for releasing the top event (dike breach or wave overtopping),
- highest water level and storm surge hydrograph,
- time of failure during storm surge,
- location of failure,
- time-dependent development of the dike gap,
- Ribe river and the discharge at the sluice (preceding inundation due to closed floodgates).

Leading failure mechanisms

As shown in Figure 4-6, the three failure mechanisms causing the top event (inundation of the hinterland) are overflow, wave overtopping and dike breaching. In Chapter 4-4, the failure probability of each failure mechanism has been calculated for each of the six representative cross-sections (see also Appendix D). The calculations showed the highest failure probabilities for the failure mechanism ‘wave overtopping’, assuming a maximum permissible overtopping rate of 20 l/(sm). The permissible overtopping rate of 20 l/(sm) is dependent on the circumstances of the adjacent hinterland (size of polder, building density, damage potential) and the dike stretch, where wave overtopping occurs (Kortenhaus & Oumeraci, 2002). Within this study the acceptable overtopping rate is set to 20 l/(sm).

As further mentioned in Chapter 4.4, wave overtopping is also the relevant failure mechanism for the sluice and the outlets. However, the volume of overtopping water over a 10 m wide sluice or over a 30 m wide outlet is very small compared to several dike kilometres, and will therefore not cause a major flooding event in the flood-prone area. Wave overtopping at the sluice or at the outlets is therefore not considered when defining relevant failure scenarios.

The failure mechanism 'overflow' is neglected because of the low probability. However, the consideration of overflow in a scenario would be comparable to the failure mechanism 'wave overtopping'.

The third failure mechanism to be considered in the scenarios is the dike breach itself. During a dike breach, a flow channel and a subsequent gap develop due to erosion. The inflow volume into the hinterland strongly depends on the size of the gap as well as on the gradient between the inner and outer water levels. These parameters are important for the inundation simulation and will be further described below.

Highest water level and storm surge hydrograph

The water level during a storm surge on the seaward side is an important parameter, not only for probabilistic calculations. The flood peak and the water level course are furthermore relevant parameters for determining the inflowing water volume through a gap or due to wave overtopping. For this purpose, a standardised water level hydrograph is derived. The standardised hydrograph is based on the five highest storm surges which have been monitored completely at four water level gauges in the Danish Wadden Sea from 1972 till 2002. The storm surge curves are related to their highest water level by means of a simultaneous plot. For every 20 cm level below the flood peak, the mean retention period and its standard deviation are calculated. Table 5-6 lists the calculated values.

Level below max. water level [cm]	Mean retention period [h]	St. deviation [h]
0	0,03	0,11
-20	2,29	1,24
-40	3,63	2,36
-60	4,62	3,15
-80	5,46	3,69
-100	7,15	5,05
-120	9,55	6,46
-140	11,64	7,36
-160	13,92	8,28
-180	16,26	9,83
-200	19,48	11,52
-220	23,47	12,48
-240	27,32	12,52

Table 5-6: Standardised storm surge for the Danish Wadden Sea.

Assuming a storm surge culmination at a maximum water level of 5,0 m DVR90, Figure 5-14 illustrates the related water level hydrograph. For the calculations of the inflowing water volume within the inundation simulation, the standardised water level hydrograph constitutes the basis for each scenario only distinguished by the assumed flood peak level.

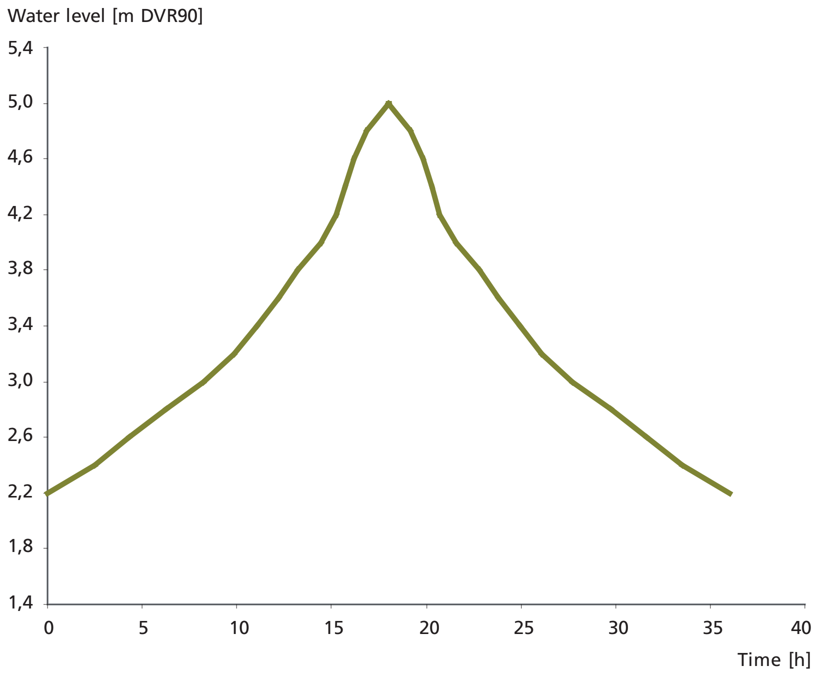

Figure 5-14: Standardised storm surge hydrograph based on a flood peak level of 5,0 m DVR90.

Time of failure during storm surge

Furthermore, the time of failure in relation to the standardised storm surge hydrograph has to be defined. A dike breach during a raising water level will result in a larger inflow volume than a breach occurring after the surge culmination during a falling water level. For reasons of simplification, the time of failure is set in relation to the flood peak. An assumed time of failure of e.g. -6 hours represents a failure event which occurs six hours before the flood peak.

Location of failure (dike breach or wave overtopping)

As mentioned before, the location of a dike breach or wave overtopping is important in the simulation of the inundation due to the flood water extension governed by the hinterland topography. Topographical elevation will limit the spreading of the flood wave, while on the other hand flood water is easily transported into the hinterland by means of the existing watercourses and their low-lying areas.

However, the precise position of a dike breach or a dike stretch with wave overtopping is not known in advance. The conditions and parameters which govern the location of a dike breach event or an overtopping event are not known yet. In the coming years, attempts will therefore be made to develop approaches which will enable a more precise positioning of an overall failure event along a flood defence system.

Within this study, the positioning of e.g. an assumed dike breach is limited to the selection of one or more dike sections. For example, the assumption of one dike breach within Section 6 is made. The precise position within Section 6 is, however, not known and will therefore not be defined. The selection of relevant sections for e.g. a dike breach is mainly governed by the calculated overall failure probabilities of each section, see Chapter 4-5. The overall failure probabilities of the sections are also graphically illustrated in Appendix F.

Time-dependent development of dike gap

In case of a dike breach, the time-dependent development of the gap has to be considered. The width of the gap through which water flows into the hinterland depends on the time-dependent gradient between outer and inner water levels as well as the geotechnical features of the dike.

Up to now, only the method of Visser (1998) has described the time-dependent breach development of a sand dike. According to Visser (1998) five stages can be distinguished in the process of a breach at a sand dike. The breach erosion starts with the flow of water through a small initial breach at the top of the dike with a trapezoidal cross-section. Within the first three stages, the flow of water increases the cross-section of the channel on the inner slope of the dike. The slope angle of the channel gets steeper and retrograde erosion decreases the width of the dike crest. After the vanishing of the crest, the inflow increases which results in increased erosion of the dike core. At the same time the gap width increases. At the end of the third stage, the dike core in the breach is completely washed out down to the dike base at polder level. At the fourth stage, the breach continues to grow laterally. At the fifth stage, the breach continues to grow until the point of time where the flow velocity becomes so small that the breach erosion stops. This point of time depends on the gradient between the outer and inner water levels. At the time where the inner water level reaches approximately 0,7 times the height of the outer water level, the flow velocity through the gap will start decrease, which results in a decreased erosion rate on the breach sides. The flow through the breach stops when the water level in the flooded hinterland equals the outside water level. At that time, the final breach width is reached.

The inner water level, however, depends on the storage capacity of the flood-prone area. In order to simplify the calculation of the inflow volume and the simulation of the inundation behaviour, two assumptions have been made:

- The time at the end of the third stage has been chosen as the starting time for calculations of the breach development and the inflow volume. At that time, the vertical erosion is ended and the dike core in the breach is completely washed out. The previous breach stages are thus not considered in the inundation scenarios within this study.
- The model by Visser (1998) only applies to a sand dike. Models on the growth of a gap at a clay-covered dike could not be found in the literature. Hence, it has been necessary to apply information about a recorded dike breach for the scenarios at the Ribe defence system.

In CUR (1990) it is stated that only a few cases have been recorded in which the growth of the gap width as a function of time is tolerably known. Two cases are represented in CUR (1990), of which the breach at the IJssel dike on January 8th, 1926 has been chosen as an assumed scenario for the growth of a possible breach at Ribe dike. This scenario has been selected due to missing data and models for a time-dependent modelling of a dike breach at Ribe dike. By performing a curve-fitting, the following function for the gap growth based on the recorded breach at the IJssel dike could be derived:

$$b = 67 \cdot t^{\frac{1}{4}} \qquad \text{(Eq. 14)}$$

where: b = gap width [m]

t = time [h]

Figure 5-15 illustrates the derived function of gap growth assumed for a dike breach at Ribe dike based on the recorded breach at the IJssel dike in 1926.

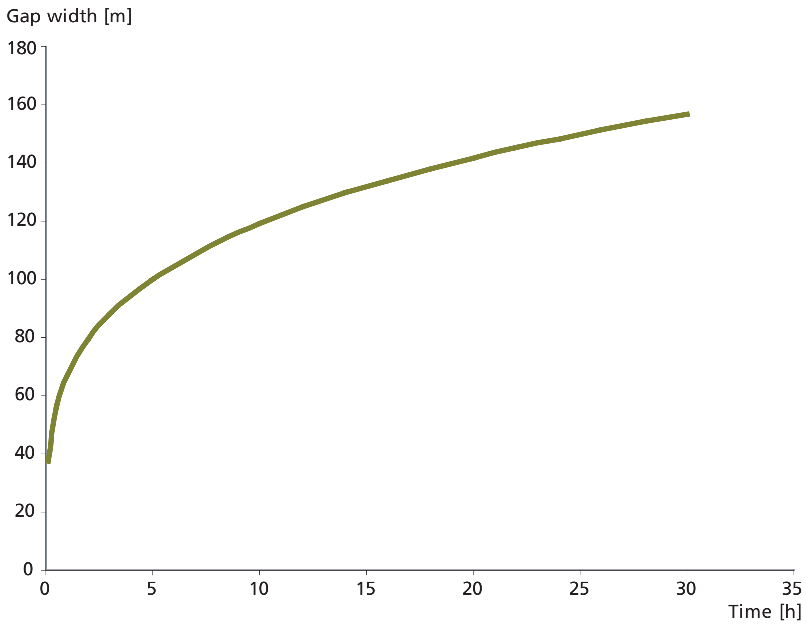

Figure 5-15: Assumed growth of a dike breach at Ribe dike.

Ribe river and the discharge at the Kammer sluice

In the case of an up-coming flood event, the floodgates of the Kammer sluice will be closed in order to prevent the intrusion of flood water into the hinterland through the sluice. The closing of the floodgates normally lasts until the outer water level has fallen below the river's water level. In some situations this may last up to several days, which involves a long interruption of the river discharge through the sluice.

Especially in combination with long precipitation events during the winter season, the closing of the floodgates cause comprehensive backwatering of the river discharge, which results in flooding of the adjacent low-lying hinterland. Therefore, in some scenarios a preceding inundation due to interruption of the river discharge is considered. The inundation volumes caused by closed gates have been calculated based on a mean discharge of 70 m^3/s. This mean discharge value has been stated by the Ribe County as valid for the Kammer sluice in case of long-lasting preceding precipitation events.

5.5.3 Description of inundation scenarios

A total of seven scenarios are defined. Three scenarios affect the southern sub-area of the flood-prone hinterland. Two scenarios affect the northern sub-area and two scenarios affect the total flood-prone area.

In five scenarios inundation occurs due to one or more dike breaches, whereas two scenarios consider wave overtopping and the failure of both gates at the sluice respectively. Three scenarios will consider a preceding inundation due to the closing of the sluice gates for several hours. The seven scenarios will be further described in the following. Furthermore, the selection of the considered dike section within each scenario is graphically illustrated in Appendix F.

Scenario Sc1

Scenario Sc1 comprises one dike breach in Section 6. The section is located directly south of the Kammer sluice which includes the flooding of the southern sub-area (see Appendix F). Section 6 is represented by the cross-section km 8,422. The failure probability of which has been calculated to $P_f = 4{,}5 \cdot 10^{-5}$. This probability value is the second highest failure probability within all six cross-sections. Furthermore, when considering only the sections which border on the southern sub-area, Section 6 has the highest failure probability.

The time of failure is assumed to be four hours before the flood peak, which is defined to reach a level of 4,90 m DVR90. At the time of failure the outer water level is calculated to 3,83 m DVR90 considering the standardised storm surge hydrograph (see Chapter 5.5.2). By subtracting the foreland height from the water level, the hydraulic fall results in 1,91 m.

Scenario Sc2

Within scenario Sc2 one dike breach is assumed in Section 2, which is represented by the cross-section km 3,156. Section 2 has a failure probability of $P_f = 3{,}1 \cdot 10^{-5}$, which is the second highest probability of all southern sections (see Chapter 4.5 and Appendix F). Actually, scenario Sc2 and scenario Sc1 are quite comparable, however, scenario Sc2 considers a preceding closing of the gates at the Kammer sluice.

The dike breach is assumed to take place 3,5 hours before the culmination of the storm surge at an outer water level of 4,21 m DVR90. The hydraulic fall is only 1,64 m due to a high foreland level of 2,57 m DVR90. Further, it is assumed that the floodgates of the sluice had to be closed 24 hours before the flood peak because of an increasing wind setup on the seaward side of the flood defence system.

Scenario Sc3

In scenario Sc3 the inundation behaviour in the northern sub-area is investigated. Therefore, scenario 3 comprises one dike breach within Section 9. Section 9 has the highest failure probability of all cross-sections.

Within scenario Sc3, the standardised water level hydrograph is calculated based on a maximum water level of 4,5 m DVR90. The breach takes place 30 minutes before the flood reaches its maximum. At that time, the outer water level is calculated to 4,41 m DVR90, which results in a hydraulic fall of 1,91 m.

Scenario Sc4

Scenario Sc4 investigates the effects of wave overtopping on a long dike stretch. Dike breach failure is not considered in scenario Sc4.

Within scenario 4 wave overtopping is assumed to occur in Section 9, which is located north of the Kammer sluice. Section 9 is represented by the cross-section km 10,403. The failure probability for wave overtopping has been calculated to $P_f = 6{,}6 \cdot 10^{-5}$ (see Table 4-7), which is the highest probability value within all cross-sections. Wave overtopping is assumed to occur along the whole stretch of Section 9, which comprises approximately 1.200 m. The overtopping rate is assumed to be 20 l/(sm) and the duration of wave overtopping is set to six hours.

Scenario Sc5

Scenario Sc5 considers three dike breaches along the defence system. The dike breaches occur in Section 6 (cross-section km 8,422), Section 2 (cross-section km 3,156) and in Section 9 (cross-section km 10,403) (see Appendix F). Two of the breaches affect the southern sub-area and one dike breach affects the northern sub-area. However, the number of breaches and the subsequent inflow volume will affect the total flood-prone area.

The maximum water level during scenario Sc5 is assumed to reach 5,0 m DVR90. The three dike breaches take place at different times before the flood peak. The time of each breach is stated in Table 5-8. Due to the differences in time as well as in foreland heights, the hydraulic fall at each gap varies between 1,52 m and 2,22 m.

Furthermore, it is assumed that the flood gates of the Kammer sluice had to be closed 14 hours before the flood peak. The preceding inundation volume is calculated based on a mean discharge of 70 m³/s.

Scenario Sc6

Scenario Sc6 comprises four dike breaches, two north of the sluice and two south of the sluice. The four affected sections are represented by the cross-sections having the four highest failure probabilities. Table 5-7 lists the affected sections and the accompanying cross-sections.

The flood peak level is set to 5,35 m DVR90. The hydraulic fall at the dike breaches varies between 1,16 m and 2,00 m. Furthermore, the scenario comprises the closing of the flood gates 14 hours before the flood peak.

Scenario Sc7

Within scenario Sc7 solely the failure of the gates at the Kammer sluice is considered. It is assumed that both gates fail 4,5 hours before flood culmination. At that time, the height of the water level is 3,0 m DVR90. The flood peak level is set to 4,0 m DVR90.

An overview of the locations and the representative cross-sections used within the inundation scenarios are provided in Table 5-7. All relevant input parameters for the calculation of the inflow volume as well as their assumed values are listed in Table 5-8.

No.	Scenario	Dike section	Rep. cross-section	Failure mechanism	Affected area
Sc 1	Scenario 1	6	8422	1 dike breach	Southern sub-area
Sc 2	Scenario 2	2	3156	1 dike breach	Southern sub-area
Sc 3	Scenario 3	9	10403	1 dike breach	Northern sub-area
Sc 4	Scenario 4	9	10403	wave overtopping	Northern sub-area
Sc 5	Scenario 5	6	8422	3 dike breaches	Total area
		2	3156		
		9	10403		
Sc 6	Scenario 6	6	8422	4 dike breaches	Total area
		2	3156		
		9	10403		
		8	9400		
Sc 7	Scenario 7	7	Sluice	failure of both gates	Southern area

Table 5-7: Overview of the locations and the representative cross-sections.

No.	Rep. cross-section	Crest height h_k [m DVR90]	Level in front of dike h_t [m DVR90]	Time of failure t_f *) [h]	Water level at time of failure h_{w_f} [m DVR90]	Highest water level h_{w_max} [m DVR90]	Mean over-topping rate [m³/sm]	Mean dis-charge Q_{Ks} K. sluice [m³/s]	Duration of closing t_{Ks} K. sluice [h]
Sc 1	8422	6,73	1,92	-4	3,83	4,90			
Sc 2	3156	6,83	2,57	-3,5	4,21	4,90		70,0	24 + 10
Sc 3	10403	6,65	2,50	-0,5	4,41	4,50			
Sc 4	10403	6,65	2,50	-3			0,02		
Sc 5	8422	6,73	1,92	-3	4,14				14 + 13
	3156	6,83	2,57	-2	4,53	5,00		70,0	
	10403	6,65	2,50	-3,5	4,02				
Sc 6	8422	6,73	1,92	-6	3,92	5,35		70,0	14 + 8,5
	3156	6,83	2,57	-5	4,11				
	10403	6,65	2,50	-7,5	3,66				
	9400	6,68	2,63	-4,5	4,20				
Sc 7	Sluice	5,88	-1,30	-4,5	3,02	4,00			

Table 5-8: Input parameters and values of the inundation scenarios.

5.5.4 Calculation of inflow volume and simulation of inundation behaviour

Before presenting the calculated inflow volume and the inundation behaviour within each scenario, the general approach which has been applied will be explained. A smaller deviation from the general approach applies to Scenario 4, which will be described during the subsequent result presentation of the calculated inflow volumes of the respective scenarios.

The determination of the inflow volumes has been performed by means of MS Excel spreadsheet calculations. Based on the assumed flood peak level the standardised storm surge hydrograph is determined by calculating the respective water level for each time step (compare Table 5-6 and Figure 5-14). The assumed time of failure (dike breach) represents the starting point for the calculation of the gap development and the inflow volume. Based on the assumed gap growth curve and the time steps in the storm surge hydrograph, the growth of the gap is calculated over the time. Furthermore, the hydraulic fall is calculated for each time step after the assumed time of failure. Having determined the gap width and the hydraulic fall, the inflow volume is calculated for each time step by means of equation Eq. 15:

$$Q = b \cdot \sqrt{\frac{8}{27} \cdot g} \cdot h^{\frac{3}{2}} \qquad \text{(Eq. 15)}$$

where: b = width of gap

g = gravity = 9,81 m/s²

h = height of hydraulic fall

Afterwards, the inflow volume accumulated over the time steps is calculated.

Due to the counteracting behaviour of the inner and outer water levels – the inner water level rises because of the inflow of flood water and the outer water level decreases according to the storm surge hydrograph - both water levels will reach the same level at a certain time. In order to determine the time where the gradient between the outer and inner water levels approaches zero, storage mass curves of the southern and northern sub-areas as well as of the total flood-prone area have been derived by calculating the storage capacity for every 0,1 m. The storage mass curves for the southern sub-area, northern sub-area and the total flood-prone area are illustrated in Figure 5-16.

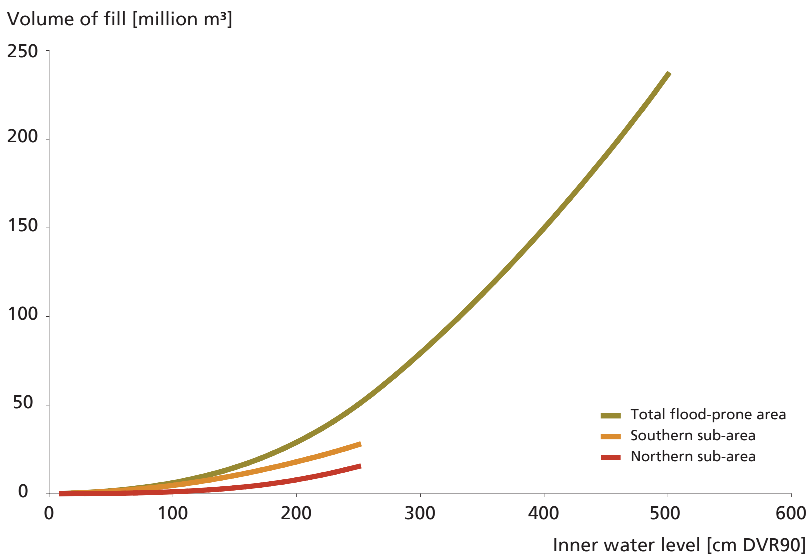

Figure 5-16: Storage mass curves for the southern and northern sub-areas as well as for the total flood-prone area.

For different values of accumulated inflow volumes, the related inner water levels are determined by the storage mass curves. By comparing the inner water level with the outer water level at a certain time step, the gradient's magnitude between both water levels is assessed. In case the inner water level has approached about 0,7 times the height of the outer water level, the inflow capacity starts decreasing. At the time of equal water levels on both sides of the gap, the inflow stops and the adapted inner water level is recorded for the subsequent determination of the damage potential.

Inundation within scenario Sc1

The inflow volume within scenario Sc1 amounts to 27,5·10^6 m³. The outer and inner water levels are balanced 10 hours after the flood peak, which results in an overall inflow duration of 14 hours from the time of failure. During that time, the gap width has extended to approximately 130 m. The inner water level in the southern sub-area appears to be 2,4 m DVR90.

Inundation within scenario Sc2

Within scenario Sc2, the preceding closing of the sluice gates results in a backwatering volume of about 6,0·106 m³ before the time of failure. About 14 hours after the flood peak (17,5 hours after the dike breach) the outer water level has decreased below the level of the dike base within the gap. The inflow therefore stops. At that time 13·10^6 m³ of flood water has flown into the southern sub-area. Together with the backwater volume of the Ribe river before the dike breach and during the flooding the inundation volume amounts to 22,5·10^6 m³, which results in an inner water level of 2,2 m DVR90. This inner water level is, however, lower than the base level of the gap.

Thus, this scenario shows that in some cases the balancing of the water levels can not be achieved during the storm surge because of a high foreland level, which stops the inflow into the hinterland at the time when the outer water level has fallen below that gap level.

Inundation within scenario Sc3

Within scenario Sc3, the northern sub-area is flooded by a total inundation volume of 5,8·10^6 m³. The growth of the gap stops nine hours after the time of failure comprising a width of 115 m due to balanced water levels. The inner water level in the northern sub-area ends up at 1,8 m DVR90.

Inundation within scenario Sc4

Scenario Sc4 comprises the failure of wave overtopping on a dike stretch of 1200 m. Here, the approach with two balanced water levels (inner and outer) is not applicable. The inflow volume is mainly governed by the duration of wave overtopping and the mean overflow rate. As earlier described, the duration of wave overtopping is set to six hours and the mean overflow rate is assumed to be 20 l/(sm). The total inundation volume amounts to $0{,}52 \cdot 10^6$ m³, which results in an inner water level of 0,7 m DVR90.

Inundation within scenario Sc5

Within scenario Sc5, three dike breaches and the backwatering of the discharge of Ribe river result in a total inundation volume of about $66{,}8 \cdot 10^6$ m³, which inundates major parts of the total flood-prone area. The volume of backwater is calculated to $6{,}8 \cdot 10^6$ m³, whereas the inflow volume through the three gaps accumulated during 16,5 hours totals $60 \cdot 10^6$ m³. The total width of all three gaps adds up to 410 m.

Inundation within scenario Sc6

Scenario Sc6 comprises four dike breaches along the flood defence system, which add up to a total width of 530 m 16 hours after the first dike breach. During that time, a total volume of $121 \cdot 10^6$ m³ flows through the four gaps into the hinterland. Additionally, the closing of the sluice gates causes a backwatering volume of $5{,}7 \cdot 10^6$ m³. The total inundation volume of $127 \cdot 10^6$ m³ results in an inner water level of 3,7 m DVR90, which can be considered as a major flooding disaster in the Ribe hinterland.

Inundation within scenario Sc7

Within scenario Sc7, both gates at the Kammer sluice fail 4,5 hours before the flood culmination. The stretch of failure is 10 m, equal to the width of the sluice opening. For reasons of simplification, a rough assumption is made while calculating the height of the hydraulic fall: For each time step, the hydraulic fall is calculated by subtracting the flood level and the mean river level. The effects of two currents being directed towards each other (discharge of the river towards the inflow of flood water) are not considered here.

The total inundation volume is calculated to be $19{,}8 \cdot 10^6$ m³, which results in an inner water level of 2,1 m DVR90 affecting the southern sub-area. Thus, scenario Sc7 comprises an inundation behaviour quite similar to the scenarios Sc1 and Sc2.

The results of all inundation scenarios are summarized in Table 5-9. The second column states the time of balanced outer and inner water levels, while the third column presents the inflow duration for each scenario. The fourth column adds up the total length of failure. Finally, the fifth and sixth column state the inflow volume and the resulting inner water level for the affected area.

No.	Time $t_{(h=hi)}$ *) [h]	Total length of failure at $t_{(h=hi)}$ [m]	Duration of in-flowing water [h]	Volume Q at $t_{(h=hi)}$ [10^6 m³]	Inner water level hi at $t_{(h=hi)}$ [m DVR90]	Affected area
Sc 1	+10	130	14	27,5	2,40	Southern sub-area
Sc 2	+14	130	17,5	22,5	2,20	Southern sub-area
Sc 3	+8,5	115	9	5,8	1,80	Northern sub-area
Sc 4	-3 till +3	1200	6	0,52	0,70	Northern sub-area
Sc 5	+13	410	16,5	66,8	2,80	Total area
Sc 6	+8,5	530	16	127,0	3,70	Total area
Sc 7	+10,5	10	15	19,8	2,10	Southern sub-area

Table 5-9: Results of the inundation scenarios.

5.5.5 Determination of the damage within each scenario

As described in Chapter 5.2, altitude lines have been interpolated at regular intervals of 0,5 m within the topography of the flood-prone hinterland. Furthermore, all elements at risk have been classed with a certain interval (Chapter 5.3), which allows in the following the selection of inundated risk elements within the respective inundation scenarios. Due to the fact that some of the depth-damage functions of the elements depend on the inundation depth (Chapter 5.4), the calculated inner water levels are sorted into matching altitude intervals. All risk elements within the intervals below the inundation interval are selected and the inundation depth is calculated by subtracting the mean altitude values of both intervals.

For example, a risk element placed within the altitude interval of 0-0,5 m DVR90 will be flooded by 1,5 m within scenario Sc3, where the inner water level has been sorted into the interval of 1,5-2,0 m DVR90. Table 5-10 states the calculated inundation levels of each scenario and indicates the sorting into the altitude intervals.

No.	Inner water level [m DVR90]	Altitude interval [m DVR90]	Mean altitude [m DVR90]	Affected area
Sc 1	2,40	2,0 - 2,5	2,25	Southern sub-area
Sc 2	2,20	2,0 - 2,5	2,25	Southern sub-area
Sc 3	1,80	1,5 - 2,0	1,75	Northern sub-area
Sc 4	0,70	0,5 - 1,0	0,75	Northern sub-area
Sc 5	2,80	2,5 - 3,0	2,75	Total area
Sc 6	3,70	3,5 - 4,0	3,75	Total area
Sc 7	2,10	2,0 - 2,5	2,25	Southern sub-area

Table 5-10: The calculated inner water levels and the sorting into the altitude intervals.

Due to the fact that the inner water level of scenarios Sc1, Sc2 and Sc7 are sorted into the same altitude interval (2,0 – 2,5 m DVR90), the three scenarios are treated as one scenario in the following assessment of the damage.

Table 5-11 states the final results of the calculated damage for the seven scenarios. In contrast to the presentation of the selected risk elements in Chapter 5.1.2, the risk elements 'traffic system' and 'electric installations' have been grouped together as 'Infrastructure'.

Table 5-11 shows clearly the highest damage within scenario Sc6. This is understandable due to the large extension of the inundation into the hinterland and the large inundation depth of up to 3,25 m in low-lying areas, which results from the four dike breaches.

For the scenarios Sc3 and Sc4, the damage is quite low. The amount of 2 million DKK (€ 268.500) is not exceeded in either scenario. Both scenarios are characterised by the fact that no buildings are inundated. Thus, no damage to movable property occurs. Within the scenarios Sc1, Sc2 and Sc7, however, buildings and movable property are flooded. The total damage for these scenarios amounts to about 19 million DKK.

Risk element	Sc1/Sc2/Sc7		Sc3		Sc4		Sc5		Sc6	
Buildings	DKK	4.937.000	DKK	0	DKK	0	DKK	54.179.000	DKK	203.555.000
	€	662.685	€	0	€	0	€	7.272.349	€	27.322.819
Movable property	DKK	4.640.000	DKK	0	DKK	0	DKK	37.538.000	DKK	146.905.000
	€	622.819	€	0	€	0	€	5.038.658	€	19.718.792
Agricultural acreages	DKK	2.208.000	DKK	933.000	DKK	211.000	DKK	7.098.000	DKK	9.489.000
January	€	296.376	€	125.235	€	28.322	€	952,752	€	1.273.691
Livestock	DKK	0	DKK	0	DKK	0	DKK	1.232.500	DKK	7.978.000
	€	0	€		€	0	€	165.436	€	1.070.872
Infrastructure	DKK	7.226.000	DKK	844.000	DKK	942.500	DKK	22.862.000	DKK	56.554.000
	€	969.933	€	113.289	€	126.510	€	3.068.725	€	7.591.141
TOTAL	DKK	19.011.000	DKK	1.777.000	DKK	1.153.500	DKK	122.909.500	DKK	424.481.000
	€	2.551.812	€	238.523	€	154.832	€	16.497.919	€	56.977.315

Table 5-11: The calculated damage for all inundation scenarios.

In the following, a closer look at the calculated damage is intended by making a few remarks on the risk elements. An illustration of the affected risk elements within each scenario as well as an illustration of the inundation extension are presented in Appendix G.

Buildings

Within scenarios Sc1, Sc2, Sc5, Sc6 and Sc7 buildings are flooded. The greatest damage is seen within scenario Sc6, nearly 4 times the damage of scenario Sc5. This leap between Sc5 and Sc6 can be explained by the extension of the inundation into the urban areas of Ribe town. Moreover, industrial buildings are flooded which normally have a higher property value compared to private property.

No buildings are affected by the flooding within the scenarios Sc3 and Sc4. On the one hand, this is due to the fact that the inundation volumes in Sc3 and Sc4 are quite small and on the other hand the fact that no buildings are located close to the defence system in the northern sub-area.

Movable property

The determination of the damage to movable property is linked to the particular property value, as already described in Chapter 5.4. Furthermore, the depth-damage functions of movable property distinguish between movable property within residential buildings (private sector) and agricultural/industrial buildings (economic sector). Table 5-12 states the calculated damage for both sectors.

Risk element	Sc1/Sc2/Sc7		Sc5		Sc6	
Movable property	DKK	2.239.000	DKK	22.533.000	DKK	59.828.000
Private sector	€	300.537	€	3.024.564	€	8.030.604
Movable property	DKK	2.401.000	DKK	15.005.000	DKK	87.077.000
Economical sector	€	322.282	€	2.014.094	€	11.688.188
Movable property	DKK	4.640.000	DKK	37.538.000	DKK	146.905.000
Total	€	622.819	€	5.038.658	€	19.718.792

Table 5-12: The damage to movable property in the private and economic sectors.

Within Sc6 the damage to the economic sector is higher than the damage within the private sector. This fact can again be explained by the extension of the inundation into Ribe town. In general, an extension of the inundation into the Ribe hinterland causes an increase of the damage to buildings as well as of the damage to movable property. Inundation of particular areas inside Ribe town may result in higher damage to economic movable property than damage to private movable property.

Agricultural acreage

Figure 5-17 shows the damage to crops within the seven scenarios for the five winter months November, December, January, February and March, where the occurrence of a storm surge is most likely. Flooding of agricultural acreage in March will cause the worst damage, since new sowing of crops for the coming harvest is out of the question.

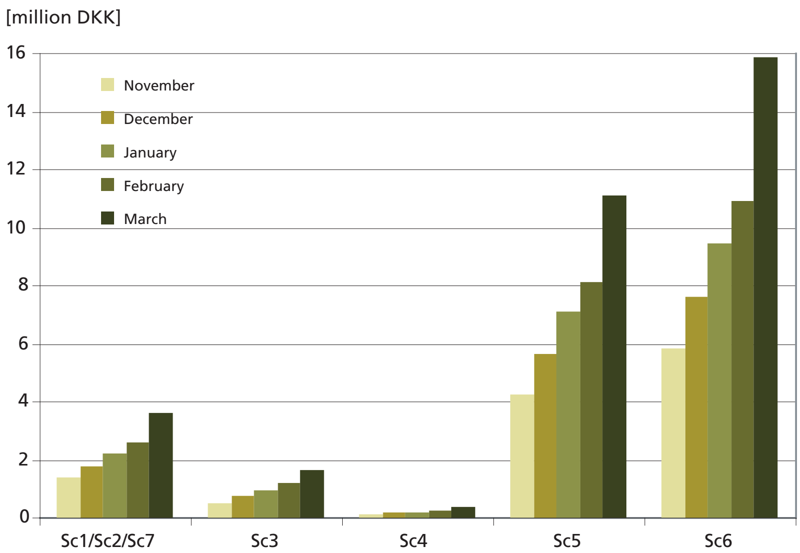

Figure 5-17: The damage to crops due to inundation in the five winter months.

Since no statistics of the occurrence of storm surges regarding the five winter months is available, the calculated damage values of January have been applied to calculate the total damage of each scenario.

Livestock

Damage to livestock is only calculated within scenarios Sc5 and Sc6. Due to the fact that livestock is geocoded by means of agricultural buildings, the damage to livestock depends on an inundation event at a particular agricultural building. Therefore, the inundation of some stock species staying on meadows is not considered in the calculated damage. A small damage of livestock is thus possible within the scenarios Sc1 – Sc4 and Sc7, too.

Infrastructure

The calculated damage to infrastructure comprises damage to roads, pumps and windmills. It is only within Sc5 and Sc6 that damage occurs to pumps and windmills, adding up to 324.000 DKK (€ 43.500) and

804.000 DKK (€ 108.000) respectively. Hence, the largest portion of the damage can be led back to damage to or cleaning work at roads. The assumed damage factor of 10 % of the road building costs (Chapter 5.4) amount to a quite high damage value. However, the cleaning work of up to 185 km road and roadside ditches (scenario Sc6) as well as the repair work of scour damage under the carriageway surfacing may add up to quite high sums.

6. Risk assessment of the Ribe flood defence system

As the final formal step of the risk analysis procedure, the risk assessment links the results of the hazard analysis and the vulnerability analysis. Thus the predicted flood risk is determined, which in some references also is defined as the specific or statistical risk (Reese, 2003).

The objective of the risk assessment is to quantify the probability of damage events in a specific area based on the results of the hazard analysis and the vulnerability analysis. As described in Chapter 5.5, inundation scenarios have been defined to determine the inundation behaviour (extension and depth) in the hinterland, which governs the damage within each scenario. The inundation extension and inundation depth depend on the inflow volume and the topography. Data about the hinterland topography is normally available or can be generated. Concerning the inflow volume, it depends on several principal parameters, which have already been described in detail in Chapter 5.5.2:

- the location and number of failure events (dike breach or wave overtopping),
- the (standardised) storm surge hydrograph,
- the time of failure or the failure water level in relation to the storm surge hydrograph,
- time-dependent development of the dike gap.

The geographical placement of one or more failure events along the defence systems together with the time-dependent inflow volume must therefore be assessed in connection with a vulnerability analysis.

However, this leads to two questions:

- Is the damage determined within each scenario multiplied by the overall flooding probability of the whole flood defence system or by the overall failure probability of the defence system section (see Chapter 4.5) where the particular scenario considers failure?
- Is the calculated flood risk of the Ribe flood defence system a single value, or should the flood risk rather be assessed as a range of risks depending on the applied scenarios?

Concerning these two questions, no information could be found in the literature. Moreover, the number of already published risk values and detailed descriptions of combining the failure probability with the damage potential are quite poor in the literature.

Therefore, considering the first question, it is decided to multiply the damage calculated within a particular scenario by the overall flooding probability of the whole flood defence system. By using this approach, it is taken into account that the structure actually also could fail in a different section than the section considered in the particular scenario.

Within this study, the different damage values depending on the scenarios lead to an assessment of the Ribe flood risk as a range of the flood risk values. Scenarios comprising a small inflow volume and subsequently little damage potential may represent a lower bound of the flood risk, whereas the scenarios with large inflow volumes and a high inundation depth may represent the upper bound of the flood risk.

Table 6-1 states the overall failure probability P_f, the damage $E(D)_{Sc}$ and the calculated risk values R for each inundation scenario.

Scenario	Overall flooding probability	Damage		Risk	
	Pf	$E(D)_{Sc}$ [DKK]	$E(D)_{Sc}$ [€]	R [DKK/year]	R [€/year]
Sc1	2,50E-04	19.011.000	2.552.000	4.753	638
Sc2	2,50E-04	19.011.000	2.552.000	4.753	638
Sc3	2,50E-04	1.777.000	239.000	444	60
Sc4	2,50E-04	1.153.500	155.000	288	39
Sc5	2,50E-04	122.909.500	16.498.000	30.727	4.125
Sc6	2,50E-04	424.481.000	56.977.000	106.120	14.244
Sc7	2,50E-04	19.011.000	2.552.000	4.753	638

Table 6-1: Predicted risk of the Ribe defence system considering each inundation scenario.

The results presented in Table 6-1 show that the statistical risk for the Ribe defence system roughly varies between 300 DKK/year and 110.000 DKK/year. This can be seen as a quite large range which, however, depends on the definition of the inundation scenarios and the assets affected by the inundation. Unfortunately, other risk values from different civil engineering disciplines could not be found in the literature in the remaining working time available. However, a risk of 110.000 DKK/year is considered as acceptably small. A detailed evaluation of the determined range of risks is, however, only applicable within the procedure of a risk evaluation, which lies beyond the scope of this study.

By comparing the risk values of the scenarios, the calculated risks within scenarios Sc1, Sc2 and Sc7 have identical values. This may lead to the conclusion that one dike breach affecting the southern sub-area results in the same risk as the failure of the sluice gates. This is, however, only valid when considering an overall flooding probability of $P_f = 2{,}5 \cdot 10^{-4}$, which includes the disregard of the sluice and the three outlets. As mentioned in Chapter 4.5, it has not been possible to finally investigate the failure probability of the Kammer sluice due to missing models within its fault tree. By comparing scenarios Sc1 and Sc2, the significance of a preceding closing of the sluice gates can be assessed. Without considering the backwatering of the Ribe river discharge in scenario Sc2, the total inflow volume will amount to about 13 million m³ due to the decrease of the outer water level below the basis of the gap. This inflow volume will result in an inundation level of approximately 1,75 m DVR90, which evidently will cause less damage in the southern sub-area and thus reduce the risk value for scenario Sc2. However, considering a backwatering volume of 9,5 million m³, the risk within this scenario will be similar to the risk of scenario Sc1. The parameters of foreland height and backwatering volume in connection with sluices or outlets therefore turn out to be important parameters to be considered within a vulnerability analysis.

The calculated risk values for scenarios Sc3 and Sc4 are very low. The small inflow volumes together with damage only to agricultural acreage and infrastructure result in risk values below 1.000 DKK per year, which are considered the lower bound of the range of risks.

The risk values calculated for scenarios Sc5 and Sc6 show that more severe failure events (three dike breaches or more) are required for larger damage values, which may by explained by the location of the assets in the Ribe flood-prone area.

To sum up one may say that the risk values strongly depend on the inundation scenarios, how they are defined and their accompanying total damage values. It is therefore recommended that the set-up and the reliability of scenarios be further investigated within future research projects (see also Chapter 7).

7. Summary, conclusion and recommendations for future work

The main objective of this study has been the performance of a risk assessment of a flood defence system located in the Danish part of the Wadden Sea. As a pilot study area the Ribe flood defence system and the accompanying flood-prone hinterland have been chosen. Based on the literature, a conceptual framework on risk handling has been worked out, which considers the performance of a risk assessment as a sub-process of a risk analysis. The procedure applied within the risk analysis has been based on the state of the art found in the literature.

The report in hand has described the procedure and the results of the risk analysis for the Ribe flood defence system. The flood risk of the flood defence system is hereby defined as the product of the flooding probability and the subsequent consequences of flooding. The flooding probability has been investigated within a hazard analysis, the results of which are summarised at first. Afterwards, the vulnerability analysis comprising the determination of the possible consequences of inundation will be summarised. This summary will be followed by a short overview of the results of the risk assessment. The summaries will be concluded by recommendations concerning the particular analysis or procedure.

Additionally, the chapter will end with some general remarks and recommendations on the procedures applied in the study.

Hazard analysis

The flood defence system in Ribe situated at the West Coast of Denmark is characterised by a flat sea dike with a sand core, clay and grass cover. The standard profile shows a 1:10 seaward slope and a crown height of 6,88 m DVR90. The system also comprises a sluice and three outlets. The flood-prone hinterland expands over 95 km².

The calculation of the overall flooding probability has been based on six cross-sections of the Ribe dike. Information about a total number of 80 input parameters describing geometrical, geotechnical and hydrodynamic boundary conditions has been collected before carrying out the probabilistic calculations based on the ProDeich model by Kortenhaus (2003) (Chapter 4.4). The Kammer sluice required further information from the literature and additional limit state equations which were programmed and applied (Figure 4-8). For calculation of the outlets again additional limit state equations were derived (Figure 4-13).

Due to the fact that deterministic design procedures form the basis of the probabilistic calculations in the ProDeich model, a deterministic calculation of the Ribe defence system was performed before calculating the overall failure probability. The results of the deterministic calculation for all dike sections (see Table 4-3) show that "grass erosion" failure on the seaward slope may occur under design conditions. However, from the context of a complete fault tree no overall failure of the sea defence system can be observed within the deterministic calculations under design conditions.

The deterministic calculations for the sluice and the outlets result in a very high wave overtopping rate under design conditions. Wave overtopping is therefore assumed to be the governing failure mechanism for the sluice and the outlets.

The probabilistic calculations based on the fault tree analysis for the dike sections result in a failure probability from $P_f = 1{\cdot}10^{-5}$ to $P_f = 1{\cdot}10^{-6}$ (Table 4-7). Similar values are obtained when scenario fault trees are used (Table 4-8), which consider the temporal dependencies of the failure mechanisms in the fault tree. These similar values are explained by the fact that the overall flooding probability is primarily governed by the failure probability of wave overtopping. A further analysis of the scenario fault trees showed that the fault trees can be simplified (see Figure 4-16). Moreover, the simplified fault trees were used to derive the key input parameters, which were identified as the wave period T_p and the water level h_w. The failure probability of the sluice and the outlets are in the order of $P_f = 10^{-1}$ which is mainly due to the high failure probability of wave overtopping.

To determine the overall flooding probability of the whole Ribe defence system, a division into several sections was made. The key parameters for the division of the dike sections were derived as the crown height and the wave period. The sluice and the outlets were defined as separate sections. The fault tree calculations including all dike sections, the Kammer sluice and the three outlets resulted in an overall flooding probability of $P_f = 9{,}5{\cdot}10^{-1}$. This result was considered to be much too high since it solely depends on the failure probabilities of the sluice and the outlets which are mainly governed by wave overtopping. The inflow volume caused by wave overtopping will, however, be very small due to the fact that the sluice and the outlets only represent a very limited stretch of the whole defence system. Therefore, a second calculation ignoring the sluice and the outlets in the fault tree resulted in an overall flooding probability of $P_f = 2{,}5{\cdot}10^{-4}$.

Overall, the Kammer sluice and the outlets are the weak points of the Ribe flood defence system where a large amount of wave overtopping can be expected. This is mainly due to a large wave height in front of the sluice and the outlets and steeper seaward slopes for the outlets. Furthermore, for a number of failure mechanisms of the sluice/outlets either no proper limit state equations are available or the amount of data is not sufficient to describe these missing failure mechanisms. For the time being, it is therefore recommended to use the overall flooding probability of $P_f = 2{,}5 \cdot 10^{-4}$ for further calculations. These results have to be seen as results of this study applying probabilistic calculations to the Ribe defence system. The results may be seen as a provisional results for the final overall flooding probability of the Ribe flood defence system.

To determine the final overall flooding probability, further investigations have to be carried out, for instance:

- Investigation of the real wave size (wave height and period) in front of the sluice and the outlets. Due to the large water depth in front of the sluice and the outlets, the wave heights of incoming waves will be less reduced in front of the sluice/outlets than in front of the dike;
- Investigation of the failure mechanism 'gates not closed', the failure mechanisms concerning the collapse of the sluice gates as well as investigation of the fault tree for the sluice and the outlets;
- Investigation of the uncertainly of the water level h_W. The water level h_W has a significant influence on many of the failure mechanisms. The sensitivity analysis showed (Chapter 4.3.1) that a variation of the threshold value or the distribution function can led to deviations in the order of several centimetres. Unfavourable combinations of different approaches may therefore lead to a large variation of the uncertainty values of the water level;
- Investigation of the approach of dividing a sea defence systems into representative sections. Within the approach of dividing a sea defence system into sections, the influence of variation of structural features (e.g. geometry of the structure or the properties of the used material) lengthwise has to be considered.

Vulnerability analysis

At first, the flood-prone area was delimited to enable the selection of the elements at risk. It was decided that the delimitation of the flood-prone area towards the remaining hinterland should consider the 5,0 m DVR90 altitude line. Within the delimited flood-prone area six risk elements of direct, tangible damage were selected. These six risk elements comprised buildings, movable property, agricultural acreage, livestock, electric installations and traffic system. Additionally, four risk elements (inhabitants, employees, vehicles, tourism) of intangible, direct/indirect damage were considered in a descriptive form.

The request of data about the risk elements from national registers, consultants and public administrations showed clear differences in the data quality and format. This fact complicated the procedure of geocoding the risk elements by means of a GIS software application. With respect to the cartographic basis used in the vulnerability analysis, altitude data in a grid net of 25x25 metres was used to generate a topographical map. The altitude data was supplemented by altitude data from road surveys.

The valuation analysis showed the location of most of the risk elements on high ground around the low-lying delta area of Ribe river. For example, only 7 % of the property value (buildings) are located below 2,5 m DVR90. About 45 % of the property value are placed up to 4,0 m DVR90 and about 30 % of the total property value are located between 4,5 and 5,0 m DVR90. This distribution of assets over altitude has been characteristical for most of the risk elements. However, a differentiation of the total profit of all kinds of crop over altitude showed an almost linear distribution, which differs remarkably from the other risk elements.

To determine the possible damage to the risk elements, seven scenarios were defined comprising different breach and overtopping scenarios. By means of these scenarios different inundation events, including inundation extension and inundation depth, were simulated and the damage caused by the inundation events was assessed. In order to assess the damage due to inundation, depth-damage functions were derived for risk elements where the damage depends on the inundation depth. In case of depth-independent damage to risk elements, damage factors were derived to quantify the damage. For buildings and movable property depth-damage functions could be derived from data about compensation payments regarding real flood damage to buildings and movable property. This data was available at the Danish Flood Compensation Council (FCC). The assessment of flood damage to agricultural acreage was performed by external experts. Their assessment comprised damage factors for different kinds of crop and inundation periods of 5, 14 and 28 days.

Based on the seven scenarios, inflow volumes between 0,5 and 127 million m^3 were calculated. Input parameters, such as a standardised storm surge hydrograph, the failure probability of defence system sections, the time-dependent development of a dike gap as well as an assumed time of failure during storm surge, were considered in the calculations of the inflow volumes. The results showed that the flood-prone area is differently inundated depending on the location and the number of failure events. However, it has to be remarked that several assumptions had to be made while defining the inundation scenarios. The calculated inflow volumes have therefore to be regarded as rough estimations.

Due to differences in inundation behaviour, damage within each scenario varies between 1,15 and 424,5 million DKK. The scenarios Sc5 and Sc6 comprising three and four dike breaches respectively result in damage exceeding 100 million DKK (€ 13,4 million). The scenarios Sc1, Sc2 and Sc7 showed comparable inundation behaviour which resulted in the same total damage for all three scenarios.

In general, the vulnerability analysis showed that the total damage calculated within each scenario depends on the definition of the scenarios, the considered risk elements, the determination of the inundation behaviour and the derived depth-damage functions. Therefore further investigations should be carried out, for instance:

- Investigations of criteria for the definition of inundation scenarios. Within this study the definition of inundation scenarios has been based on several assumptions of which reliability has not been further investigated. Therefore, generic criteria should be worked out to enable a more reliability-based definition of inundation scenarios;
- Investigations of further risk elements, which have not been considered in this study. Together with an investigation of further/new risk elements, a standardised overview of risk elements to be considered within a vulnerability analysis would be recommendable in order to allow comparability with other vulnerability analyses. Efforts should also be put into indirect and intangible damage categories. Furthermore, a close inspection of the different data sources (registers, consultants, public administrations) available in Denmark would make the procedure of a vulnerability analysis more efficient;
- Investigations of improvements for the determination of the inundation behaviour. Numerical modelling should be applied to simulate the inundation velocity, the inundation depth and duration as well as the inundation extension within a flood-prone area more accurately. Further research also has to be dedicated to the breach process of a clay-covered dike;
- Investigations of the depth-damage functions. The applied depth-damage functions have to be further developed and verified by means of real data. With this, the data about real flood damage and about the subsequent compensation payments collected by the Flood Compensation Council (FCC) could be very valuable.

Risk assessment

Within the risk assessment, risk values varying between 300 DKK/year and 110.000 DKK/year were calculated. In this connection, the risk values calculated for scenarios Sc3 and Sc4 represent the lower bound of the range of risks for the Ribe flood defence system. On the other hand, the upper bound is represented by the calculated risk value considering the damage caused in scenario Sc6.

The risk assessment made it clear that the range of risk values depends on the inundation scenarios and the damage, which was determined on the basis of the inundation extension and depth. The determination of these factors required, however, several assumptions, such as the location and number of failure events, the time of failure, the water level at the time of failure and a standardised storm surge hydrograph. The reliability of these assumptions was not analysed within the damage analysis.

For example, the location and number of one or more dike breaches was chosen mainly on the basis of the overall failure probabilities calculated for the 15 sections of the defence system. These failure probabilities were calculated by the ProDeich model based on six representative cross-sections (Kortenhaus, 2003). The division of the defence system into 15 sections was based on two key selection criteria, the wave period T_p and the crown height h_k. This simple approach of dividing a defence system into sections has to be further developed in future, prompted by the following objectives:

- The variation of the values of relevant input parameters along the defence system (length effect) has to be considered. Wave attack on the seaward slope may for example vary locally because of changing foreland geometry, or a varying crown height due to consolidation of different magnitude along the defence system may influence the probability of wave overtopping.
- The variation of the input parameter along the defence system has to be considered in the probabilistic calculations in order to obtain a more proper overall flooding probability of the defence system. In this connection, spatial and temporal correlations between different defence structures (dike, sluice, foreland, etc.) within one defence system have to be considered.
- Furthermore, an improved approach of considering the parameter variation (length effect) will give reliability-based indications of the location of failure (dike breach) along the defence, which will be useful in the process of defining inundation scenarios.

General conclusions

Probabilistic considerations are increasingly being applied in actual practice, also within the field of coastal protection. The risk analysis procedure described in this report is considered to be a starting point of reliability-based design of flood defence systems on a feasibility level. This study has shown that it is indeed possible to consider more stochastic parameters than just the water level and the wave run-up when analysing the safety of a flood defence system. Despite the fact that many questions are still open and problems regarding the feasibility remain unsolved, the risk analysis procedure applied has resulted in a considerable increase in information about the Ribe flood defence system and the protected hinterland, which should improve the decision-making basis.

Considering the hazard of failure of the flood defence system, the study has contributed to a detailed description of all possible failure mechanisms at a sea dike. Furthermore, significant failure mechanisms and their limit state equations for a sluice and an outlet have been derived. First attempts of dividing the flood defence system into representative sections and considerations with respect to the length effect have been made.

As part of an assessment of the consequences of failure of the defence system, the vulnerability analysis has shown that only a small number of all assets and the possible damage may be considered in full. For some damage types the tangible property is difficult to assess. The selection and definition of the inundation scenarios are only possible events marked by a chance order. The assessment of the inundation extension and thus the dimension of the damage is only possible to a certain degree of accuracy. However, to calculate the flood risk and to assess the importance of the flood defence system as a defence structure for the inhabitants and their assets, a vulnerability analysis is indispensable.

Finally, when considering the aforementioned conclusions and recommendations, investigations regarding the setting of standards for the performance of risk analyses in the form of e.g. standardized probabilistic guidelines or general frameworks for the performance of vulnerability analyses are recommended.

8. References

Buijs, F. (2003): Reliability analysis of the Caldicot Levels' flood defence system by using Dutch reliability methods for flood defences. M.Sc. Thesis, Delft University of Technology & HR Wallingford.

BYGD (1989): Ribe, Hedeby, Slesvig, Lybeck og Hamburg. Tværforbindelser over Jyllands rod i 1250 år. Published by BYGD, Esbjerg (in Danish).

CPSL (2001): Final Report of the Trilateral Working Group on Coastal Protection and Sea Level Rise. Wadden Sea Ecosystem No. 13. Common Wadden Sea Secretariat, Wilhelmshaven, Germany.

CUR (1990): Probabilistic design of flood defences. Centre for Civil Engineering Research, Codes and Specification, CUR, No. 141, Gouda, Holland, 154 pages.

DEFRA (2002): Risk, Performance and Uncertainty in Flood and Coastal Defence – A Review. Flood and Coastal Defence R&D Programme, Technical Report FD2302/TR1 (HR Wallingford Report SR 587), London.

EAK (2002): Empfehlungen für Küstenschutzwerke. Kuratorium für Forschung im Küsteningenieurwesen, Die Küste, Vol. 65, 589 pages (in German).

Faber, M.H.; Stewart, M.G. (2003): Risk assessment for civil engineering facilities: Critical overview and discussion. Reliability Engineering and System Safety, Vol. 80, pp. 173-184.

Hawkes, P.J.; Gouldby, B.P., Tawn, J.A.; Owen, M.W. (2002): The joint probability of waves and water levels in coastal engineering design. Journal of Hydraulic Research, Vol. 40, No. 3, pp. 241-251.

Jensen, J. (1985): Über instationäre Entwicklungen der Wasserstände an der deutschen Nordseeküste. Journal of Leichtweiss-Institute, Technical University of Braunschweig, Vol. 88, pp. 151-319 (in German).

Kortenhaus, A. (2003): Probabilistische Methoden für Nordseedeiche. Ph.D. Thesis, Technical University of Braunschweig, Leichtweiss-Institute, Braunschweig, Germany, 154 pages (in German).

Kortenhaus, A. & Oumeraci, H. (2002): Probabilistische Bemessungsmethoden für Seedeiche – ProDeich. Technical University of Braunschweig, Leichtweiss-Institute, Research Report No. 877 (in German).

Kortenhaus, A.; Oumeraci, H.; Weissmann, R.; Richwein, W. (2002): Failure mode and fault tree analysis for sea and estuary dikes. Proceedings 28. International Conference on Coastal Engineering (ICCE), Cardiff, Wales, UK.

Lang, H.-J.; Huder, J.; Amann, P. (2003): Bodenmechanik und Grundbau: Das Verhalten von Böden und Fels und die wichtigsten grundbaulichen Konzepte. Berlin: Springer-Verlag, 317 pages (in German).

Maniak, U. (2004): Hydrologie und Wasserwirtschaft: Eine Einführung für Ingenieure. Berlin: Springer-Verlag, 650 pages (in German).

Meadowcroft, I.C.; Van Lany, P.; Allsop, N.W.H.; Reeve, D.E. (1994): Risk assessment for coastal and tidal defence schemes. Proceedings 24th International Conference Coastal Engineering (ICCE), ASCE, Kobe, Japan, vol. 3.

Napp, N. (1999): Konzept zur Abschätzung des Überflutungsrisikos von Hochwasserschutzanlagen am Beispiel des privaten Hochwasserschutzes im Hamburger Hafen. M.Sc. Thesis, Technical University of Braunschweig, Leichtweiss-Institute, 164 pages (in German).

Oumeraci, H. (2001): Conceptual framework for risk-based design of coastal flood defences: A suggestion. Proceedings of International Workshop on Advanced Design on Maritime Structures in the 21st century (ADMS21), Goda, Y.; Takahashi, S. (eds.), PHRI, Yokosuka, Japan, Paper R-1, pp. 331-348.

Oumeraci, H.; Kortenhaus, A. (2002): Risk-based design of coastal flood defences: A suggestion for a conceptual framework. Proceedings 28. International Conference on Coastal Engineering (ICCE), Cardiff, Wales, UK.

Oumeraci, H.; Kortenhaus, A.; Lambrecht, H.-J. (2004): Berechnung der Versagenswahrscheinlichkeit eines Küstenschutzsystems in Ribe/Dänemark. Technical University of Braunschweig, Leichtweiss-Institute, Research Report No. 899, 67 pages (in German).

Oumeraci, H.; Muttray, M. (2001): Bemessungswellenparameter von Strukturen mit verschiedenen Reflexionseigenschaften. Final Report DFG-Projekt, OU 1/3-3, Braunschweig, Germany, 93 pages (in German).

Plate, E.J. (1993): Statistik und angewandte Wahrscheinlichkeitslehre für Bauingenieure. Publisher for architects and technical science, Berlin, Germany, 685 pages.

Reese, S. (2003): Die Vulnerabilität des schleswig-hosteinischen Küstenraumes durch Sturmfluten. Fallstudien von der Nord- und Ostseeküste. Ph.D. Thesis, Christian-Albrechts University, Kiel (in German).

Ribe Amtsråd (1966): Ribe Marsken. Betænkning vedrørende færdselsdæmning til Mandø, digesikring af marsken, afvanding af marsken. Published by Vestkystens Bogtrykkeri, Esbjerg (in Danish).

Ribe Tourist Office (2004): Ribe – Denmark's oldest town. Information brochure.

TAW (1997): Leidraad waterkerende kunstwerken en bijzondere constructies. Technische Adviescommissie voor de Waterkeringen (TAW), Delft, The Netherlands, 59 pages (in Dutch).

TAW (2000): Van overschijdingskans naar overstromingskans. Adviesrapport met Achtergrondrapport, Technische Adviescommissie voor de Waterkeringen, Den Haag, The Netherlands, 25 pages (in Dutch).

Tougaard, S. & Meesenburg, H. (1974): Den Jyske Vestkyst. En geografisk fortæling I flyfoto og kort. Published by BYGD, Esbjerg (in Danish).

Schüttrumpf, H. & Oumeraci, H. (2002): Schäden an See- und Stromdeichen. Journal of Leichtweiss-Institute, Technical University of Braunschweig, No. 149, pp. 129-172 (in German).

Visser, P.J. (1998): Breach erosion in sand-dikes. Proceedings 26th International Conference Coastal Engineering (ICCE), ASCE, Copenhagen, Denmark, vol. 3, pp. 3516-3528.

Voortman, H.G. (2003): Risk-based design of large-scale flood defence systems. Ph.D. thesis, Delft University of Technology, Delft, Holland.

Vrouwenvelder, A.W.C.M. (1993): Rekenmethoden voor een probabilistische dijkringanalyse. TNO 93-CON-R1332, (in Dutch).

Westrich, B.; Siebel, R.; Zweschper, B. (2003): Überströmbare Erddämme und Deiche - erosionssichere Deckwerke, Bodenverfestigung, Bemessungsgrundlagen. In: Herrmann, R.A. and Jensen, J., Symposium „Sicherung von Dämmen und Deichen", Institut für Geotechnik, Forschungsstelle Wasserwirtschaft und Umwelt, Siegen, Germany, 15 pages (in German).